

NOAA Technical Report NESDIS 142-4



Regional Climate Trends and Scenarios for the U.S. National Climate Assessment

Part 4. Climate of the U.S. Great Plains

Washington, D.C.
January 2013



U.S. DEPARTMENT OF COMMERCE
National Oceanic and Atmospheric Administration
National Environmental Satellite, Data, and Information Service

NOAA TECHNICAL REPORTS

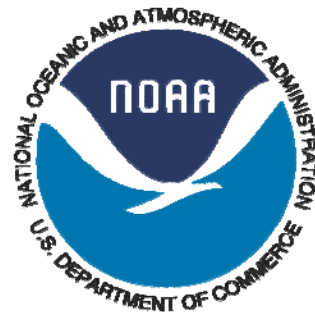
National Environmental Satellite, Data, and Information Service

The National Environmental Satellite, Data, and Information Service (NESDIS) manages the Nation's civil Earth-observing satellite systems, as well as global national data bases for meteorology, oceanography, geophysics, and solar-terrestrial sciences. From these sources, it develops and disseminates environmental data and information products critical to the protection of life and property, national defense, the national economy, energy development and distribution, global food supplies, and the development of natural resources.

Publication in the NOAA Technical Report series does not preclude later publication in scientific journals in expanded or modified form. The NESDIS series of NOAA Technical Reports is a continuation of the former NESS and EDIS series of NOAA Technical Reports and the NESC and EDS series of Environmental Science Services Administration (ESSA) Technical Reports.

Copies of earlier reports may be available by contacting NESDIS Chief of Staff, NOAA/ NESDIS, 1335 East-West Highway, SSMC1, Silver Spring, MD 20910, (301) 713-3578.

NOAA Technical Report NESDIS 142-4



Regional Climate Trends and Scenarios for the U.S. National Climate Assessment

Part 4. Climate of the U.S. Great Plains

Kenneth E. Kunkel, Laura E. Stevens, Scott E. Stevens, and Liqiang Sun

Cooperative Institute for Climate and Satellites (CICS), North Carolina State University
and NOAA's National Climatic Data Center (NCDC)
Asheville, NC

Emily Janssen and Donald Wuebbles

University of Illinois at Urbana-Champaign
Champaign, IL

Michael C. Kruk and Devin P. Thomas

ERT Inc.
NOAA's National Climatic Data Center (NCDC)
Asheville, NC

Martha D. Shulski, Natalie A. Umphlett, and Kenneth G. Hubbard

High Plains Regional Climate Center
University of Nebraska-Lincoln
Lincoln, NE

Kevin Robbins and Luigi Romolo

Southern Regional Climate Center
Louisiana State University
Baton Rouge, LA

Adnan Akyuz

North Dakota State Climate Office
North Dakota State University
Fargo, ND

Tapan B. Pathak

University of Nebraska-Lincoln
Lincoln, NE

Tony R. Bergantino

Wyoming State Climate Office
University of Wyoming
Laramie, WY

J. Greg Dobson

National Environmental Modeling and Analysis Center
University of North Carolina at Asheville
Asheville, NC

U.S. DEPARTMENT OF COMMERCE

Rebecca Blank, Acting Secretary

National Oceanic and Atmospheric Administration

Dr. Jane Lubchenco, Under Secretary of Commerce for Oceans and Atmosphere
and NOAA Administrator

National Environmental Satellite, Data, and Information Service

Mary Kicza, Assistant Administrator

PREFACE

This document is one of series of regional climate descriptions designed to provide input that can be used in the development of the National Climate Assessment (NCA). As part of a sustained assessment approach, it is intended that these documents will be updated as new and well-vetted model results are available and as new climate scenario needs become clear. It is also hoped that these documents (and associated data and resources) are of direct benefit to decision makers and communities seeking to use this information in developing adaptation plans.

There are nine reports in this series, one each for eight regions defined by the NCA, and one for the contiguous U.S. The eight NCA regions are the Northeast, Southeast, Midwest, Great Plains, Northwest, Southwest, Alaska, and Hawai'i/Pacific Islands.

These documents include a description of the observed historical climate conditions for each region and a set of climate scenarios as plausible futures – these components are described in more detail below.

While the datasets and simulations in these regional climate documents are not, by themselves, new, (they have been previously published in various sources), these documents represent a more complete and targeted synthesis of historical and plausible future climate conditions around the specific regions of the NCA.

There are two components of these descriptions. One component is a description of the historical climate conditions in the region. The other component is a description of the climate conditions associated with two future pathways of greenhouse gas emissions.

Historical Climate

The description of the historical climate conditions was based on an analysis of core climate data (the data sources are available and described in each document). However, to help understand, prioritize, and describe the importance and significance of different climate conditions, additional input was derived from climate experts in each region, some of whom are authors on these reports. In particular, input was sought from the NOAA Regional Climate Centers and from the American Association of State Climatologists. The historical climate conditions are meant to provide a perspective on what has been happening in each region and what types of extreme events have historically been noteworthy, to provide a context for assessment of future impacts.

Future Scenarios

The future climate scenarios are intended to provide an internally consistent set of climate conditions that can serve as inputs to analyses of potential impacts of climate change. The scenarios are not intended as projections as there are no established probabilities for their future realization. They simply represent an internally consistent climate picture using certain assumptions about the future pathway of greenhouse gas emissions. By “consistent” we mean that the relationships among different climate variables and the spatial patterns of these variables are derived directly from the same set of climate model simulations and are therefore physically plausible.

These future climate scenarios are based on well-established sources of information. No new climate model simulations or downscaled data sets were produced for use in these regional climate reports.

The use of the climate scenario information should take into account the following considerations:

1. All of the maps of climate variables contain information related to statistical significance of changes and model agreement. This information is crucial to appropriate application of the information. Three types of conditions are illustrated in these maps:
 - a. The first condition is where most or all of the models simulate statistically significant changes and agree on the direction (whether increasing or decreasing) of the change. If this condition is present, then analyses of future impacts and vulnerabilities can more confidently incorporate this direction of change. It should be noted that the models may still produce a significant range of magnitude associated with the change, so the manner of incorporating these results into decision models will still depend to a large degree on the risk tolerance of the impacted system.
 - b. The second condition is where the most or all of the models simulate changes that are too small to be statistically significant. If this condition is present, then assessment of impacts should be conducted on the basis that the future conditions could represent a small change from present or could be similar to current conditions and that the normal year-to-year fluctuations in climate dominate over any underlying long-term changes.
 - c. The third condition is where most or all of the models simulate statistically significant changes but do not agree on the direction of the change, i.e. a sizeable fraction of the models simulate increases while another sizeable fraction simulate decreases. If this condition is present, there is little basis for a definitive assessment of impacts, and, separate assessments of potential impacts under an increasing scenario and under a decreasing scenario would be most prudent.
2. The range of conditions produced in climate model simulations is quite large. Several figures and tables provide quantification for this range. Impacts assessments should consider not only the mean changes, but also the range of these changes.
3. Several graphics compare historical observed mean temperature and total precipitation with model simulations for the same historical period. These should be examined since they provide one basis for assessing confidence in the model simulated future changes in climate.
 - a. Temperature Changes: Magnitude. In most regions, the model simulations of the past century simulate the magnitude of change in temperature from observations; the southeast region being an exception where the lack of century-scale observed warming is not simulated in any model.
 - b. Temperature Changes: Rate. The *rate* of warming over the last 40 years is well simulated in all regions.
 - c. Precipitation Changes: Magnitude. Model simulations of precipitation generally simulate the overall observed trend but the observed decade-to-decade variations are greater than the model observations.

In general, for impacts assessments, this information suggests that the model simulations of temperature conditions for these scenarios are likely reliable, but users of precipitation simulations may want to consider the likelihood of decadal-scale variations larger than simulated by the models. It should also be noted that accompanying these documents will be a web-based resource with downloadable graphics, metadata about each, and more information and links to the datasets and overall descriptions of the process.

1. INTRODUCTION.....	5
2. REGIONAL CLIMATE TRENDS AND IMPORTANT CLIMATE FACTORS	10
2.1. DESCRIPTION OF DATA SOURCES	10
2.2. GENERAL DESCRIPTION OF GREAT PLAINS CLIMATE	11
2.3. IMPORTANT CLIMATE FACTORS	14
2.3.1. <i>Drought</i>	14
2.3.2. <i>Floods</i>	15
2.3.3. <i>Winter Storms</i>	17
2.3.4. <i>Convective Storms</i>	18
2.3.5. <i>Heat Waves</i>	18
2.3.6. <i>Cold Waves</i>	19
2.3.7. <i>Hurricane Climatology</i>	20
2.4. CLIMATIC TRENDS	21
2.4.1. <i>Temperature</i>	22
2.4.2. <i>Precipitation</i>	24
2.4.3. <i>Extreme Heat and Cold</i>	26
2.4.1. <i>Extreme Precipitation</i>	28
2.4.2. <i>Freeze-Free Season</i>	29
2.4.3. <i>Atlantic Tropical Storm Trends</i>	30
2.4.4. <i>Sea Level Rise</i>	31
3. FUTURE REGIONAL CLIMATE SCENARIOS	32
3.1. DESCRIPTION OF DATA SOURCES	32
3.2. ANALYSES.....	34
3.3. MEAN TEMPERATURE	35
3.4. EXTREME TEMPERATURE.....	42
3.5. OTHER TEMPERATURE VARIABLES	47
3.6. TABULAR SUMMARY OF SELECTED TEMPERATURE VARIABLES	50
3.7. MEAN PRECIPITATION.....	53
3.8. EXTREME PRECIPITATION	58
3.9. TABULAR SUMMARY OF SELECTED PRECIPITATION VARIABLES	62
3.10. COMPARISON BETWEEN MODEL SIMULATIONS AND OBSERVATIONS	64
4. SUMMARY	73
5. REFERENCES.....	76
6. ACKNOWLEDGEMENTS	82
6.1. REGIONAL CLIMATE TRENDS AND IMPORTANT CLIMATE FACTORS	82
6.2. FUTURE REGIONAL CLIMATE SCENARIOS	82

1. INTRODUCTION

The Global Change Research Act of 1990¹ mandated that national assessments of climate change be prepared not less frequently than every four years. The last national assessment was published in 2009 (Karl et al. 2009). To meet the requirements of the act, the Third National Climate Assessment (NCA) report is now being prepared. The National Climate Assessment Development and Advisory Committee (NCADAC), a federal advisory committee established in the spring of 2011, will produce the report. The NCADAC Scenarios Working Group (SWG) developed a set of specifications with regard to scenarios to provide a uniform framework for the chapter authors of the NCA report.

This climate document was prepared to provide a resource for authors of the Third National Climate Assessment report, pertinent to the states of Montana, North Dakota, South Dakota, Wyoming, Nebraska, Kansas, Oklahoma, and Texas; hereafter referred to collectively as the Great Plains. The specifications of the NCADAC SWG, along with anticipated needs for historical information, guided the choices of information included in this description of Great Plains climate. While guided by these specifications, the material herein is solely the responsibility of the authors and usage of this material is at the discretion of the 2013 NCA report authors.

This document has two main sections: one on historical conditions and trends, and the other on future conditions as simulated by climate models. The historical section concentrates on temperature and precipitation, primarily based on analyses of data from the National Weather Service's (NWS) Cooperative Observer Network, which has been in operation since the late 19th century. Additional climate features are discussed based on the availability of information. The future simulations section is exclusively focused on temperature and precipitation.

With regard to the future, the NCADAC, at its May 20, 2011 meeting, decided that scenarios should be prepared to provide an overall context for assessment of impacts, adaptation, and mitigation, and to coordinate any additional modeling used in synthesizing or analyzing the literature. Scenario information for climate, sea-level change, changes in other environmental factors (such as land cover), and changes in socioeconomic conditions (such as population growth and migration) have been prepared. This document provides an overall description of the climate information.

In order to complete this document in time for use by the NCA report authors, it was necessary to restrict its scope in the following ways. Firstly, this document does not include a comprehensive description of all climate aspects of relevance and interest to a national assessment. We restricted our discussion to climate conditions for which data were readily available. Secondly, the choice of climate model simulations was also restricted to readily available sources. Lastly, the document does not provide a comprehensive analysis of climate model performance for historical climate conditions, although a few selected analyses are included.

The NCADAC directed the “use of simulations forced by the A2 emissions scenario as the primary basis for the high climate future and by the B1 emissions scenario as the primary basis for the low climate future for the 2013 report” for climate scenarios. These emissions scenarios were generated by the Intergovernmental Panel on Climate Change (IPCC) and are described in the IPCC Special Report on Emissions Scenarios (SRES) (IPCC 2000). These scenarios were selected because they

¹ <http://thomas.loc.gov/cgi-bin/bdquery/z?d101:SN00169:|TOM:/bss/d101query.html>

incorporate much of the range of potential future human impacts on the climate system and because there is a large body of literature that uses climate and other scenarios based on them to evaluate potential impacts and adaptation options. These scenarios represent different narrative storylines about possible future social, economic, technological, and demographic developments. These SRES scenarios have internally consistent relationships that were used to describe future pathways of greenhouse gas emissions. The A2 scenario “describes a very heterogeneous world. The underlying theme is self-reliance and preservation of local identities. Fertility patterns across regions converge very slowly, which results in continuously increasing global population. Economic development is primarily regionally oriented and per capita economic growth and technological change are more fragmented and slower than in the other storylines” (IPCC 2000). The B1 scenario describes “a convergent world with...global population that peaks in mid-century and declines thereafter...but with rapid changes in economic structures toward a service and information economy, with reductions in material intensity, and the introduction of clean and resource-efficient technologies. The emphasis is on global solutions to economic, social, and environmental sustainability, including improved equity, but without additional climate initiatives” (IPCC 2000).

The temporal changes of emissions under these two scenarios are illustrated in Fig. 1 (left panel). Emissions under the A2 scenario continually rise during the 21st century from about 40 gigatons (Gt) CO₂-equivalent per year in the year 2000 to about 140 Gt CO₂-equivalent per year by 2100. By contrast, under the B1 scenario, emissions rise from about 40 Gt CO₂-equivalent per year in the year 2000 to a maximum of slightly more than 50 Gt CO₂-equivalent per year by mid-century, then falling to less than 30 Gt CO₂-equivalent per year by 2100. Under both scenarios, CO₂ concentrations rise throughout the 21st century. However, under the A2 scenario, there is an acceleration in concentration trends, and by 2100 the estimated concentration is above 800 ppm. Under the B1 scenario, the rate of increase gradually slows and concentrations level off at about 500 ppm by 2100. An increase of 1 ppm is equivalent to about 8 Gt of CO₂. The increase in concentration is considerably smaller than the rate of emissions because a sizeable fraction of the emitted CO₂ is absorbed by the oceans.

The projected CO₂ concentrations are used to estimate the effects on the earth’s radiative energy budget, and this is the key forcing input used in global climate model simulations of the future. These simulations provide the primary source of information about how the future climate could evolve in response to the changing composition of the earth’s atmosphere. A large number of modeling groups performed simulations of the 21st century in support of the IPCC’s Fourth Assessment Report (AR4), using these two scenarios. The associated changes in global mean temperature by the year 2100 (relative to the average temperature during the late 20th century) are about +6.5°F (3.6°C) under the A2 scenario and +3.2°F (1.8°C) under the B1 scenario with considerable variations among models (Fig. 1, right panel).

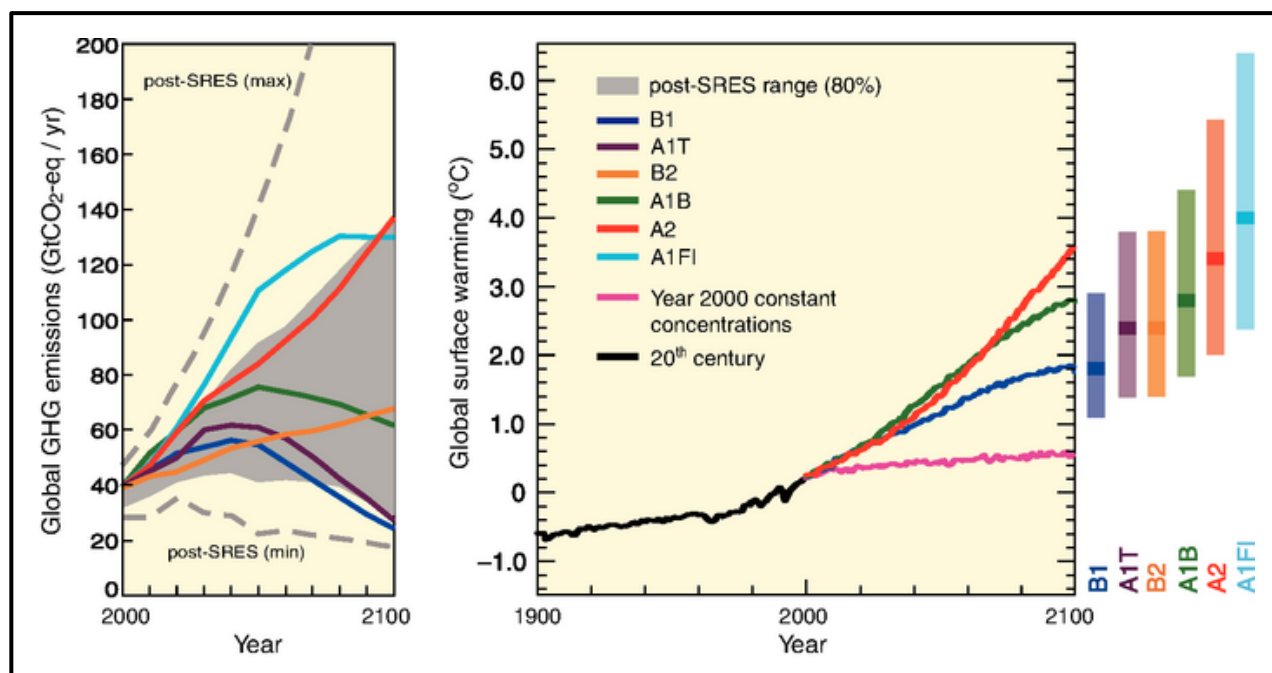


Figure 1. Left Panel: Global GHG emissions (in GtCO₂-eq) in the absence of climate policies: six illustrative SRES marker scenarios (colored lines) and the 80th percentile range of recent scenarios published since SRES (post-SRES) (gray shaded area). Dashed lines show the full range of post-SRES scenarios. The emissions include CO₂, CH₄, N₂O and F-gases. Right Panel: Solid lines are multi-model global averages of surface warming for scenarios A2, A1B and B1, shown as continuations of the 20th-century simulations. These projections also take into account emissions of short-lived GHGs and aerosols. The pink line is not a scenario, but is for Atmosphere-Ocean General Circulation Model (AOGCM) simulations where atmospheric concentrations are held constant at year 2000 values. The bars at the right of the figure indicate the best estimate (solid line within each bar) and the likely range assessed for the six SRES marker scenarios at 2090-2099. All temperatures are relative to the period 1980-1999. From IPCC AR4, Sections 3.1 and 3.2, Figures 3.1 and 3.2, IPCC (2007b).

In addition to the direct output of the global climate model simulations, the NCADAC approved “the use of both statistically- and dynamically-downscaled data sets”. “Downscaling” refers to the process of producing higher-resolution simulations of climate from the low-resolution outputs of the global models. The motivation for use of these types of data sets is the spatial resolution of global climate models. While the spatial resolution of available global climate model simulations varies widely, many models have resolutions in the range of 100-200 km (~60-120 miles). Such scales are very large compared to local and regional features important to many applications. For example, at these scales mountain ranges are not resolved sufficiently to provide a reasonably accurate representation of the sharp gradients in temperature, precipitation, and wind that typically exist in these areas.

Statistical downscaling achieves higher-resolution simulations through the development of statistical relationships between large-scale atmospheric features that are well-resolved by global models and the local climate conditions that are not well-resolved. The statistical relationships are developed by comparing observed local climate data with model simulations of the recent historical climate. These relationships are then applied to the simulations of the future to obtain local high-

resolution projections. Statistical downscaling approaches are relatively economical from a computational perspective, and thus they can be easily applied to many global climate model simulations. One underlying assumption is that the relationships between large-scale features and local climate conditions in the present climate will not change in the future (Wilby and Wigley 1997). Careful consideration must also be given when deciding how to choose the appropriate predictors because statistical downscaling is extremely sensitive to the choice of predictors (Norton et al. 2011).

Dynamical downscaling is much more computationally intensive but avoids assumptions about constant relationships between present and future. Dynamical downscaling uses a climate model, similar in most respects to the global climate models. However, the climate model is run at a much higher resolution but only for a small region of the earth (such as North America) and is termed a “regional climate model (RCM)”. A global climate model simulation is needed to provide the boundary conditions (e.g., temperature, wind, pressure, and humidity) on the lateral boundaries of the region. Typically, the spatial resolution of an RCM is 3 or more times higher than the global model used to provide the boundary conditions. With this higher resolution, topographic features and smaller-scale weather phenomena are better represented. The major downside of dynamical downscaling is that a simulation for a region can take as much computer time as a global climate model simulation for the entire globe. As a result, the availability of such simulations is limited, both in terms of global models used for boundary conditions and time periods of the simulations (Hayhoe 2010).

Section 3 of this document (Future Regional Climate Scenarios) responds to the NCADAC directives by incorporating analyses from multiple sources. The core source is the set of global climate model simulations performed for the IPCC AR4, also referred to as the Climate Model Intercomparison Project phase 3 (CMIP3) suite. These have undergone extensive evaluation and analysis by many research groups. A second source is a set of statistically-downscaled data sets based on the CMIP3 simulations. A third source is a set of dynamically-downscaled simulations, driven by CMIP3 models. A new set of global climate model simulations is being generated for the IPCC Fifth Assessment Report (AR5). This new set of simulations is referred to as the Climate Model Intercomparison Project phase 5 (CMIP5). These scenarios do not incorporate any CMIP5 simulations as relatively few were available at the time the data analyses were initiated. As noted earlier, the information included in this document is primarily concentrated around analyses of temperature and precipitation. This is explicitly the case for the future scenarios sections; due in large part to the short time frame and limited resources, we capitalized on the work of other groups on future climate simulations, and these groups have devoted a greater effort to the analysis of temperature and precipitation than other surface climate variables.

Climate models have generally exhibited a high level of ability to simulate the large-scale circulation patterns of the atmosphere. These include the seasonal progression of the position of the jet stream and associated storm tracks, the overall patterns of temperature and precipitation, the occasional occurrence of droughts and extreme temperature events, and the influence of geography on climatic patterns. There are also important processes that are less successfully simulated by models, as noted by the following selected examples.

Climate model simulation of clouds is problematic. Probably the greatest uncertainty in model simulations arises from clouds and their interactions with radiative energy fluxes (Dufresne and Bony 2008). Uncertainties related to clouds are largely responsible for the substantial range of

global temperature change in response to specified greenhouse gas forcing (Randall et al. 2007). Climate model simulation of precipitation shows considerable sensitivities to cloud parameterization schemes (Arakawa 2004). Cloud parameterizations remain inadequate in current GCMs. Consequently, climate models have large biases in simulating precipitation, particularly in the tropics. Models typically simulate too much light precipitation and too little heavy precipitation in both the tropics and middle latitudes, creating potential biases when studying extreme events (Bader et al. 2008).

Climate models also have biases in simulation of some important climate modes of variability. The El Niño-Southern Oscillation (ENSO) is a prominent example. In some parts of the U.S., El Niño and La Niña events make important contributions to year-to-year variations in conditions. Climate models have difficulty capturing the correct phase locking between the annual cycle and ENSO (AchutaRao and Sperber 2002). Some climate models also fail to represent the spatial and temporal structure of the El Niño - La Niña asymmetry (Monahan and Dai 2004). Climate simulations over the U.S. are affected adversely by these deficiencies in ENSO simulations.

The model biases listed above add additional layers of uncertainty to the information presented herein and should be kept in mind when using the climate information in this document.

The representation of the results of the suite of climate model simulations has been a subject of active discussion in the scientific literature. In many recent assessments, including AR4, the results of climate model simulations have been shown as multi-model mean maps (e.g., Figs. 10.8 and 10.9 in Meehl et al. 2007). Such maps give equal weight to all models, which is thought to better represent the present-day climate than any single model (Overland et al. 2011). However, models do not represent the current climate with equal fidelity. Knutti (2010) raises several issues about the multi-model mean approach. These include: (a) some model parameterizations may be tuned to observations, which reduces the spread of the results and may lead to underestimation of the true uncertainty; (b) many models share code and expertise and thus are not independent, leading to a reduction in the true number of independent simulations of the future climate; (c) all models have some processes that are not accurately simulated, and thus a greater number of models does not necessarily lead to a better projection of the future; and (d) there is no consensus on how to define a metric of model fidelity, and this is likely to depend on the application. Despite these issues, there is no clear superior alternative to the multi-model mean map presentation for general use. Tebaldi et al. (2011) propose a method for incorporating information about model variability and consensus. This method is adopted here where data availability make it possible. In this method, multi-model mean values at a grid point are put into one of three categories: (1) models agree on the statistical significance of changes and the sign of the changes; (2) models agree that the changes are not statistically significant; and (3) models agree that the changes are statistically significant but disagree on the sign of the changes. The details on specifying the categories are included in Section 3.

2. REGIONAL CLIMATE TRENDS AND IMPORTANT CLIMATE FACTORS

2.1. Description of Data Sources

One of the core data sets used in the United States for climate analysis is the National Weather Service's Cooperative Observer Network (COOP), which has been in operation since the late 19th century. The resulting data can be used to examine long-term trends. The typical COOP observer takes daily observations of various climate elements that might include precipitation, maximum temperature, minimum temperature, snowfall, and snow depth. While most observers are volunteers, standard equipment is provided by the National Weather Service (NWS), as well as training in standard observational practices. Diligent efforts are made by the NWS to find replacement volunteers when needed to ensure the continuity of stations whenever possible. Over a thousand of these stations have been in operation continuously for many decades (NOAA 2012a).

For examination of U.S. long-term trends in temperature and precipitation, COOP data is the best available resource. Its central purpose is climate description (although it has many other applications as well); the number of stations is large, there have been relatively few changes in instrumentation and procedures, and it has been in existence for over 100 years. However, there are some sources of temporal inhomogeneities in station records, described as follows:

- One instrumental change is important. For much of the COOP history, the standard temperature system was a pair of liquid-in-glass (LIG) thermometers placed in a radiation shield known as the Cotton Region Shelter (CRS). In the 1980s, the NWS began replacing this system with an electronic maximum-minimum temperature system (MMTS). Inter-comparison experiments indicated that there is a systematic difference between these two instrument systems, with the newer electronic system recording lower daily maximum temperatures (T_{max}) and higher daily minimum temperatures (T_{min}) (Quayle et al. 1991; Hubbard and Lin 2006; Menne et al. 2009). Menne et al. (2009) estimate that the mean shift (going from CRS/LIG to MMTS) is -0.52K for T_{max} and +0.37K for T_{min} . Adjustments for these differences can be applied to monthly mean temperature to create homogeneous time series.
- Changes in the characteristics and/or locations of sites can introduce artificial shifts or trends in the data. In the COOP network, a station is generally not given a new name or identifier unless it moves at least 5 miles and/or changes elevation by at least 100 feet (NWS 1993). Site characteristics can change over time and affect a station's record, even if no move is involved (and even small moves \ll 5 miles can have substantial impacts). A common source of such changes is urbanization around the station, which will generally cause artificial warming, primarily in T_{min} (Karl et al. 1988), the magnitude of which can be several degrees in the largest urban areas. Most research suggests that the overall effect on national and global temperature trends is rather small because of the large number of rural stations included in such analyses (Karl et al. 1988; Jones et al. 1990) and because homogenization procedures reduce the urban signal (Menne et al. 2009).
- Station siting can cause biases. Recent research by Menne et al. (2010) and Fall et al. (2011) examined this issue in great detail. The effects on mean trends was found to be small in both studies, but Fall et al. (2011) found that stations with poor siting overestimate (underestimate) minimum (maximum) temperature trends.

- Changes in the time that observations are taken can also introduce artificial shifts or trends in the data (Karl et al. 1986; Vose et al. 2003). In the COOP network, typical observation times are early morning or late afternoon, near the usual times of the daily minimum and maximum temperatures. Because observations occur near the times of the daily extremes, a change in observation time can have a measurable effect on averages, irrespective of real changes. The study by Karl et al. (1986) indicates that the difference in monthly mean temperatures between early morning and late afternoon observers can be in excess of 2°C. There has, in fact, been a major shift from a preponderance of afternoon observers in the early and middle part of the 20th century to a preponderance of morning observers at the present time. In the 1930s, nearly 80% of the COOP stations were afternoon observers (Karl et al. 1986). By the early 2000s, the number of early morning observers was more than double the number of late afternoon observers (Menne et al. 2009). This shift tends to introduce an artificial cooling trend in the data.

A recent study by Williams et al. (2011) found that correction of known and estimated inhomogeneities lead to a larger warming trend in average temperature, principally arising from correction of the biases introduced by the changeover to the MMTS and from the biases introduced by the shift from mostly afternoon observers to mostly morning observers.

Much of the following analysis on temperature, precipitation, and snow is based on COOP data. For some of these analyses, a subset of COOP stations with long periods of record was used, specifically less than 10% missing data for the period of 1895-2011. The use of a consistent network is important when examining trends in order to minimize artificial shifts arising from a changing mix of stations.

2.2. General Description of Great Plains Climate

The Great Plains region is characterized by a highly diverse climate with large spatial variations. The great latitudinal range of this region leads to a very wide range in temperatures; the region includes both some of the coldest and hottest regions of the coterminous U.S. as well as some of the wetter and drier regions.

In addition to the latitudinal range, several geographic factors contribute to this variability. Because the mountains to the west of the region largely block moisture from the Pacific Ocean, the Gulf of Mexico is the major source of moisture for this region. Intrusions of moisture from the Gulf of Mexico are more infrequent the further north and west one goes. The lack of mountain ranges to the north means that the region is exposed to outbreaks of Arctic air that can bring bitter cold during the winter. The polar jet stream is often located near or over the region during the winter, with frequent storm systems bringing cloudy skies, windy conditions, and precipitation. Eastern and southern parts of the region are characteristically warm and humid during the warmer half of the year due to a semi-permanent high pressure system in the subtropical Atlantic that draws warm, humid ocean air into the area. Summer also tends to be the rainiest season, with short-lived rainfall and thunderstorms. Precipitation tends to be erratic, and severe droughts occur from time to time.

Potentially dangerous storms occur in every season. Winter can bring major snowstorms, damaging ice storms, or both. Warmer months, typically March-October, have heat waves and convective storms, including thunderstorms and lightning, flood-producing rainstorms, hail, and deadly

tornadoes. This area has the highest incidence of tornadoes in the world due to the unique confluence of several geographical factors. Hurricanes are a major weather phenomenon for the coastal region of Texas.

In far southwestern portions of the Great Plains, an important feature of the climate is a summer peak in precipitation caused by a continental-scale shift in wind flow known as the North American Monsoon (NAM). Although this feature is most prominent in Arizona and New Mexico, it also extends into far West Texas; in fact, more than 40% of mean annual precipitation at El Paso, TX falls in July, August, and September, the NAM season (Douglas et al. 1993).

The Great Plains has a very wide range of annual average temperature (Fig. 2). The coldest annual average temperatures of less than 30°F occur in the higher mountain areas of Wyoming and Montana and along the northern border with Canada. By contrast, the average annual temperatures in south Texas are greater than 70°F.

Average annual precipitation (Fig. 3) also exhibits an extremely large range, illustrating the particular geographic features that determine the frequency of high moisture transport from oceanic sources. The far southeastern part of the region receives more than 60 inches per year, while some of the far western areas receive less than 10 inches per year.

The Great Plains region includes 10 of the top 100 metropolitan statistical areas by population (U.S. Census Bureau 2011). These are Dallas (rank #4), Houston (#5), San Antonio (#24), Kansas City (#29), Austin (#34), Oklahoma City (#43), Tulsa (#54), Omaha (#58), El Paso (#65), and Wichita (#86). These urban centers experience the typical types of climate sensitivities that are unique to, or exacerbated by, the specific characteristics of the urban environment. Temperature extremes can have large impacts on human health, particularly in the urban core where the urban heat island effect raises summer temperatures. Severe storms, both winter and summer, result in major disruptions to surface and air transportation. Extreme rainfall causes a host of problems, including storm sewer overflow, flooding of homes and roadways, and contamination of municipal water supplies. Climate extremes combined with the urban pollution sources can create air quality conditions that are detrimental to human health. Both Dallas and Houston are designated as nonattainment areas for ozone standards (USEPA 2011).

Within the Great Plains region there are a number of Native American tribes and tribal lands. The majority of the tribal land, in terms of area, is located in the Dakotas, Montana, Wyoming, and Oklahoma. Water availability is a concern as most tribal land is located in areas with low annual average precipitation.

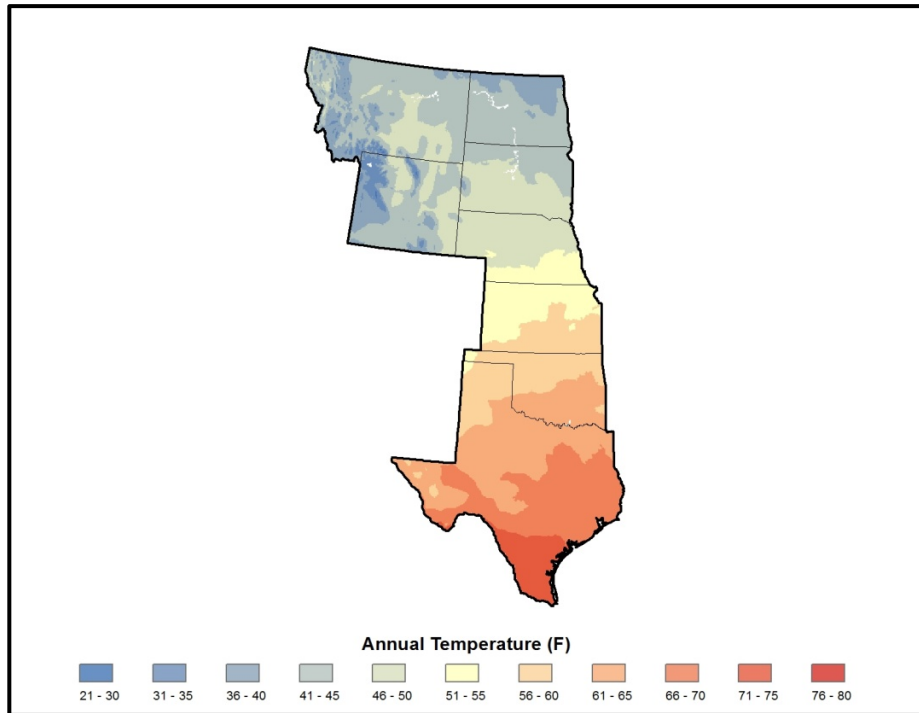


Figure 2. Average (1981-2010) annual temperature ($^{\circ}\text{F}$) for the Great Plains region. Based on a new gridded version of COOP data from the National Climatic Data Center, the CDDv2 data set (R. Vose, personal communication, July 27, 2012).

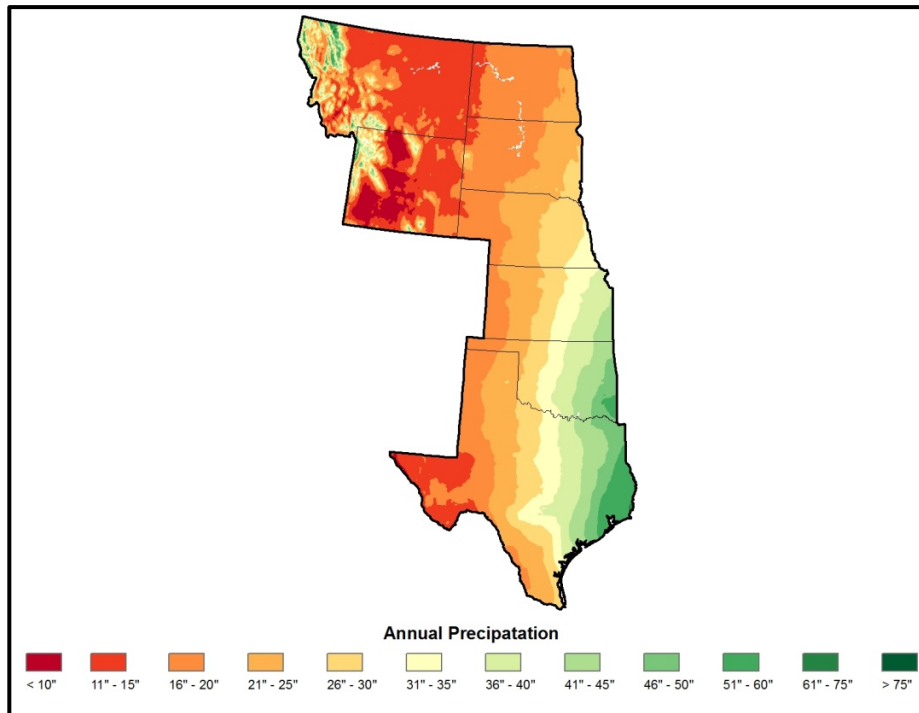


Figure 3. Average (1981-2010) annual precipitation (inches) for the Great Plains region. Based on a new gridded version of COOP data from the National Climatic Data Center, the CDDv2 data set (R. Vose, personal communication, July 27, 2012).

Agriculture is very important in this region and is highly diverse, reflective of the diverse climate conditions. Unirrigated summer crop production occurs in the eastern parts of the region with significant output of soybeans and wheat. In western parts of the region, there are large areas of irrigated crop production, particularly corn, cotton, and alfalfa. Unirrigated agricultural production in particular is critically dependent on weather. Rainfall, heat stress, pests, ozone levels, and extreme events such as heavy precipitation, flooding, or drought can seriously affect production. The Ogallala aquifer is a major source of water for irrigation, but this resource is being depleted (Rosenberg et al. 1999). The Great Plains is also a major producer of livestock, especially dairy and beef cattle, hogs, and others.

Major river basins in the Great Plains region include the Souris-Red-Rainy, Missouri, Arkansas-Red-White, and Texas-Gulf. The largest of these is the Missouri basin, encompassing more than 529,000 square miles. Periodically, these rivers reach and exceed flood stage due to high springtime snowmelt runoff from the Rocky Mountains and/or excessive rainfall. A tributary of the Missouri River is the Platte River with North and South Forks both originating in Colorado. It is a highly managed and over-appropriated river system and drains an arid, relatively high elevation portion of the Great Plains. Areas of the region could see hydrological impacts for this basin and others in a warmer climate (Ojima et al. 1999).

2.3. Important Climate Factors

The Great Plains region experiences a wide range of extreme weather and climate events that affect human society, ecosystems, and infrastructure. This discussion is meant to provide general information about these types of weather and climate phenomena. These include:

2.3.1. Drought

Various types of drought can occur throughout the Great Plains. For example, *meteorological drought* (measured solely by the severity and duration of a dry period) occurs in some portion of the Great Plains nearly every year. Other types of drought are measured by the dryness relative to the needs for water in various sectors. *Agricultural drought* largely refers to climate related problems in food production for farmers and cattlemen. Lush pastures can quickly wilt and dry up, leaving ranchers with less hay and grazing resources than required for their cattle herds. Farmers may find their rain-fed crops undergoing severe stress due to water shortage, and as a result, yields will be reduced. Water supplies for cattle and irrigation may be adversely impacted when lakes, reservoirs, and ground water are affected by drought conditions. *Hydrological drought* occurs when water supply is reduced due to periods of precipitation shortages. The hydrologic storage systems are negatively impacted, with less water available for irrigation, navigation, hydropower and recreation.

Drought can occur in any area of the Great Plains and can vary in intensity and duration. The Dust Bowl is by far the most famous drought over the past 100 years, but prolonged drought has occurred recently as well. For instance, Wyoming, which is the 5th driest state, experienced moderate to severe drought conditions for nearly a decade beginning in 1999.

The 2011 drought in the southern Great Plains was the most intense event in that area in the observational record extending back to 1895, based on the Palmer Drought Severity Index (NOAA 2011b). In Texas, the summer of 2011 was both the warmest on record and the driest on record. In

Oklahoma, the summer was the also the warmest on record and the second driest on record. Losses from this drought are estimated at \$12 billion with 95 fatalities (NOAA 2011a). The most prolonged drought in the southern Great Plains was in the 1950s. From a paleoclimatic perspective using tree rings as a proxy for drought, the 2011 drought in Texas is approximately equal in intensity to the worst droughts of the past 429 years. Also based on the tree ring evidence, the drought of the 1950s is not exceeded in length in the last 429 years. This confirms the unusual nature of both the 1950s and 2011 events.

2.3.2. Floods

Floods that occur in the Great Plains can be categorized into several types. One occurs when melting of a heavy snow pack in the mountains leads to flooding of rivers downstream and dangerously full reservoirs. For instance, floods in the Red River basin occur primarily during April and May and are caused by rapid spring snowmelt that may be accompanied by rain. In general, the later that snowmelt begins in spring the more likely it will be accelerated by high temperatures and/or rainfall making flooding more likely. A second type is associated with short-duration heavy rainfall, usually from summer convective storms. These strong storms occur on the plains when warm moist air from the south meets cooler air from the north. A third type occurs when heavy precipitation is persistent over many days to weeks, which can produce flooding on the largest river systems. Finally, along the gulf coast, heavy precipitation from hurricane rain bands can produce flooding over wide areas.

Geographical proximity to heavy rainfall is not necessary to experience flood effects. In the plains, many of the creek beds are usually dry due to lack of precipitation sufficient to maintain water flow. However, the dry creeks can suddenly fill with torrents of rapidly moving floodwaters. Loss of life may result from storms that occur miles upstream to unsuspecting individuals.

Topography and synchrony of spring melt makes the Red River of the North and the Red River Valley one of the most flood-prone areas in the U.S. The Red River flows north along the gently sloped Red River Valley. In the region of Fargo-Halstad, the gradient of the Red River averages 5 inches per mile of length. In the region of Drayton-Pembina, however, the gradient drops to 1.5 inches per mile. During floods, the Red River at Drayton tends to pool due to lack of slope - the region becoming essentially a massive, shallow lake. The Red River flows northward, but, at the same time, spring thaw proceeds steadily northward along the Valley. Thus, along the Red River, runoff from the southern portion of the Valley progressively joins with fresh, melted waters from more northerly localities. Therefore the synchrony of melting creates natural ice jams in the downstream every year, making the Valley one of the most flood-prone areas in the US. Based on more than 100 years of river stage data collected in Fargo, the Red River exceeded major flood stages (30 feet from a reference level and higher) 16 times. In the spring of 1997, record floods occurred along the Red River due to snowfall totals exceeding average by 1.5 to 2.5 times (Kunkel 2003); this record was exceeded in the 2009 floods (NDSU 2012). A time series of annual peak stream flow (Fig. 4) exhibits a strong upward trend over the 20th and early 21st centuries.

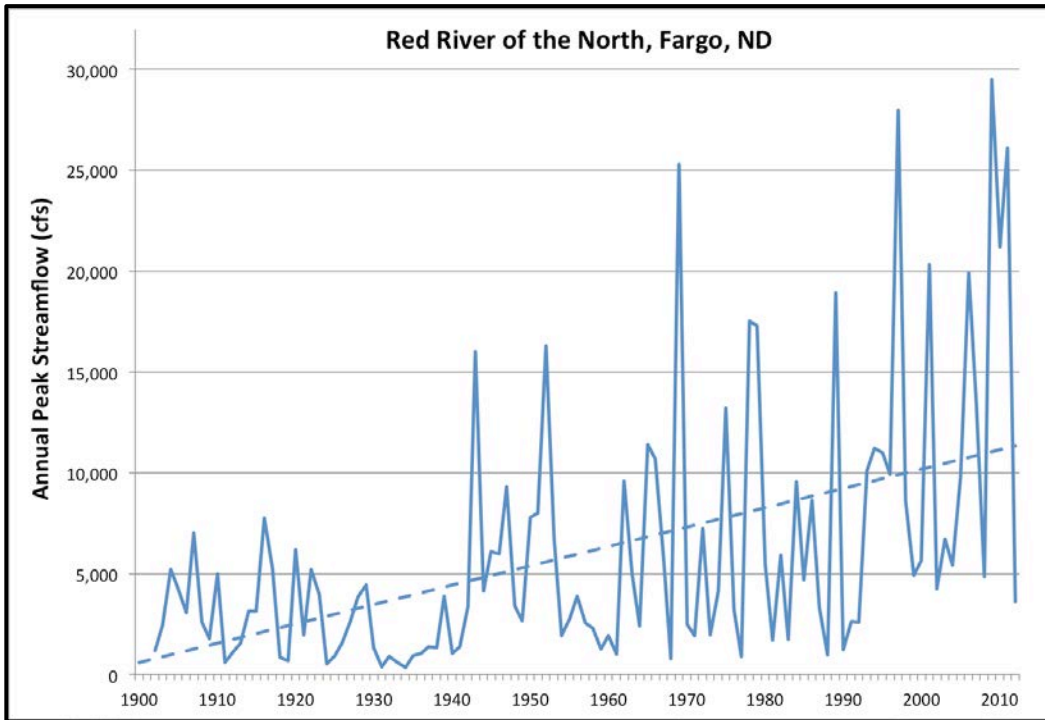


Figure 4. Annual peak streamflow (cfs) of the Red River of the North, Fargo, ND.

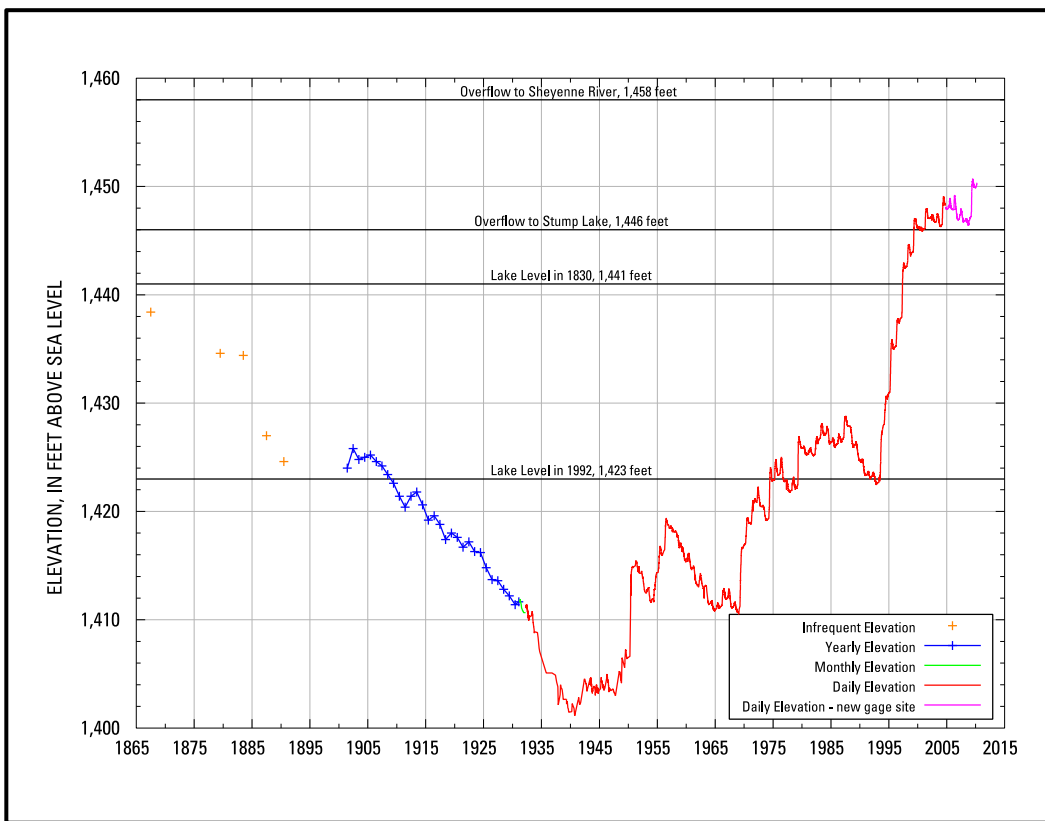


Figure 5. Devils Lake, ND elevation change since 1865 (USGS 2011).

The Devils Lake Basin is a 3,810-square-mile subbasin in the Red River of the North Basin. The elevation of the lake has fluctuated in time, and Fig. 5 shows the elevation change since 1865 (USGS 2011). However, continuous lake level measurements did not start until the early 1930s. The graphic shows that there has been a general rise in the lake levels since 1941 with a steady rise since 1993 from the 1992 elevation of 1423 feet to 1452.05 feet in 2010 (record elevation level during the instrumental era). In March 1993, Devils Lake had a surface area of 44,230 acres. At its June 2009 record elevation, it covered about 169,000 acres – an increase of 124,800 inundated acres, or about 195 square miles. Evidence shows that variation in the lake elevation is mostly part of the natural cycle of hydro-climate variability (Hoerling 2010).

2.3.3. Winter Storms

This portion of the country is highly susceptible to the impacts of winter storm systems, which can produce heavy snows, high winds with blowing snow and reduced visibility, low wind chill temperatures and produce the conditions for later snowmelt flooding. Major impacts include a disruption of transportation and commerce, high snow removal costs, and loss of life and livestock due to cold exposure. Recent research on winter storm classification shows promise for evaluating associated societal impacts (Cerruti and Decker 2011). For the southern Great Plains region, severe winter storms are less common, but ice storm events are generally more frequent than in the north (Changnon et al. 2006). Winter storms affecting the Plains region normally originate and strengthen on the leeward (east) side of the Rocky Mountains. There are two frequent locations for winter storm genesis; one in the north (sometimes termed an Alberta Low), and one in the south (the Colorado Low). These systems track in an eastward direction in association with the jet stream and prevailing winds at this latitude.

Blizzard conditions are not uncommon for the northern Great Plains and represent high impact events (Black 1971). These are defined by the National Weather Service as winds of 35 mph or greater with considerable snowfall and reduction in visibility to less than 0.25 miles prevailing for 3 hours or longer. The probability of a blizzard occurring in a given year is greater than 50% for the Dakotas and western Nebraska, the highest probability in the nation (Schwartz and Schmidlin 2002). The peak blizzard frequency for the northern Plains occurs in January and in March for the central Plains. Although blizzards were rare in the 1980s and most of the 1990s, during the winter of 1996 - 1997 there were nine blizzards and four winter storms that produced all-time record seasonal snowfalls of 60 to 120 inches over most of North Dakota (Enz 2003). Work has been done to investigate winter season severity associations with large-scale atmospheric circulation processes, and there has been found a weak tendency for an increase in blizzards during La Niña winters.

Snow represents an important natural resource and is a significant component of the climate system with the physical characteristics to modify the surface energy budget. In the northern Plains, natural or structural fences are sometimes installed to capture windblown snow on the landscape for use in springtime recharge for water resources and/or to keep roadways clear during winter storm events. The period of time with snow on the ground in the Plains varies quite significantly across the region, with increasing duration in a northward progression. Snow cover is episodic and associated with winter storm events in the southern Plains, whereas the ground generally remains covered throughout the season for the northern Plains states. Snowfall represents one of the most difficult meteorological variables to accurately measure. However, high quality surface observing stations in the region show trends in seasonal snowfall amounts over time. These trends vary regionally with a

general increase in the northern and western high Plains and a decrease in seasonal snowfall for the eastern southern Plains (Kunkel et al. 2009).

Freezing rain occasionally affects the region. Most areas from central Texas to the Canadian border experience from 1 to 3 days per year with freezing rain (Changnon and Karl 2003). Extreme eastern portions of the region from northeast Oklahoma to southeastern North Dakota experience 3 to 4 days per year.

2.3.4. Convective Storms

This region of the country experiences a high frequency of convective storms during the spring and summer months. Hazards from these events range from downbursts, heavy downpours, and lightning, to hail, tornadoes, and flash flooding. Severe storms peak in the spring for the southern Plains while the peak in storm activity is in summer for the northern Plains. The occurrence of lightning strikes is at a maximum in the southeast portion of the region (particularly the Texas Gulf coast) and gradually decreases to the northwest with the fewest strikes in the mountains of Wyoming and Montana. The central and southern portion of the Great Plains is often referred to as 'tornado alley' due to the frequency of these events here compared to elsewhere in the U.S. [e.g., more than 100 per year on average in Texas and more than 50 per year in Kansas and Oklahoma, Brooks et al. (2003)]. All tornadoes are capable of producing damage; however, violent tornadoes often result in significant damage and destruction. In May 2007, nearly 95% of Greensburg, KS, was completely destroyed by an EF5 tornado where 11 lives were lost. The event was part of a larger-scale tornado outbreak over a four-state region throughout the Plains. Hail events associated with convective storm events are most common in the central and southern Plains of the U.S. While most hail is smaller in size, some can be quite large and damaging to life and property. In fact, the largest circumference hailstone of 18.75 inches (1.34 lbs and 7.0 inch diameter) was reported in Aurora, NE, in June of 2003. A close second occurred in July 2010 near Vivian, SD, which was heavier (1.94 lbs) and greater in diameter (8.0 inches).

2.3.5. Heat Waves

The great north-south extent of the Great Plains region lends itself to a wide range of temperatures. Statewide extreme temperatures of 115°F and higher have been recorded for each of the states in the region; however, exposure to prolonged heat (i.e. a heat wave) varies widely. For instance, summer high temperatures of 95°F and higher are quite common for areas of Texas and Oklahoma, but temperatures that high are quite uncommon in areas of the Dakotas. The east-west gradient of moisture that exists in the region has an impact on the magnitude of the effects of heat waves. In the eastern portion of the Great Plains, moisture from the Gulf of Mexico can exacerbate the effects of heat waves as the combination of high temperatures and humidity can create dangerous conditions for humans (Changnon et al. 1996; McGeehin and Mirabelli 2001) as well as livestock (Mader 2003; St. Pierre et al. 2003), and crops (Herrero and Johnson 1980). Alternatively, the dryness of the western portion of the Great Plains allows for an increased human tolerance for heat.

Some examples of historic heat waves in the Great Plains region include the Dust Bowl of the 1930s (Schubert et al. 2004) and the 1980 summer heat wave and drought (Karl and Quayle 1981). Most recently, the heat wave and drought of the summer of 2011 across the southern portions of the Great Plains region had major impacts on human livelihood, crops, livestock, water supplies, and more. According to the National Oceanic and Atmospheric Administration's National Climatic Data

Center, both Texas and Oklahoma recorded their warmest summer on record (records date back to 1895). The Dallas-Fort Worth area endured 40 consecutive days of 100°F+ heat in 2011, which was the second longest streak of 100°F+ days on record (period of record 1898-2011); 1980 held on to the record of 42 days. Most areas of Texas and Oklahoma experienced at least 40 total days of 100°F+ heat (Fig. 6). On average, Amarillo, TX sees roughly 5 days per year over 100 °F, Dallas, TX 16 days, and Oklahoma City, OK 11 days. In 2011, Amarillo had 50 days, Dallas had 73, and Oklahoma City had 63. This heat wave was exacerbated by the excessively dry conditions which contributed to higher temperatures because of reduced evaporative cooling at the land surface. Although not as long lasting, the intense heat made its way to the northern portions of the region, impacting crops and cattle. For instance, in South Dakota, unusually warm and humid conditions took their toll on livestock, and at least 1700 head of cattle perished (Aberdeen American News 2011).

2.3.6. Cold Waves

Arctic air routinely plunges south into the Great Plains region during the winter months. As stated before, the large latitudinal extent of the region lends itself to a wide range of temperatures, and this is especially the case in the winter months. While statewide extreme maximum temperatures are similar across the Great Plains, the large latitudinal extent of the region leads to a large variation of statewide extreme minimum temperatures, ranging from -23°F in Texas to -70°F in Montana. Cold waves can impact a wide range of sectors such as human health (Kalkstein and Davis 1989; Mäkinen 2007) and agriculture including both crops and livestock (Young 1981; Gu et al. 2008).

Many memorable cold waves have affected the region over the years (O'Connor and Fean 1955; Quiroz 1984; Kocin et al. 1988; Nielsen-Gammon 2011). Major cold air outbreaks are typically associated with a negative phase North Atlantic Oscillation index and positive Arctic sea level pressure anomalies (Walsh et al. 2001). When compared to past data, relatively few cold waves have occurred in the region since 2000; however one recent cold wave to affect the region is the Easter Freeze of April 2007 (NWS 2008). Unseasonably warm temperatures in March were followed by an arctic outbreak in April. The early warmth in the spring season caused many plants to develop early, including fruit trees and pastures. In many areas of the Great Plains, the average last spring freeze dates occur in April and May, making early growing plants highly susceptible to a freeze event. Ultimately, the April 2007 freeze event caused at least 2 billion dollars in freeze-related losses from an area stretching from Colorado through Virginia. While most of the damage to agricultural and horticultural crops was confined to areas east, in the Great Plains, winter wheat damage was reported. In addition, counties in northwestern Nebraska, the eastern half of Kansas, and nearly all of Oklahoma were declared disaster areas by the USDA Farm Services Agency. Although loss information was not available for all states, it was estimated that there was at least a 400 million dollar loss in the Great Plains region alone.

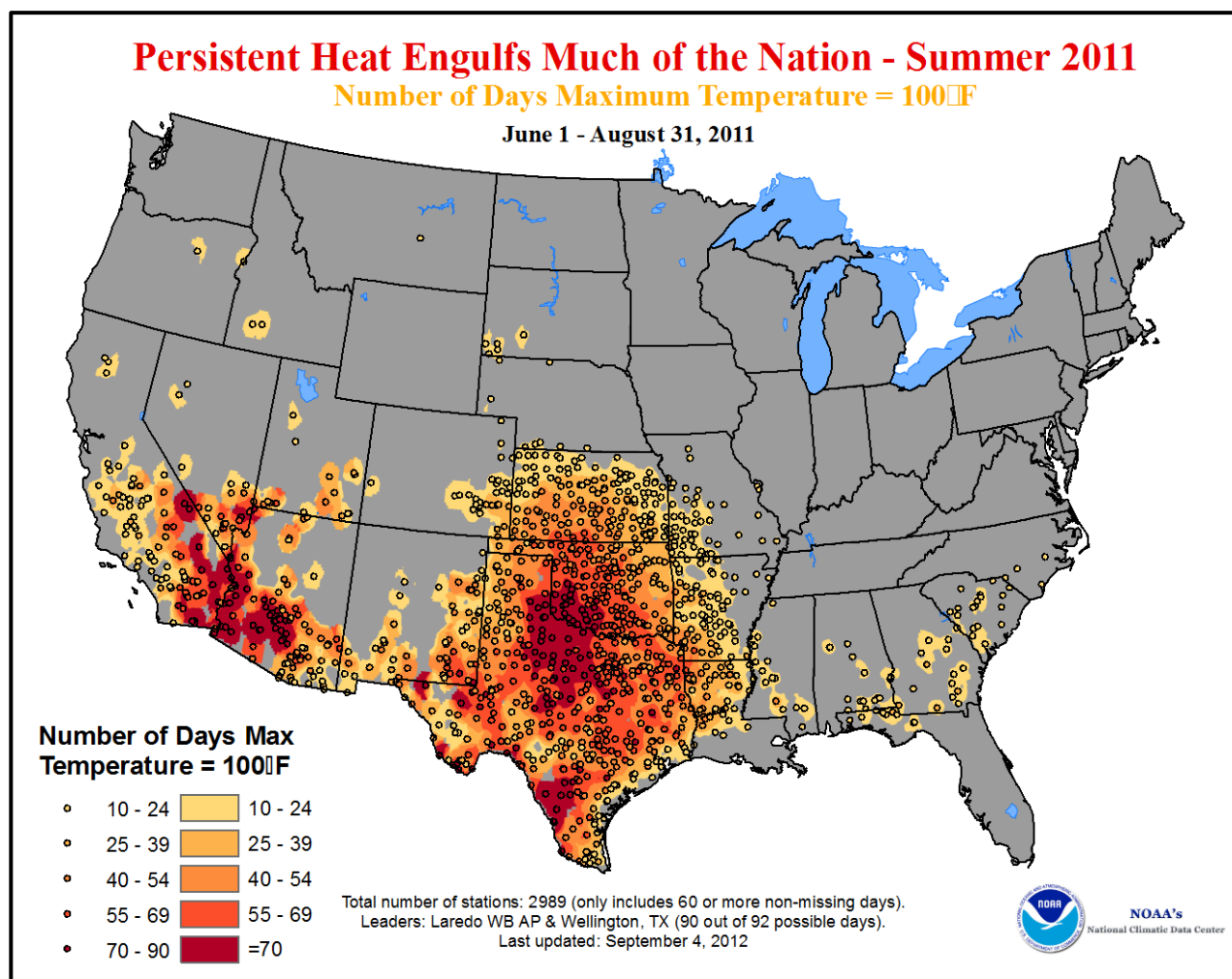


Figure 6. Number of days with maximum temperature exceeding 100°F in Summer 2011 across the contiguous U.S. (NOAA 2011c). Data from NOAA's National Climatic Data Center (NCDC).

2.3.7. Hurricane Climatology

With a gulf coastline of roughly 367 miles, Texas regularly experiences tropical storms and hurricanes. An extensive report on the climatology of hurricanes and tropical storms making landfall on the Texas coastline is found in Roth (2010). According to this report, the Texas coastline averages approximately 0.8 named storms per year, or about three storms every four years. This generally equates to about 0.4 tropical storms per year and 0.4 hurricanes per year. Roth (2010) also indicates that any given fifty mile coastal segment has an annual probability strike of approximately one storm per six years. Over the period of 1900 to 2010, these coastal areas have endured over 85 known tropical storms and hurricanes, the latter of which make up approximately half the events. The busiest decade occurred in the 1940s, when the coast was hit by eight hurricanes and six tropical storms. The most recent decade has also seen above average storm counts with a total of 10 named storms making landfall, five of which were hurricanes. Perhaps the most memorable tropical storm event was the Galveston Category Four hurricane that made landfall in September, 1900. This storm resulted in approximately eight thousand fatalities.

As in other regions, the major impacts of tropical cyclones along the coast can be attributed to storm surge, high winds, and flooding from heavy rainfall. According to Roth (2010), the tropical storm/hurricane rainfall record for Texas occurred in early August, 1978 at Bluff, Texas, with a storm total of 46 inches. Roth (2010) also lists eight other occurrences where storm rainfall totals were in excess of 30 inches. In addition to torrential rainfall, hurricanes have also resulted in devastating winds. In August 1970, wind speeds of 180 miles per hour were recorded at Aransas Pass (Roth 2010). There have also been nine instances where tropical cyclone wind speeds were recorded in excess of 131 miles per hour (lower limit wind speed for a Category Four Hurricane) (Roth 2010). Information on storm surges is not readily available; however, Roth (2010) notes that storm surges have reached heights of twenty feet, with several instances of measured surges at or above ten feet. A detailed description of gulf storm surges can also be found in Needham and Keim (2011).

The effects of hurricanes can extend well beyond the immediate coastal areas (Kruk et al. 2010). On occasion, the remnants of hurricanes will track northward and westward into the interior of the Great Plains. Such storms have caused heavy rainfall events from interior Texas to as far north as Nebraska (Fig. 7). Over much of Oklahoma and interior Texas, between 3 and 6% of all days with more than 2 inches of rain are caused by tropical cyclones (Knight and Davis 2009).

2.4. Climatic Trends

The temperature and precipitation data sets used to examine trends were obtained from NOAA's National Climatic Data Center (NCDC). The NCDC data is based on NWS Cooperative Observer Network (COOP) observations, as described in Section 2.1. Some analyses use daily observations for selected stations from the COOP network. Other analyses use a new national gridded monthly data set at a resolution of 5 x 5 km, for the time period of 1895-2011. This gridded data set is derived from bias-corrected monthly station data and is named the "Climate Division Database version 2 beta" (CDDv2) and is scheduled for public release in January 2013 (R. Vose, NCDC, personal communication, July 27, 2012).

The COOP data were processed using 1901-1960 as the reference period to calculate anomalies. In Section 3, this period is used for comparing net warming between model simulations and observations. There were two considerations in choosing this period for this purpose. Firstly, while some gradually-increasing anthropogenic forcing was present in the early and middle part of the 20th century, there is a pronounced acceleration of the forcing after 1960 (Meehl et al. 2003). Thus, there is an expectation that the effects of that forcing on surface climate conditions should accelerate after 1960. This year was therefore chosen as the ending year of the reference period. Secondly, in order to average out the natural fluctuations in climate as much as possible, it is desirable to use the longest practical reference period. Both observational and climate model data are generally available starting around the turn of the 20th century, thus motivating the use of 1901 as the beginning year of the reference period. We use this period as the reference for historical time series appearing in this section in order to be consistent with related figures in Section 3.

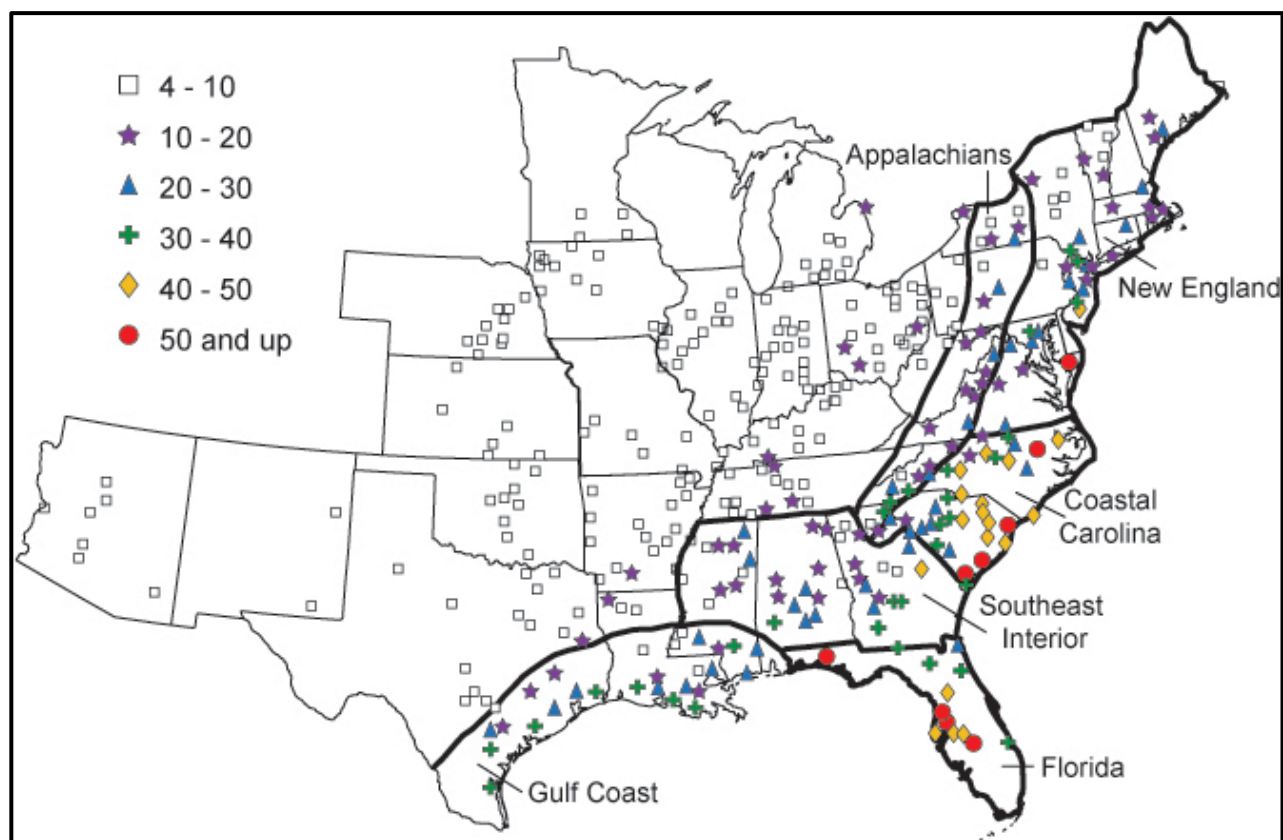


Figure 7. Percent of heavy events associated with tropical cyclones (TC) at individual stations (delineated by color and symbol type) and regional groupings (delineated by thick black lines). Only stations with at least 1 TC-associated event are plotted. Republished with permission of the American Geophysical Union, from Kunkel et al. (2010); permission conveyed through Copyright Clearance Center, Inc.

2.4.1. Temperature

Figure 8 shows annual and seasonal time series of temperature anomalies for the period of 1895-2011, for the northern and southern Great Plains. Temperatures for the Great Plains as a whole have generally been above the 1901-1960 average for the last 20 years, annually and for all seasons. Annually, all but 3 of the last 20 years have been above the 1901-1960 average. The warmest years on record were 1934 and 2006. The heat that occurred during the Dust Bowl era is very evident in the summer time series. The warmest summer on record was 1936, with the second warmest being a virtual tie between 1934 and 2011. Eight of the ten summers during the last decade (2002-2011) have been above the 1901-1960 average. Temperatures during the other seasons have also generally been above average. States in the northern portion of the Great Plains region have experienced the most change in their long-term average temperatures. For instance, North Dakota's annual average temperature increased 0.26°F per decade during the last 130 years, the fastest increase in the nation.

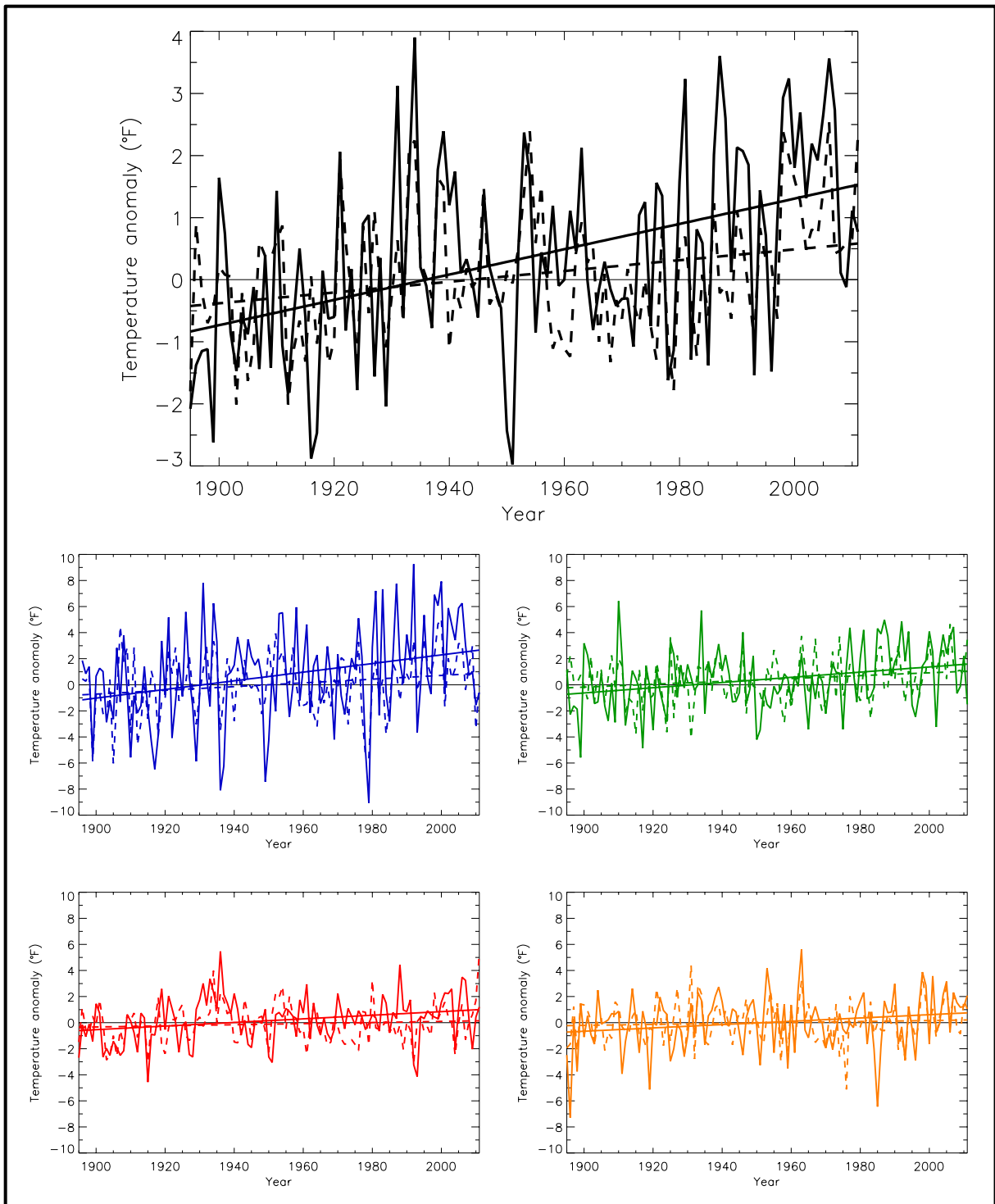


Figure 8. Temperature anomaly (deviations from the 1901-1960 average, °F) for annual (black), winter (blue), spring (green), summer (red), and fall (orange), for the northern (solid lines) and southern (dashed lines) U.S. Great Plains. Dashed lines indicate the best fit by minimizing the chi-square error statistic. Based on a new gridded version of COOP data from the National Climatic Data Center, the CDDv2 data set (R. Vose, personal communication, July 27, 2012). Note that the annual time series is on a unique scale. Trends are upward and statistically significant annually and for all seasons, except summer and fall for the southern Great Plains.

Table 1 shows temperature trends for the period of 1895-2011, calculated using the CDDv2 data set. Values are only displayed for trends that are statistically significant at the 95% confidence level. Temperature trends are statistically significant for all seasons for the northern Great Plains. For the southern Great Plains, values are not significant for both summer and fall. Warming is greater in the northern Great Plains than in the south.

Table 1. 1895-2011 trends in temperature anomaly (°F/decade) and precipitation anomaly (inches/decade) for the northern Great Plains (top) and southern Great Plains (bottom), for each season as well as the year as a whole. Based on a new gridded version of COOP data from the National Climatic Data Center, the CDDv2 data set (R. Vose, personal communication, July 27, 2012). Only values statistically significant at the 95% confidence level are displayed. Statistical significance of trends was assessed using Kendall's tau coefficient. The test using tau is a non-parametric hypothesis test.

Region	Season	Temperature (°F/decade)	Precipitation (inches/decade)
Northern Great Plains	Winter	+0.33	—
	Spring	+0.20	—
	Summer	+0.14	—
	Fall	+0.13	—
	Annual	+0.20	—
Southern Great Plains	Winter	+0.14	—
	Spring	+0.11	—
	Summer	—	—
	Fall	—	—
	Annual	+0.09	—

2.4.2. Precipitation

Figure 9 shows annual and seasonal time series of precipitation anomalies for the period of 1895-2011, for both the northern and southern Great Plains again, calculated using the CDDv2 data set. The variability of precipitation is greater in the southern Great Plains than in the north. Annual precipitation for the entire Great Plains region was greater than the 1901-1960 average during the 1990s, less than the average during the early 2000s, and greater than the average during the last few years, except for 2011. The early 1950s were the driest multi-year period, and included the single driest year on record, 1956. The 1930s were nearly as dry. The wettest single year on record was 1941. Summer precipitation anomalies are very similar to the annual behavior, except that the 1930s were the driest multi-year period. In fact, the driest summer on record is 1936 for Oklahoma, Kansas, Nebraska, South Dakota, and North Dakota. The flood year of 1993 was the second wettest summer on record, after 1915. The severe impacts of the 1930s in the Great Plains can be attributed mainly to the conditions during the summers, which were much more severe than during the multi-year dry period of the 1950s. For the region as a whole, 1934 and 1936 were the two hottest summers on record and the two driest summers on record. This combination of heat and dryness, along with the close temporal proximity of these two extreme summers, is unique in the record.

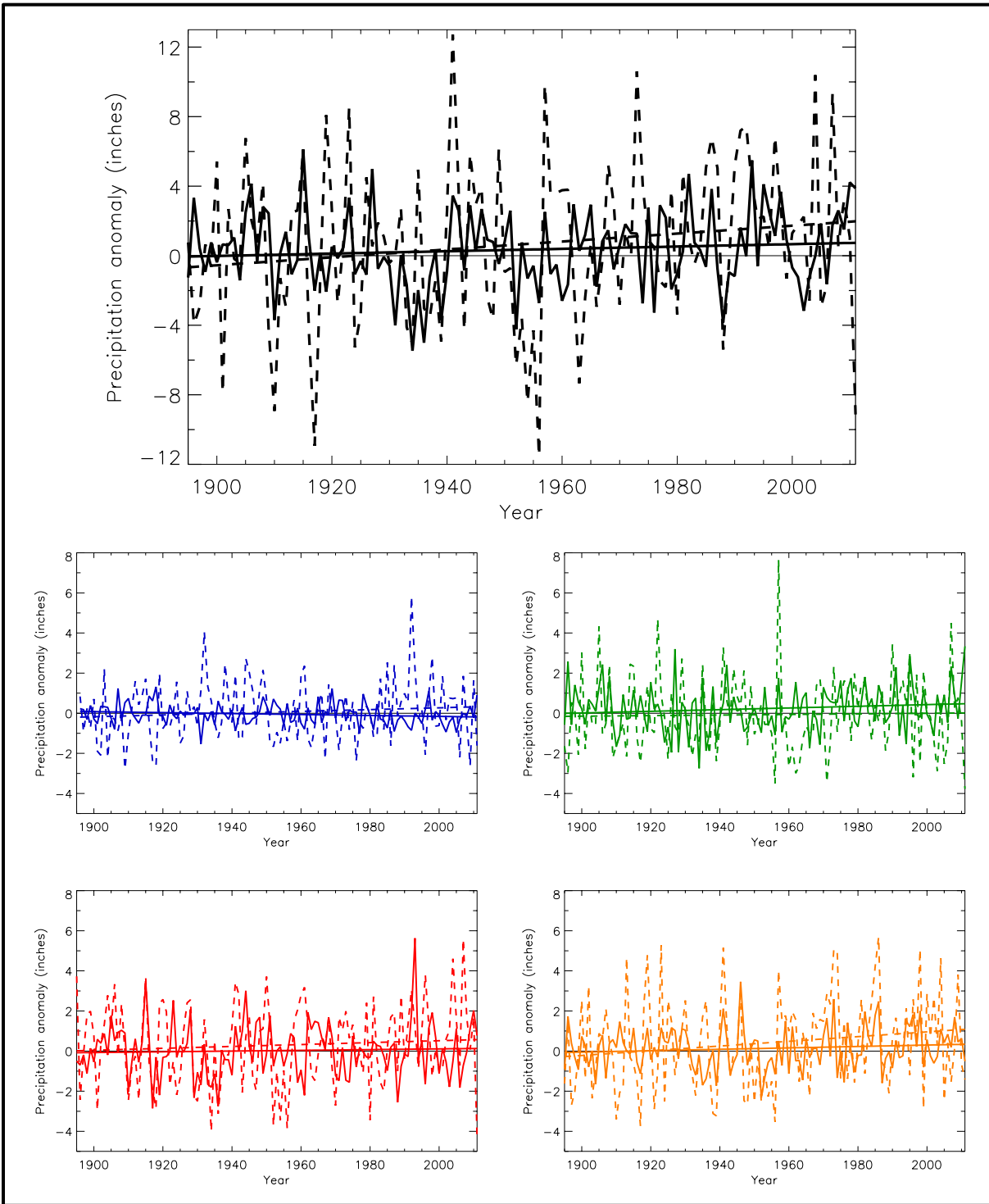


Figure 9. Precipitation anomaly (deviations from the 1901-1960 average, inches) for annual (black), winter (blue), spring (green), summer (red), and fall (orange), for the northern (solid lines) and southern (dashed lines) U.S. Great Plains. Dashed lines indicate the best fit by minimizing the chi-square error statistic. Based on a new gridded version of COOP data from the National Climatic Data Center, the CDDv2 data set (R. Vose, personal communication, July 27, 2012). Note that the annual time series is on a unique scale. Trends are not statistically significant for any season.

Trends in precipitation for the period of 1895-2011 can be seen in Table 1. Trends in precipitation are not statistically significant for any season. The nominal annual upward trends seen in Fig. 9 are not statistically significant.

See <http://charts.srcc.lsu.edu/trends/> (LSU 2012) for a comparative seasonal or annual climate trend analysis of a specified state from the Great Plains region, using National Climate Data Center (NCDC) monthly and annual temperature and precipitation datasets.

2.4.3. Extreme Heat and Cold

Large spatial variations in the temperature climatology of this region result in analogous spatial variations in the definition of “extreme temperature”. We define here extremes as relative to a location’s overall temperature climatology, in terms of local frequency of occurrence.

Figure 10 shows time series of an index intended to represent heat and cold wave events. This index specifically reflects the number of 4-day duration episodes with extreme hot and cold temperatures, exceeding a threshold for a 1 in 5-year recurrence interval, calculated using daily COOP data from long-term stations. Extreme events are first identified for each individual climate observing station. Then, annual values of the index are gridding the station values and averaging the grid box values.

There is a large amount of interannual variability in extreme cold periods and extreme hot periods, reflecting the fact that, when they occur, such events affect large areas and thus large numbers of stations in the region simultaneously experience an extreme event exceeding the 1 in 5-year threshold.

The occurrence of heat waves, as illustrated by the heat wave index time series shown in Fig. 10, is dominated by the severe heat of the 1930s (during this decade, the index averaged more than 4 times the long-term mean value). The highest number of heat waves, by far, occurred in 1934 and 1936. Since the 1930s, the two years with the highest number of heat waves were 1954 and 2011. There is no overall trend in the occurrence of heat waves.

The frequency of extreme cold periods has been generally low since 1990 (averaging about 65% below the long-term mean), with the exception of 1996 when a severe cold wave in early February affected large areas. Other recent years with widespread severe cold included 1983 and 1989. The 1950s were a period of few severe cold waves (averaging about 60% below the long-term mean). A separate analysis of the northern and southern parts of the region indicates that the recent tendency toward fewer cold waves is more prominent in the north than in the south.

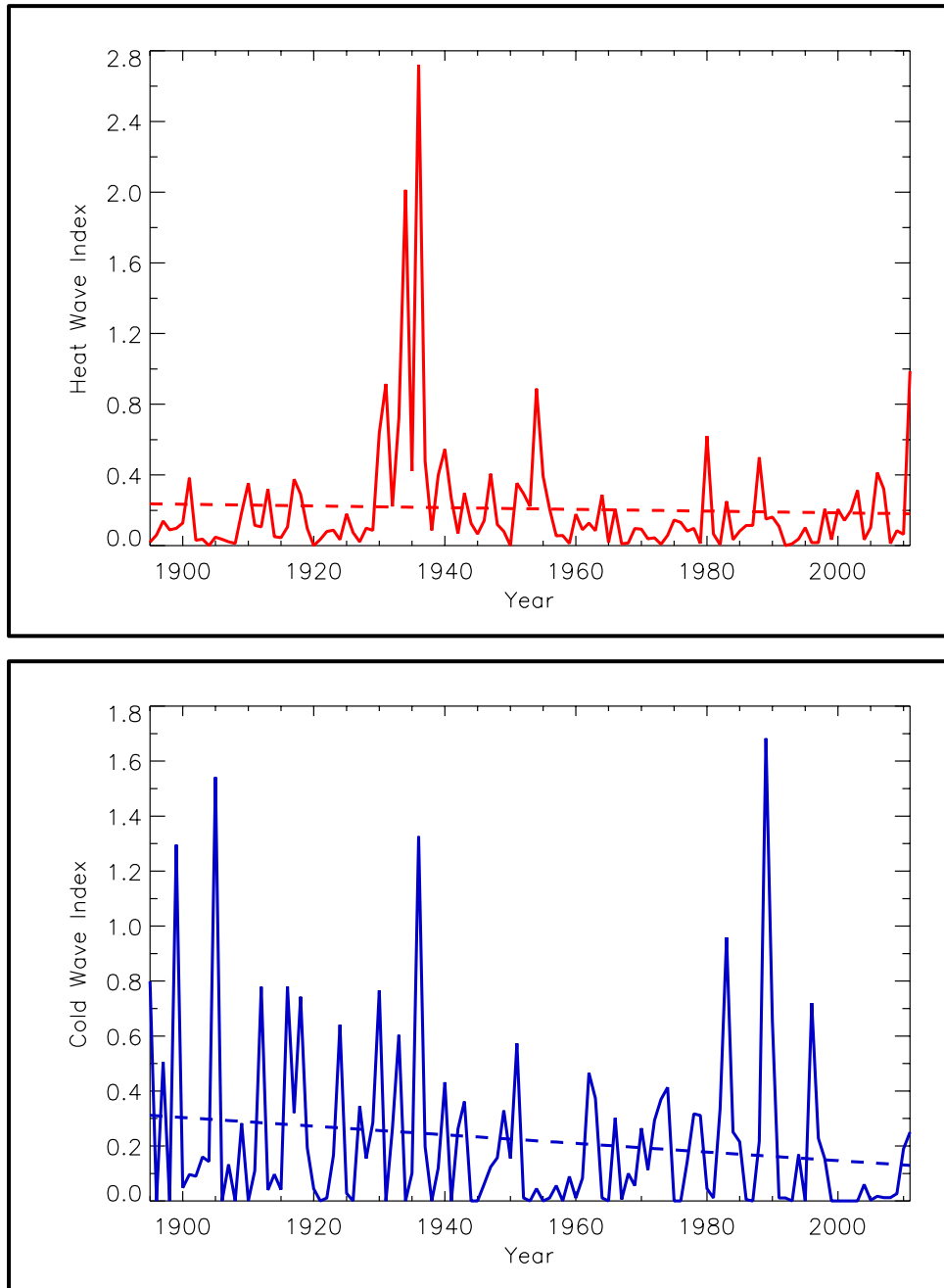


Figure 10. Time series of an index for the occurrence of heat waves (top) and cold waves (bottom), defined as 4-day periods that are hotter and colder, respectively, than the threshold for a 1 in 5-year recurrence, for the Great Plains region. The dashed line is a linear fit. Based on daily COOP data from long-term stations in the National Climatic Data Center's Global Historical Climate Network data set. Only stations with less than 10% missing daily temperature data for the period 1895-2011 are used in this analysis. Events are first identified for each individual station by ranking all 4-day period mean temperature values and choosing the highest (heat waves) and lowest (cold waves) non-overlapping $N/5$ events, where N is the number of years of data for that particular station. Then, event numbers for each year are averaged for all stations in each $1 \times 1^\circ$ grid box. Finally, a regional average is determined by averaging the values for the individual grid boxes. This regional average is the index. The most intense heat waves occurred in the 1930s, although there is no overall trend. There is also no statistically significant trend in cold wave events, however, the number of intense cold wave events has been very low during the last 15 years.

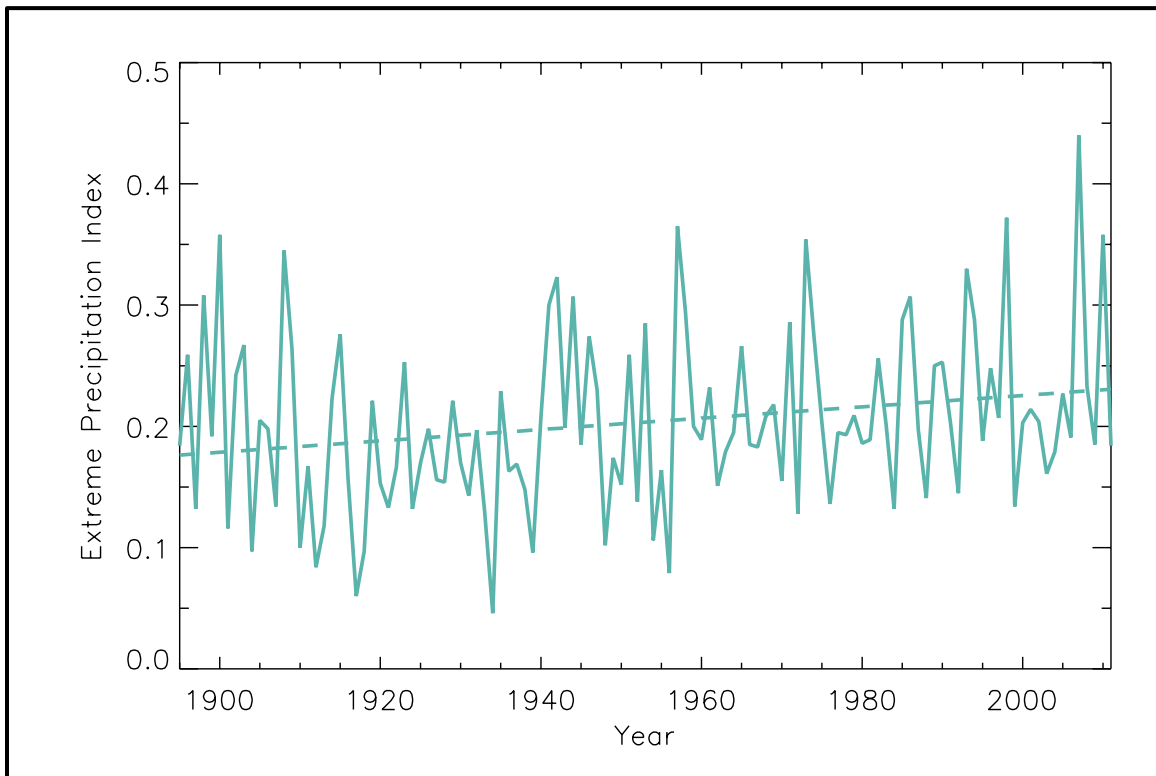


Figure 11. Time series of extreme precipitation index for the occurrence of 1-day, 1 in 5-year extreme precipitation, for the Great Plains region. The dashed line is a linear fit. Based on daily COOP data from long-term stations in the National Climatic Data Center’s Global Historical Climate Network data set. Only stations with less than 10% missing daily precipitation data for the period 1895-2011 are used in this analysis. Events are first identified for each individual station by ranking all daily precipitation values and choosing the top $N/5$ events, where N is the number of years of data for that particular station. Then, event numbers for each year are averaged for all stations in each $1 \times 1^\circ$ grid box. Finally, a regional average is determined by averaging the values for the individual grid boxes. This regional average is the extreme precipitation index. The overall trend is upward and statistically significant.

2.4.1. Extreme Precipitation

There are many different metrics that have been used in research studies to examine temporal changes in extreme precipitation. Here, we define the threshold for an extreme event based on a recurrence interval. This type of definition is commonly used for design applications, for example, in the design of runoff control structures. The analysis was performed using daily COOP data from long-term stations for a range of recurrence intervals, from one to twenty years. The results were not very sensitive to the exact choice. Results are presented for the five-year threshold, as an intermediate value. The duration of the extreme event is another choice for a metric. A range of durations was analyzed, from one to ten days, but the results were also not very sensitive to the choice. Results are presented (Fig. 11) for 1-day duration events, which is the shortest duration possible because of the daily time resolution of the COOP data.

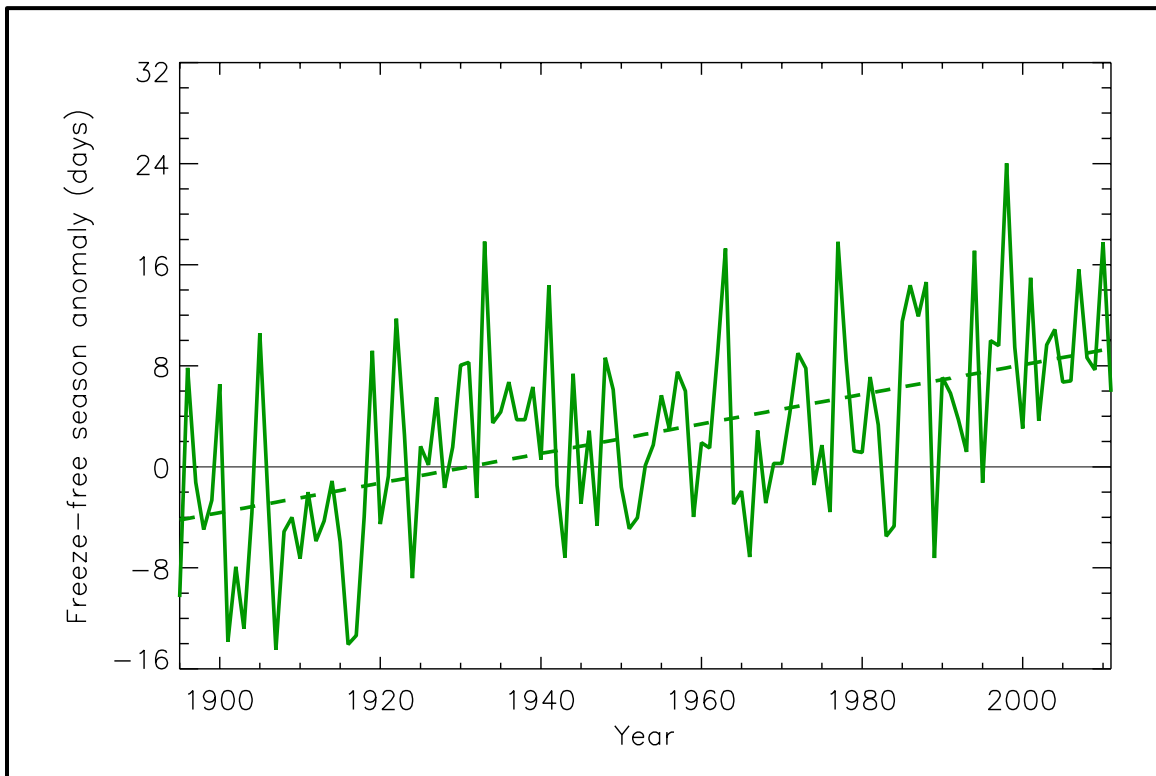


Figure 12. Time series of freeze-free season anomalies shown as the number of days per year, for the Great Plains region. Length of the freeze-free season is defined as the period between the last occurrence of 32°F in the spring and first occurrence of 32°F in the fall. The dashed line is a linear fit. Based on daily COOP data from long-term stations in the National Climatic Data Center's Global Historical Climate Network data set. Only stations with less than 10% missing daily temperature data for the period 1895-2010 are used in this analysis. Freeze events are first identified for each individual station. Then, event dates for each year are averaged for 1x1° grid boxes. Finally, a regional average is determined by averaging the values for the individual grid boxes. There is an overall statistically significant upward trend.

Despite the substantial interannual and decadal-scale variability in the number of extreme precipitation events, there is an upward trend, which is statistically significant at the 95% confidence level. Since 1990, there have been a number of years with a high number of extreme events. The highest value overall for 1-day events occurred in 2007. The 1940s were characterized by a high number of extreme events that followed a period of low values in the 1930s. The high number of extreme events in the early part of the record is primarily a feature of the northern part of the region.

2.4.2. Freeze-Free Season

Figure 12 shows a time series of freeze-free season length, calculated using daily COOP data from long-term stations. Freeze-free season length has been generally increasing since the early 20th century, with the trend over the entire time period (1895-2011) being statistically significant. The last occurrence of 32°F in the spring has been occurring earlier and the first occurrence of 32°F in the fall has been happening later. The longest freeze-free season occurred in 1998. The average freeze-free season length during 1991-2010 was about 6 days longer than during 1961-1990. Shifts

in planting dates have occurred as well. A preliminary study by Pathak et al. (2012), using data from the High Plains Regional Climate Center's Automated Weather Data Network (AWDN), shows a one to three week shift in the dates when soil temperature reaches 55°F across Nebraska when the recent decade (2000-2009) is compared to the previous decade (1990-1999). Trends for when the soil temperature reaches 50°F, 60°F, 65°F, and 70°F are similar. These trends in the last two decades show a potential for shifting agricultural planting to earlier dates in Nebraska.

2.4.3. Atlantic Tropical Storm Trends

A primary concern among scientists pertains to the quality of the historical record. Many studies argue that the quality of the tropical cyclone data for the north Atlantic basin is insufficient for the determination of trends in storm counts (Landsea et al. 2006). Goldenberg et al. (2001) state that this data prior to 1944, which precedes aircraft reconnaissance, is not considered reliable and caution should be exercised with its usage in research analyses. The issue of data quality is also considered by Owens and Landsea (2003), citing 1944 as the start of complete and reliable data for the North Atlantic region. By contrast, other studies indicate that these issues of data quality are not substantial enough to preclude trend analyses (Emanuel 2005; Webster et al. 2005; Hoyos et al. 2006; Holland and Webster 2007; Elsner et al. 2008).

Data quality issues aside, many studies have addressed the issues of trends in tropical cyclone activity in the North Atlantic Basin, and how climate change may impact the frequency and intensity of tropical cyclones. Holland and Webster (Holland and Webster 2007) examine tropical storm and hurricane frequency for the North Atlantic Ocean over the past century. Their study identifies three distinct regimes (1905-1930; 1931-1994; 1995-2005). Their findings illustrate a marked increase of approximately fifty percent in each regime over time. Their observed increase in tropical cyclone frequency is commensurate with observed increases in Atlantic sea surface temperatures. Holland and Webster (2007) conclude that observed increases are the combined result of both natural variability and anthropogenic-induced greenhouse warming. Emanuel (2005), Mann and Emanuel (2006), and Webster et al. (2005) also conclude that increases in Atlantic tropical cyclone activity are likely being driven by greenhouse-induced warming. Goldenberg et al. (2001), on the other hand, maintain that natural variability in the Atlantic Multidecadal Oscillation (AMO) may be the primary driver behind the observed increasing trends.

Landsea (2007) asserts that when data are adjusted for missing storms, a significant trend is not evident. These findings are also consistent with other studies which claim that observed increases in storm activity over the past century are not entirely obvious, despite the observed increases in Atlantic sea surface temperatures (e.g., Elsner et al. 2008; Vecchi and Knutson 2008; Knutson et al. 2010). In a study by Elsner et al. (2008), results indicate an increasing trend in the intensity of strong tropical cyclones. Their study examines trends in lifetime-maximum wind speeds and notes an upward trend over time for the North Atlantic, owing to increases in oceanic energy resulting from increases in Atlantic sea surface temperatures.

A recent assessment of the state of knowledge about trends in hurricanes (Kunkel et al. 2012) concluded that attribution of trends to anthropogenic forcing remains controversial due to data heterogeneity, deficient quantification of internal variability, and lack of scientific consensus about physical linkages between climate forcing and tropical cyclone activity.

Many studies have examined the future of Atlantic tropical cyclone activity. Though a bulk of these studies conclude that global warming will more than likely result in an increase in the frequency and intensity of events (e.g., IPCC 2007a), a debate remains as to how the climatology of tropical storms will ultimately be affected. Knutson et al. (2010) caution that it is not entirely clear whether the variability of tropical cyclone activity has exceeded that which is expected by natural causes. The authors note that modeling studies suggest a shift toward stronger storms, with decreases in global-scale frequency on the order of six to thirty-four percent. Bengtsson et al. (2007) examine tropical cyclones in the northern hemisphere using the Max Planck Institute coupled ECHAM5/MPI-OM and atmosphere (ECHAM5) models. Their results indicate a reduction in storm numbers between the nineteenth and twentieth centuries, with no significant change in the number of intense storms. When focusing on the twenty-first century, Bengtsson et al. (2007) find that tropical cyclone counts decrease by approximately ten percent, whereas the frequency of intense storms increase by approximately one third. Reductions in storm count may be the result of the combined effect of a reduction in vertical circulation and an increase in static stability. A study by Vecchi and Soden (2007) examines eighteen of the models used for the 2007 IPCC climate report. Their findings demonstrate that for the twenty-first century, there is a modeled increase in vertical wind shear over the critical tropical storm season months of June to November. These findings are based on the typical A1B scenario (doubling of carbon dioxide to 720ppm by 2100). The authors note that modeled increases in vertical wind shear should be considered in projections of future cyclone activity. Increases in wind shear support a reduction in the number of tropical cyclone events. However, it is difficult how to assess how this may impact storm intensity.

2.4.4. Sea Level Rise

Changes in sea level can result from either a rise in oceanic water level, land subsidence, or a combined effect of these two variables. It is therefore a very difficult process to study and model. Kolker et al. (2011) note that the primary driver of subsidence in the Gulf of Mexico may be subsurface fluid withdrawal. Unfortunately, research which focuses on subsidence in Texas is not well documented. Additionally, fewer studies exist which examine the combined effect of subsidence and sea-level changes. One study by Penland and Ramsey (1990) examines sea-level rises in the Gulf of Mexico for the period of 1908 to 1988. Their results show that the highest observed sea level rises over their study period are observed along the Louisiana coastline. They note that Galveston, Texas, is experiencing an average sea-level rise of approximately 0.63 cm per year, which is slightly lower than the Louisiana rate of 1.04 cm per year. According to Church and White (2006), global sea-level rise has averaged approximately 1.7 mm per year over the past century. According to Donoghue (2011) and NOAA (2010), sea-level rises along the Texas coast have ranged from as low as 1.93 mm per year (1963-2010), to as high as 6.39 mm per year at Galveston Pier. Port Isabel, Texas, and Padre Island, Texas, have averaged approximately 3.64 and 3.84 mm per year of sea level rise, respectively (Donoghue 2011). The study of Donoghue (2011) notes that changes in sea level within the northern Gulf of Mexico have reflected that which has been observed globally.

3. FUTURE REGIONAL CLIMATE SCENARIOS

As noted above, the physical climate framework for the 2013 NCA report is based on climate model simulations of the future using the high (A2) and low (B1) SRES emissions scenarios. The resulting climate conditions are to be viewed as scenarios, not forecasts, and there are no explicit or implicit assumptions about the probability of occurrence of either scenario.

3.1. Description of Data Sources

This summary of future regional climate scenarios is based on the following model data sets:

- **Coupled Model Intercomparison Project phase 3 (CMIP3)** – Fifteen coupled Atmosphere-Ocean General Circulation Models (AOGCMs) from the World Climate Research Programme (WCRP) CMIP3 multi-model dataset (PCMDI 2012), as identified in the 2009 NCA report (Karl et al. 2009), were used (see Table 2). The spatial resolution of the great majority of these model simulations was 2-3° (a grid point spacing of approximately 100-200 miles), with a few slightly greater or smaller. All model data were re-gridded to a common resolution before processing (see below). The simulations from all of these models include:
 - a) Simulations of the 20th century using best estimates of the temporal variations in external forcing factors (such as greenhouse gas concentrations, solar output, volcanic aerosol concentrations); and
 - b) Simulations of the 21st century assuming changing greenhouse gas concentrations following both the A2 and B1 emissions scenarios. One of the fifteen models did not have a B1 simulation.

These model simulations also serve as the basis for the following downscaled data set.

- **Downscaled CMIP3 (Daily_CMIP3)** – These temperature and precipitation data are at 1/8° (~8.6 miles latitude and ~6.0-7.5 miles longitude) resolution. The CMIP3 model data were initially downscaled on a monthly timescale using the bias-corrected spatial disaggregation (BCSD) method, for the period of 1961-2100. The starting point for this downscaling was an observationally-based gridded data set produced by Maurer et al. (2002). The climate model output was adjusted for biases through a comparison between this observational gridded data set and the model's simulation of the 20th century. Then, high-resolution gridded data for the future were obtained by applying change factors calculated as the difference between the model's present and future simulations (the so-called "delta" method).

Daily statistically-downscaled data were then created by randomly sampling historical months and adjusting the values using the "delta" method (Hayhoe et al. 2004; 2008). Eight models with complete data for 1961-2100 were available and used in the Daily_CMIP3 analyses (Table 2).

- **North American Regional Climate Change Assessment Program (NARCCAP)** – This multi-institutional program is producing regional climate model (RCM) simulations in a coordinated experimental approach (NARCCAP 2012). At the time that this data analysis was initiated, simulations were available for 9 different combinations of an RCM driven by a general circulation model (GCM); during the development of these documents, two additional simulations became available and were incorporated into selected products. These 11 combinations involved four different GCMs and six different RCMs (see Table 3). The mean temperature and precipitation maps include all 11 combinations. For calculations and graphics

involving the distribution of NARCCAP models, analyses of only the original 9 model combinations were used. For graphics of the number of days exceeding thresholds and the number of degree days, the values were obtained from the Northeast Regional Climate Center, where only 8 of the model combinations were analyzed.

Each GCM-RCM combination performed simulations for the periods of 1971-2000, 1979-2004 and 2041-2070 for the high (A2) emissions scenario only. These simulations are at a resolution of approximately 50 km (~30 miles), covering much of North America and adjacent ocean areas. The simulations for 1971-2000 and 2041-2070 are “driven” (time-dependent conditions on the lateral boundaries of the domain of the RCM are provided) by global climate model simulations. The 1979-2004 simulations are driven by the NCEP/DOE Reanalysis II data set, which is an estimate of the actual time-dependent state of the atmosphere using a model that incorporates observations; thus the resulting simulations are the RCM’s representation of historical observations. From this 1979-2004 simulation, the interval of 1980-2000 was selected for analysis.

Table 2. Listing of the 15 models used for the CMIP3 simulations (left column). The 8 models used in the daily statistically-downscaled (Daily_CMIP3) analyses are indicated (right column).

CMIP3 Models	Daily_CMIP3
CCSM3	X
CGCM3.1 (T47)	X
CNRM-CM3	
CSIRO-Mk3.0	
ECHAM5/MPI-OM	X
ECHO-G	X
GFDL-CM2.0	
GFDL-CM2.1	
INM-CM3.0	
IPSL-CM4	X
MIROC3.2 (medres)	X
MRI-CGCM2.3.2	X
PCM	X
UKMO-HadCM3	
UKMO-HadGEM1 ²	

² Simulations from this model are for the A2 scenario only.

Table 3. Combinations of the 4 GCMs and 6 RCMs that make up the 11 NARCCAP dynamically-downscaled model simulations.

		GCMs			
		CCSM3	CGCM3.1	GFDL-CM2.1	UKMO-HadCM3
RCMs	CRCM	X	X		
	ECPC			X ³	
	HRM3			X ⁴	X
	MM5I	X			X ³
	RCM3		X	X	
	WRFG	X	X		

3.2. Analyses

Analyses are provided for the periods of 2021-2050, 2041-2070, and 2070-2099, with changes calculated with respect to an historical climate reference period (either 1971-1999, 1971-2000, or 1980-2000). These future periods will sometimes be denoted in the text by their midpoints of 2035, 2055, and 2085, respectively.

As noted above, three different intervals were used as the reference period for the historical climatology. Although a uniform reference period would be ideal, there were variations in data availability and in the needs of the author teams. For the NARCCAP maps of mean temperature and precipitation, the 1971-2000 period was used as the reference because that represents the full historical simulation period. The 1971-1999 period (rather than 1971-2000) was used as the reference for CMIP3 maps because some of the CMIP3 models' 20th century simulations ended in 1999, but we wanted to keep the same starting date of 1971 for both CMIP3 and NARCCAP mean temperature and precipitation maps. The 1980-2000 period was used as the historical reference for some of the NARCCAP maps (days over thresholds and degree days) because this is the analyzed period of the reanalysis-driven simulation, and we were requested to provide maps of the actual values of these variables for both the historical period and the future period, and not just a difference map. A U.S.-wide climatology based on actual observations was not readily available for all of these variables, and we chose to use the reanalysis-driven model simulation as an alternative. Since the reanalysis data set approximates observations, the reanalysis-driven RCM simulation will be free from biases arising from a driving GCM. To produce the future climatology map of actual values, we added the (future minus historical) differences to the 1980-2000 map values. For consistency then, the differences between future and present were calculated using the 1980-2000 subset of the 1971-2000 GCM-driven simulation.

Three different types of analyses are represented, described as follows:

³ Data from this model combination were not used for simulations of the number of days exceeding thresholds or degree days.

⁴ Data from these model combinations were not used for simulations of the number of days exceeding thresholds or degree days, or calculations and graphics involving the distribution of NARCCAP models.

- **Multi-model mean maps** – Model simulations of future climate conditions typically exhibit considerable model-to-model variability. In most cases, the future climate scenario information is presented as multi-model mean maps. To produce these, each model’s data is first re-gridded to a common grid of approximately 2.8° latitude (~190 miles) by 2.8° longitude (~130-170 miles). Then, each grid point value is calculated as the mean of all available model values at that grid point. Finally, the mean grid point values are mapped. This type of analysis weights all models equally. Although an equal weighting does not incorporate known differences among models in their fidelity in reproducing various climatic conditions, a number of research studies have found that the multi-model mean with equal weighting is superior to any single model in reproducing the present-day climate (Overland et al. 2011). In most cases, the multi-model mean maps include information about the variability of the model simulations. In addition, there are several graphs that show the variability of individual model results. These should be examined to gain an awareness of the magnitude of the uncertainties in each scenario’s future values.
- **Spatially-averaged products** – To produce these, all the grid point values within the Great Plains region boundaries are averaged and represented as a single value. This is useful for general comparisons of different models, periods, and data sources. Because of the spatial aggregation, this product may not be suitable for many types of impacts analyses.
- **Probability density functions (pdfs)** – These are used here to illustrate the differences among models. To produce these, spatially-averaged values are calculated for each model simulation. Then, the distribution of these spatially-averaged values is displayed. This product provides an estimate of the uncertainty of future changes in a tabular form. As noted above, this information should be used as a complement to the multi-model mean maps.

3.3. Mean Temperature

Figure 13 shows the spatial distribution of multi-model mean simulated differences in average annual temperature for the three future time periods (2035, 2055, 2085) relative to the model reference period of 1971-1999, for both emissions scenarios, for the 14 (B1) or 15 (A2) CMIP3 models. The statistical significance regarding the change in temperature between each future time period and the model reference period was determined using a 2-sample *t*-test assuming unequal variances for those two samples. For each period (present and future climate), the mean and standard deviation were calculated using the 29 or 30 annual values. These were then used to calculate *t*. In order to assess the agreement between models, the following three categories were determined for each grid point, similar to that described in Tebaldi et al. (2011):

- *Category 1*: If less than 50% of the models indicate a statistically significant change then the multi-model mean is shown in color. Model results are in general agreement that simulated changes are within historical variations;
- *Category 2*: If more than 50% of the models indicate a statistically significant change, and less than 67% of the significant models agree on the sign of the change, then the grid points are masked out, indicating that the models are in disagreement about the direction of change;
- *Category 3*: If more than 50% of the models indicate a statistically significant change, and more than 67% of the significant models agree on the sign of the change, then the multi-model mean is shown in color with hatching. Model results are in agreement that simulated changes are statistically significant and in a particular direction.

It can be seen from Fig. 13 that spatial variations in simulated temperature changes are quite small, especially for the low (B1) emissions scenario. This is consistent with global analyses that show relatively gradual spatial changes on a global scale (Meehl et al. 2007), a probable consequence of the generally high instantaneous spatial coherence of temperature and the smoothing effect of multi-model averaging. As also seen in the climatology, warming tends to be slightly larger in the north, especially in the Dakotas. The increase in temperature seen over the past 20 years is simulated to continue, and the differences between the A2 and B1 scenarios are also simulated to increase over time. For 2035, both A2 and B1, values range between 1.5 and 3.5°F. For 2055, warming in B1 ranges between 2.5 and 4.5°F and for A2, ranges from 3.5 to 6.5°F. By 2085, the temperature increases are in the 3.5-6.5°F range for B1 and 5.5-9.5°F range for A2. Simulated temperature increases in 2085 are slightly larger than those in 2055 for the low emissions scenario (2.5-5.5°F), but are much larger for A2 at 5.5-8.5°F. The CMIP3 models indicate that temperature changes across the U.S. Great Plains, for all three future time periods and both emissions scenarios, are statistically significant. The models also agree on the sign of change, with all grid points satisfying category 3 above, i.e. the models are in agreement on temperature increases throughout the region for each future time period and scenario.

Figure 14 shows the multi-model mean simulated annual and seasonal 30-year average temperature change between 2041-2070 and 1971-2000 for the high (A2) emissions scenario, for 11 NARCCAP regional climate model simulations. The annual changes are simulated to be quite uniform and generally in the range of 4-5°F, except for coastal Texas where the warming is smaller. The seasonal changes show more spatial variability. Winter differences range from 3 to 6.5°F, and the greatest warming occurs near the Canadian border. Springtime warming is generally smaller than the winter season, ranging from 2.5 to 4.5°F, with the largest increases simulated in southwest Texas. Summer shows a large amount of warming, ranging from 3.5 to 6.5°F, with a localized maximum in southwest Kansas. Warming in the fall ranges between 3.5 and 5.5°F, with the greatest temperature increases occurring in the central portion of the region. The agreement between models was again assessed using the three categories described in Fig. 13. The models agree on the sign of change, with all grid points satisfying category 3, annually, and for all seasons.

Figure 15 shows the simulated change in annual mean temperature for each future time period with respect to 1971-1999, for both emissions scenarios, averaged over the entire Great Plains region for the 14 (B1) or 15 (A2) CMIP3 models. In addition, averages for 9 of the NARCCAP simulations and the 4 GCMs used in the NARCCAP experiment are shown for 2055 (A2 scenario only) with respect to 1971-2000. Both the multi-model mean and individual model values are shown. For the high (A2) emissions scenario, the CMIP3 models simulate average temperature increases of 2.9°F by 2035, 4.7°F by 2055, and nearly 8°F by 2085. The increases for the low (B1) emissions scenario are nearly as large in 2035 at around 2.6°F, but by 2085 the increase of 4.6°F is over 3°F smaller than in the A2 scenario. For 2055, the average temperature change simulated by the NARCCAP models is 0.4°F less than the mean of the CMIP3 GCMs for the A2 scenario.

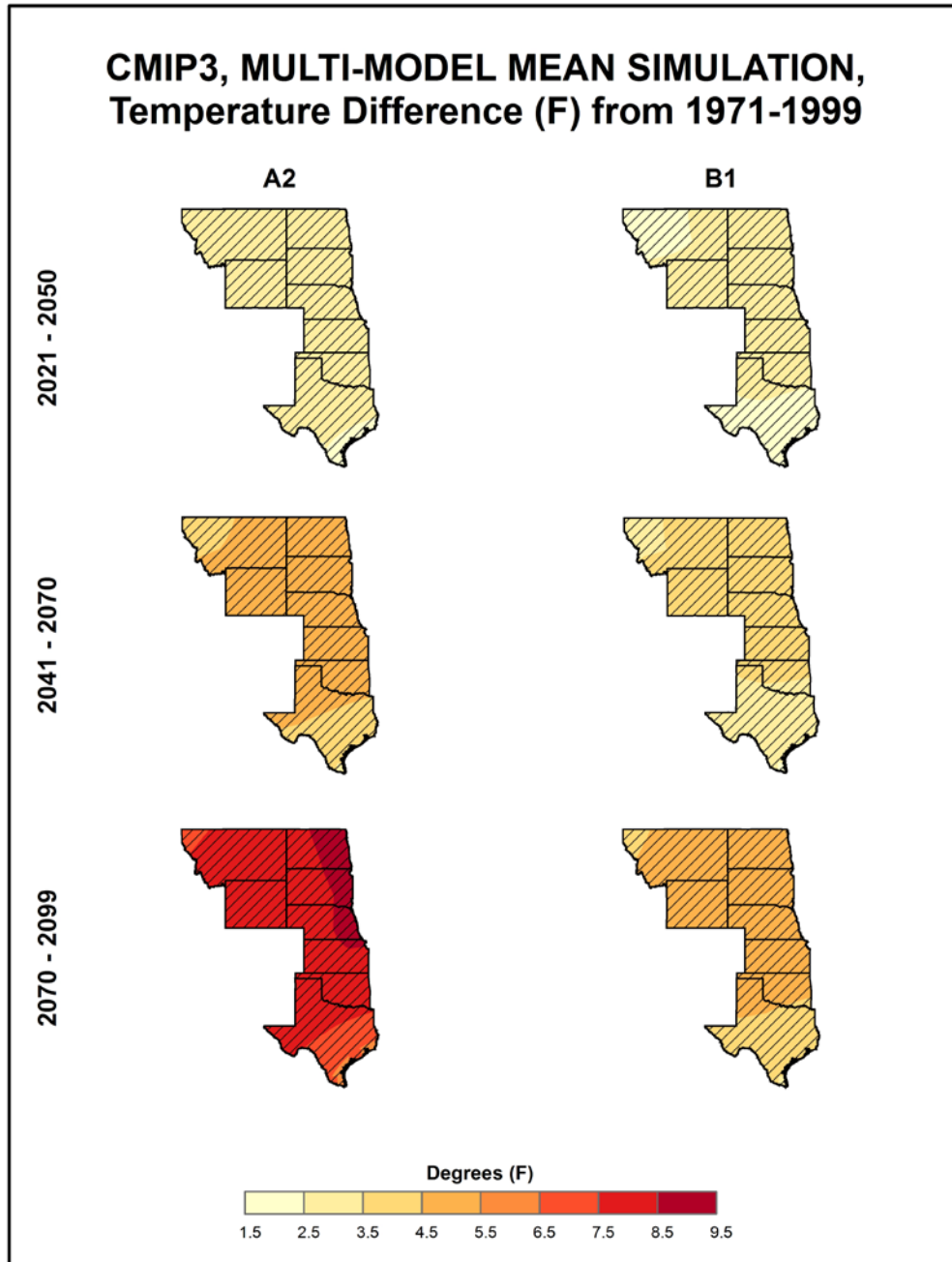


Figure 13. Simulated difference in annual mean temperature ($^{\circ}\text{F}$) for the Great Plains region, for each future time period (2021-2050, 2041-2070, and 2070-2099) with respect to the reference period of 1971-1999. These are multi-model means for the high (A2) and low (B1) emissions scenarios from the 14 (B1) or 15 (A2) CMIP3 global climate simulations. Color with hatching (category 3) indicates that more than 50% of the models show a statistically significant change in temperature, and more than 67% agree on the sign of the change (see text). Temperature changes increase throughout the 21st century, more rapidly for the high emissions scenario.

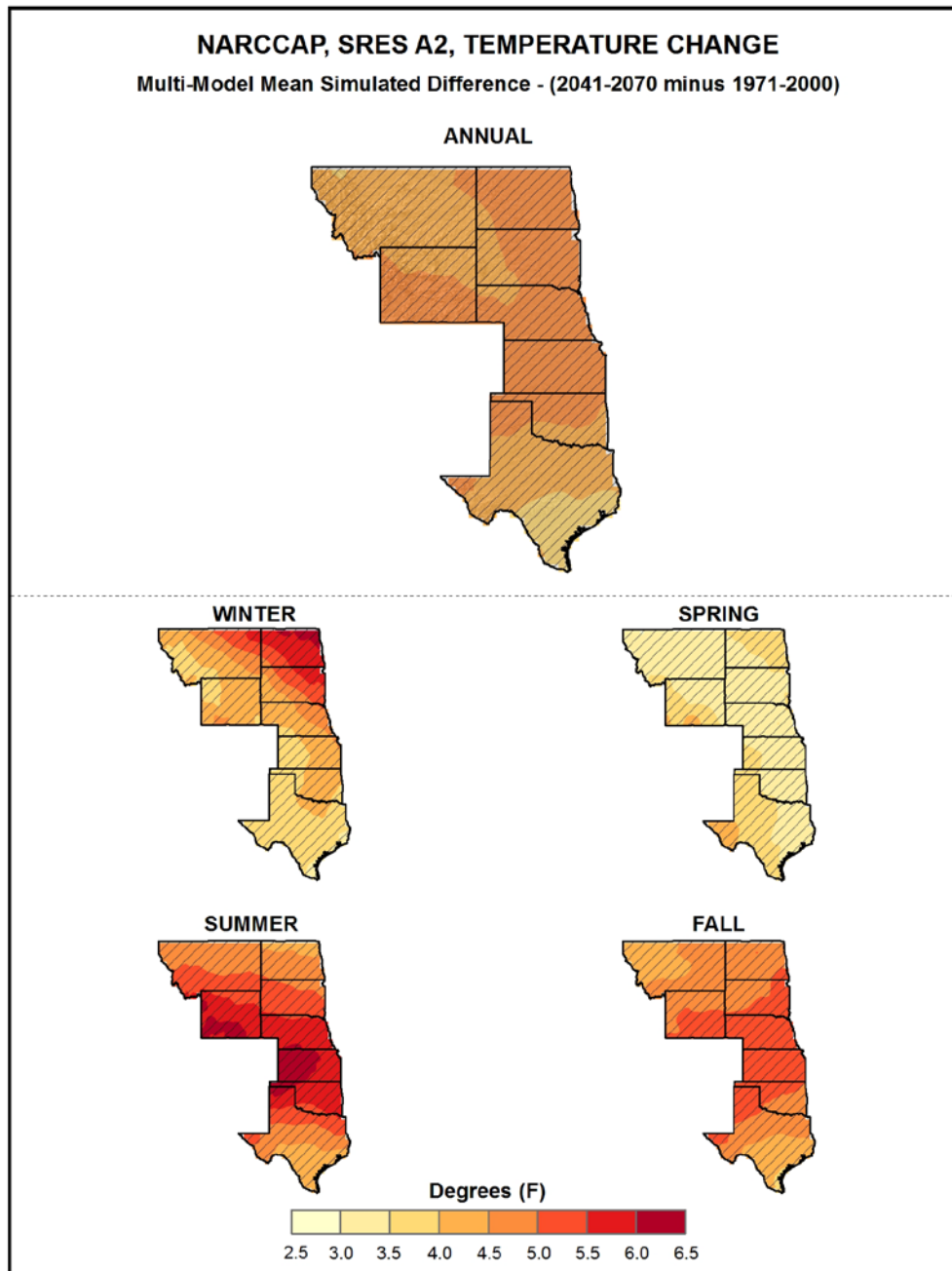


Figure 14. Simulated difference in annual and seasonal mean temperature ($^{\circ}\text{F}$) for the Great Plains region, for 2041-2070 with respect to the reference period of 1971-2000. These are multi-model means from 11 NARCCAP regional climate simulations for the high (A2) emissions scenario. Color with hatching (category 3) indicates that more than 50% of the models show a statistically significant change in temperature, and more than 67% agree on the sign of the change (see text). Note that the color scale is different from that of Fig. 13. Temperature changes for the NARCCAP simulations are similar to those for the CMIP3 global models (Fig. 13, middle left panel). Seasonal changes are of greatest magnitude in summer, and least in spring, and are in Category 3 (statistically significant for most models) throughout the region.

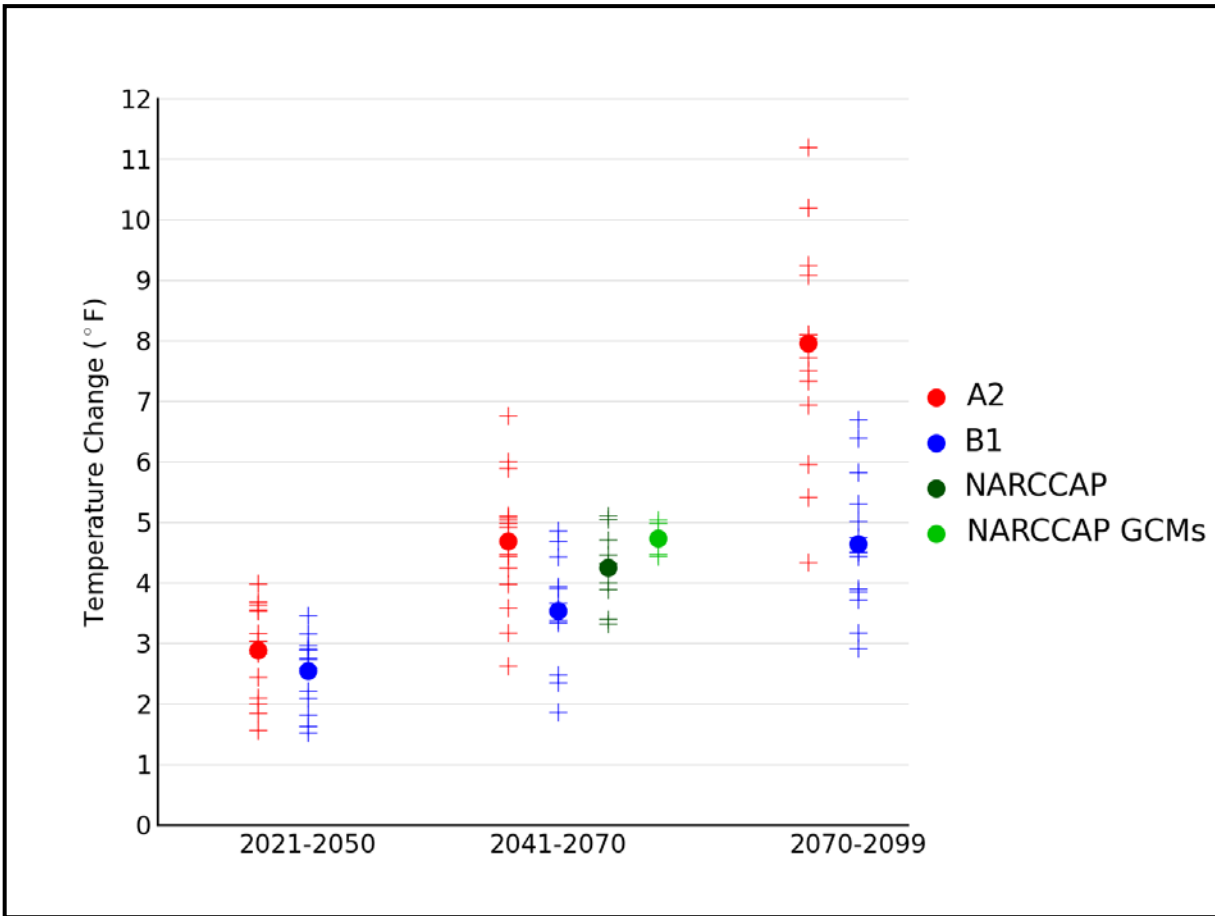


Figure 15. Simulated annual mean temperature change ($^{\circ}\text{F}$) for the Great Plains region, for each future time period (2021-2050, 2041-2070, and 2070-2099) with respect to the reference period of 1971-1999 for the CMIP3 models and 1971-2000 for the NARCCAP models. Values are given for the high (A2) and low (B1) emissions scenarios for the 14 (B1) or 15 (A2) CMIP3 models. Also shown for 2041-2070 (high emissions scenario only) are values for 9 NARCCAP models, as well as for the 4 GCMs used to drive the NARCCAP simulations. The small plus signs indicate each individual model and the circles depict the multi-model means. The range of model temperature changes is large compared to the mean differences between A2 and B1 in the early and middle 21st century. By the end of the 21st century, the difference between A2 and B1 is comparable to the range of B1 simulations.

A key overall feature is that the simulated temperature changes are similar in value for the high and low emissions scenarios for 2035, but largely different for 2085. This indicates that early in the 21st century, the multi-model mean temperature changes are relatively insensitive to the emissions pathway, whereas late 21st century changes are quite sensitive to the emissions pathway. This arises because atmospheric CO₂ concentrations resulting from the two different emissions scenarios do not considerably diverge from one another until around 2050 (see Fig. 1). It can also be seen from Fig. 15 that the range of individual model changes is quite large, with considerable overlap between the A2 and B1 results, even for 2085. The range of temperature changes for the GCMs used to drive the NARCCAP simulations is small relative to the range for all CMIP3 models. This may be largely responsible for the relatively small range of the NARCCAP models.

Figure 16 shows the change in seasonal mean temperature for each future time period with respect to 1971-1999 for the high (A2) emissions scenario, averaged over the entire Great Plains region for the 15 CMIP3 models. Again, both the multi-model mean and individual model values are shown. Temperature increases are simulated to be largest in the summertime, with multi-model means of around 3.4°F in 2035, 5.4°F in 2055, and 9.1°F in 2085. Springtime is predicted to experience the least amount of warming, ranging from 2.5°F in 2035 to 7.0°F in 2085. The range of temperature changes for the individual models increases with each time period and is large relative to the differences between seasons.

The distribution of changes in annual mean temperature for each future time period with respect to 1971-1999 for both emissions scenarios among the 14 (B1) or 15 (A2) CMIP3 models is shown in Table 4. Temperature changes simulated by the individual models vary from the lowest value of 1.6°F (in 2035 for the B1 scenario) to the highest value of 11.2°F (in 2085 for the A2 scenario). The interquartile range (the difference between the 75th and 25th percentiles) varies between 0.5 and 2.0°F across the three time periods. The NARCCAP simulated temperature changes have a smaller range than the comparable CMIP3 simulations, varying from 3.3°F to 5.1°F.

Table 4. Distribution of the simulated annual mean change in temperature (°F) from the 14 (B1) or 15 (A2) CMIP3 models for the Great Plains region. The lowest, 25th percentile, median, 75th percentile and highest values are given for the high (A2) and low (B1) emissions scenarios, and for each future time period (2021-2050, 2041-2070, and 2070-2099) with respect to the reference period of 1971-1999. Also shown are values from the distribution of 9 NARCCAP models for 2041-2070, A2 only, with respect to 1971-2000.

Scenario	Period	Lowest	25th Percentile	Median	75th Percentile	Highest
A2	2021-2050	1.6	2.3	3.0	3.5	4.0
	2041-2070	2.6	4.1	4.9	5.1	6.8
	2070-2099	4.3	7.1	8.0	9.1	11.2
	<i>NARCCAP (2041-2070)</i>	<i>3.3</i>	<i>3.9</i>	<i>4.3</i>	<i>4.7</i>	<i>5.1</i>
B1	2021-2050	1.5	2.1	2.8	2.9	3.5
	2041-2070	1.9	3.4	3.6	3.9	4.9
	2070-2099	2.9	3.9	4.5	5.2	6.7

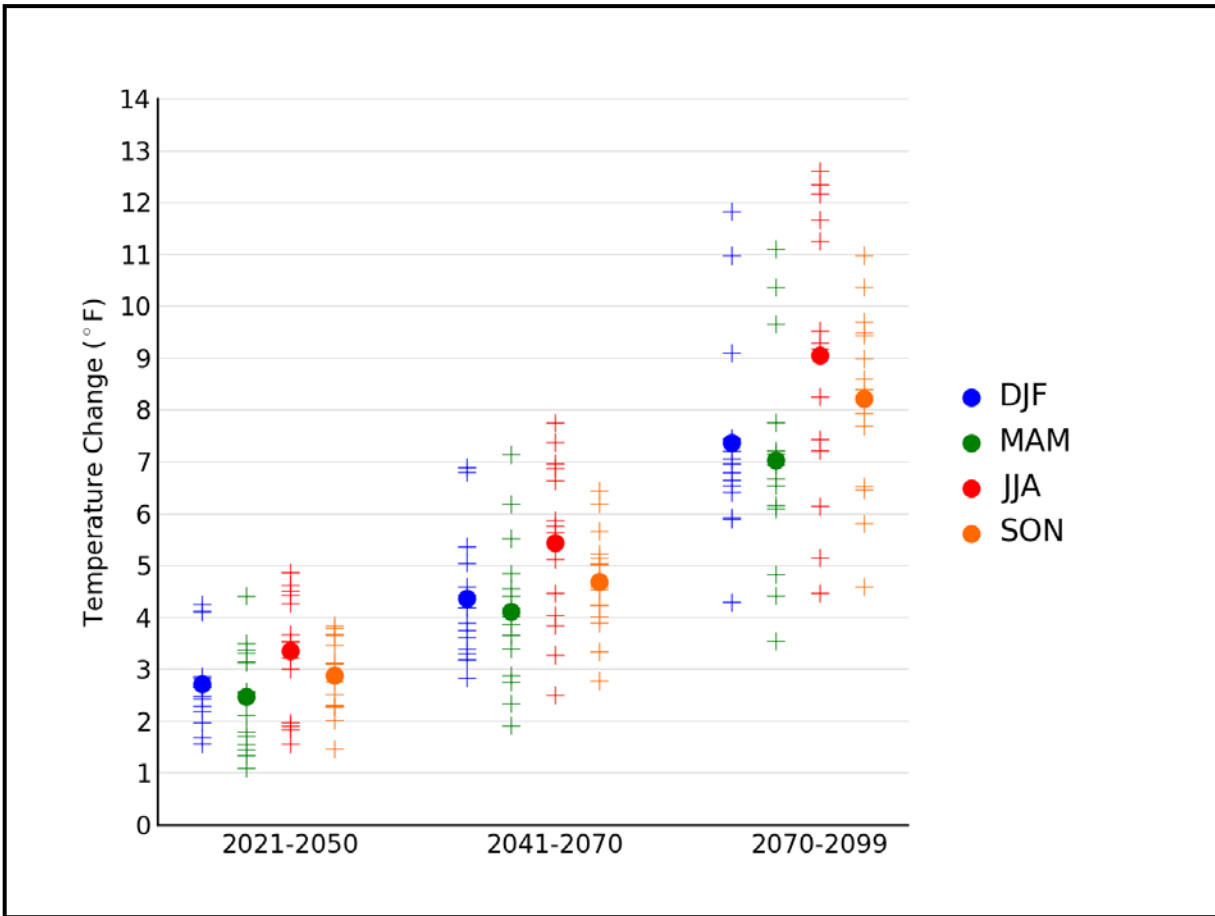


Figure 16. Simulated seasonal mean temperature change ($^{\circ}\text{F}$) for the Great Plains region, for each future time period (2021-2050, 2041-2070, and 2070-2099) with respect to the reference period of 1971-1999. Values are given for all 15 CMIP3 models for the high (A2) emissions scenario. The small plus signs indicate each individual model and the circles depict the multi-model means. Seasons are indicated as follows: winter (DJF, December-January-February), spring (MAM, March-April-May), summer (JJA, June-July-August), and fall (SON, September-October-November). The range of individual model changes is large compared to the differences among seasons and comparable to the differences between periods.

This table also illustrates the overall uncertainty arising from the combination of model differences and emission pathway. Following the high (A2) emissions scenario, for 2035, the simulated changes range from 1.6°F to 4.0°F and are almost entirely due to differences in the individual models. By 2085, the range of simulated changes has increased to 4.3°F to 11.2°F, with roughly equal contributions to the range from model differences and emission pathway uncertainties.

3.4. Extreme Temperature

A number of metrics of extreme temperatures were calculated from the NARCCAP dynamically-downscaled and CMIP3 daily statistically-downscaled (Daily_CMIP3) data sets. Maps of a few select variables and a table summarizing all of the results follow. Each figure of NARCCAP data includes three map panels and the calculations used in each panel require some explanation. One panel (top) shows the difference between the 2055 period (2041-2070) simulation for the high (A2) emissions scenario and the 1980-2000 subset of the 1971-2000 simulation driven by the GCM. Since biases in the RCM simulations can arise from biases either in the driving global climate model or in the RCM, these two simulations include both sources of biases. It is usually assumed that such biases will be similar for historical and future periods. When taking the difference of these, the biases should at least partially cancel. As noted above, we were requested to include actual values of the variables, not just the future minus historical differences. We decided that the best model representation of the present-day values is the 1980-2000 simulation because it is driven by reanalysis data (NOAA 2012b) and thus will not include biases from a driving global climate model (although the reanalysis data used to drive the RCM is not a perfect representation of the actual state of the atmosphere). Any biases should be largely from the RCM. Thus, the lower left panel in the following figures shows the actual values from the 1980-2000 simulation. The lower right panel shows the actual values for the future period, calculated by adding the differences (the 2041-2070 simulation minus the 1980-2000 subset of the 1971-2000 simulation) to the 1980-2000 simulation. If our assumption that the differencing of present and future at least partially cancels out model biases is true, then the predominant source of biases in the future values in the lower right hand panel is from the RCM simulation of the present-day, 1980-2000. The agreement among models was once again assessed using the three categories described in Fig. 13.

The selection of threshold temperatures to calculate extremes metrics is somewhat arbitrary because impacts-relevant thresholds are highly variable due to the very diverse climate of the U.S., with the exception of the freezing temperature, which is a universal physical threshold. In terms of high temperature thresholds, the values of 90°F, 95°F, and 100°F have been utilized in various studies of heat stress, although it is obvious that these thresholds have very different implications for the impacts on northern, cooler regions compared to southern, warmer regions. The threshold of 95°F has physiological relevance for maize production because the efficiency of pollination drops above that threshold. The low temperature thresholds of 10°F and 0°F also have varying relevance on impacts related to the background climate of a region. Fortunately, our analysis results are not qualitatively sensitive to the chosen thresholds. Thus, the results for these somewhat arbitrary choices nevertheless provide general guidance into scenarios of future changes.

Figure 17 shows the spatial distribution of the multi-model mean change in the average annual number of days with a maximum temperature exceeding 95°F between 2055 and the model reference period of 1980-2000, for the high (A2) emissions scenario, for 8 NARCCAP regional climate model simulations. The largest simulated increases of more than 30 days occur in the southwest corner of Texas. Changes of more than 20 days are indicated for a large area from Texas

north to southeast Wyoming. The smallest increases of less than 10 days are seen in the far north of the region and in high elevation areas, where the model reference period also exhibits the fewest number of days greater than 95°F. The NARCCAP models indicate that the changes in the number of 95°F days across the majority of the Great Plains are statistically significant. The models also agree on the sign of change, with these grid points satisfying category 3, i.e. the models are in agreement that the number of days above 95°F will increase throughout the region for these scenarios. For a portion of western Wyoming and Montana, however, the changes are not statistically significant for most models (category 1). In these areas where the historical number of days is very small, the models are in agreement that the increases in temperature are not sufficiently large to substantially increase the number of such days under this scenario.

Figure 18 shows the NARCCAP multi-model mean change in the average annual number of days with a minimum temperature of less than 10°F between 2055 and the model reference period of 1980-2000, for the high (A2) emissions scenario. The largest decreases are simulated for the northern half of the region, compared to little or no change in southern areas. The greatest changes are simulated to occur near the Canadian border and in high elevation areas, with some areas indicating decreases of 25 days or more. The smallest decreases occur in Texas, where the occurrence of cold days in the climatology is rare. The majority of grid points satisfy category 3, with the models indicating that the changes in the number days below 10°F across the Great Plains are statistically significant. The models also agree on the sign of change, i.e. they are in agreement that the number of days with a minimum temperature of less than 10°F will decrease throughout the region under this scenario. In southeastern Oklahoma and Texas, however, the changes are not statistically significant (category 1) because the number of days in the historical period is very small.

Figure 19 shows the NARCCAP multi-model mean change in the average annual number of days with a minimum temperature of less than 32°F between 2055 and the model reference period of 1980-2000, for the high (A2) emissions scenario. Model simulated decreases are largest (decreases of more than 32 days) in the northwestern part of the region. The least amount of change is simulated in south Texas, where the number of freezes in the historical period is low. The NARCCAP models indicate that the changes in the number of days below freezing across the Great Plains are statistically significant. The models also agree on the sign of change, with all grid points satisfying category 3, i.e. the models are in agreement that the number of days below 32°F will decrease throughout the region under this scenario.

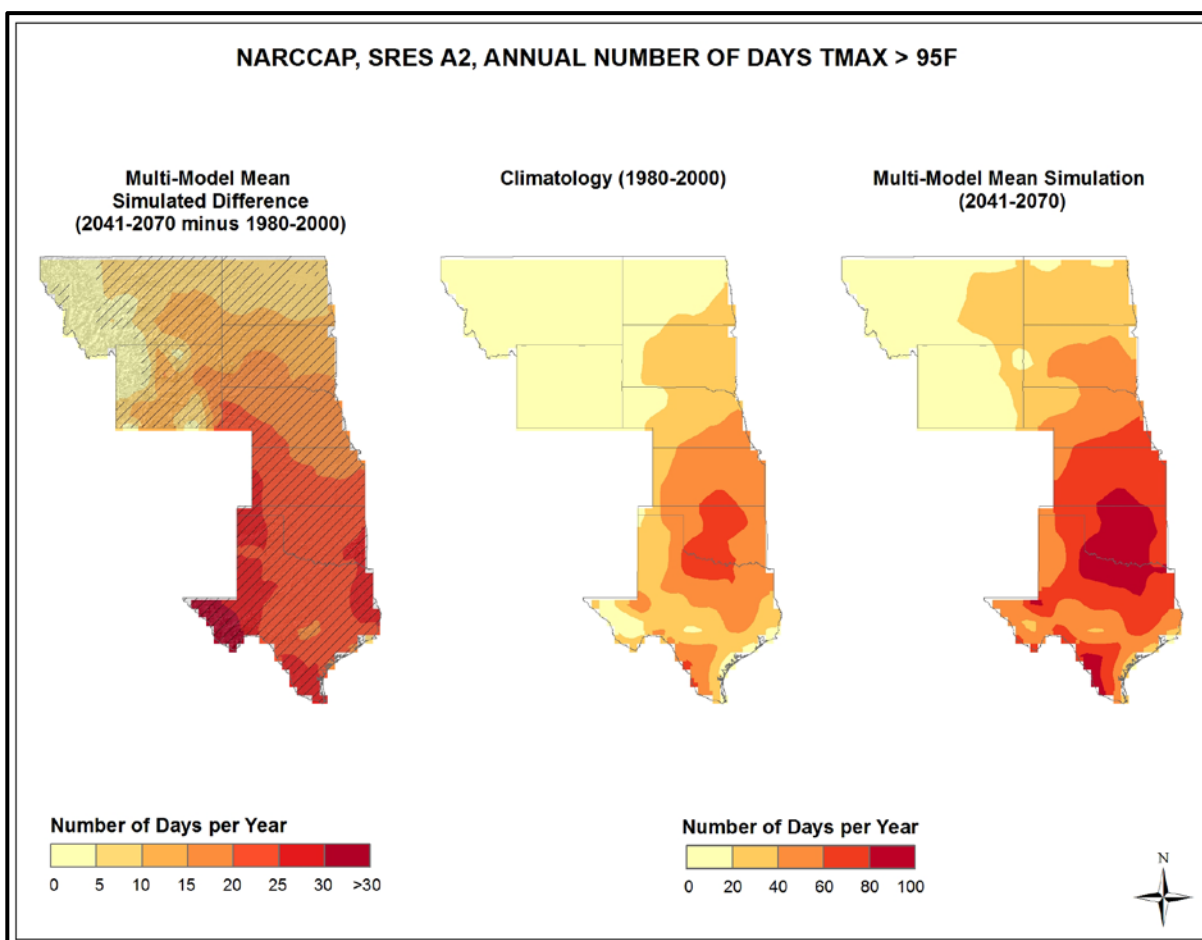


Figure 17. Simulated difference in the mean annual number of days with a maximum temperature greater than 95°F ($T_{max} > 95^{\circ}\text{F}$) for the Great Plains region, for the 2041-2070 time period with respect to the reference period of 1980-2000 (left). Color only (category 1) indicates that less than 50% of the models show a statistically significant change in the number of days. Color with hatching (category 3) indicates that more than 50% of the models show a statistically significant change in the number of days, and more than 67% agree on the sign of the change (see text). Mean annual number of days with $T_{max} > 95^{\circ}\text{F}$ for the 1980-2000 reference period (center). Simulated mean annual number of days with $T_{max} > 95^{\circ}\text{F}$ for the 2041-2070 future time period (right). These are multi-model means from 8 NARCCAP regional climate simulations for the high (A2) emissions scenario. Note that left and right color scales are different. Increases are largest in southwest Texas, and least in high elevation areas.

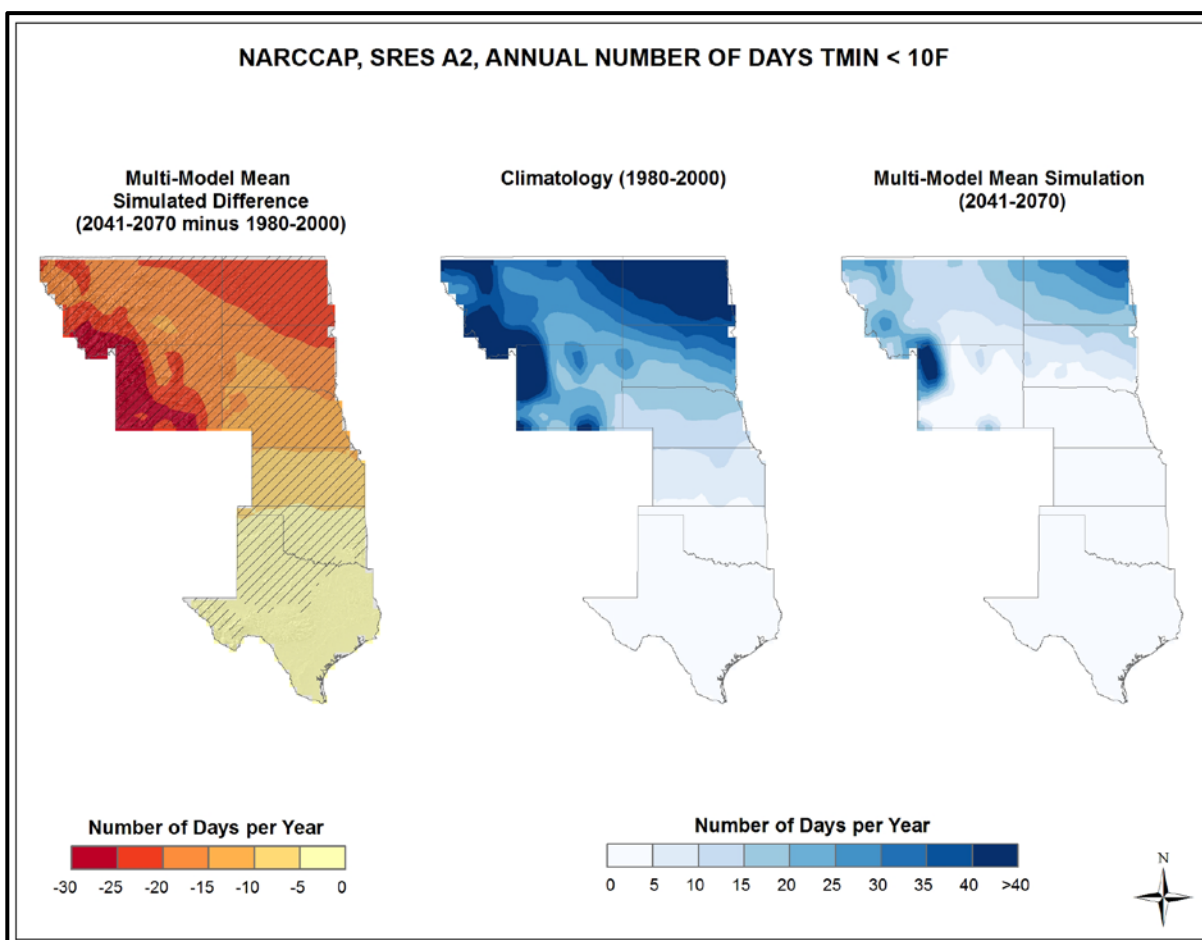


Figure 18. Simulated difference in the mean annual number of days with a minimum temperature less than 10°F ($T_{min} < 10^{\circ}F$) for the Great Plains region, for the 2041-2070 time period with respect to the reference period of 1980-2000 (left). Color only (category 1) indicates that less than 50% of the models show a statistically significant change in the number of days. Color with hatching (category 3) indicates that more than 50% of the models show a statistically significant change in the number of days, and more than 67% agree on the sign of the change (see text). Mean annual number of days with $T_{min} < 10^{\circ}F$ for the 1980-2000 reference period (center). Simulated mean annual number of days with $T_{min} < 10^{\circ}F$ for the 2041-2070 future time period (right). These are multi-model means from 8 NARCCAP regional climate simulations for the high (A2) emissions scenario. Decreases are largest in the north and in high elevation areas, and become smaller southward, in a pattern similar to the present-day climatology.

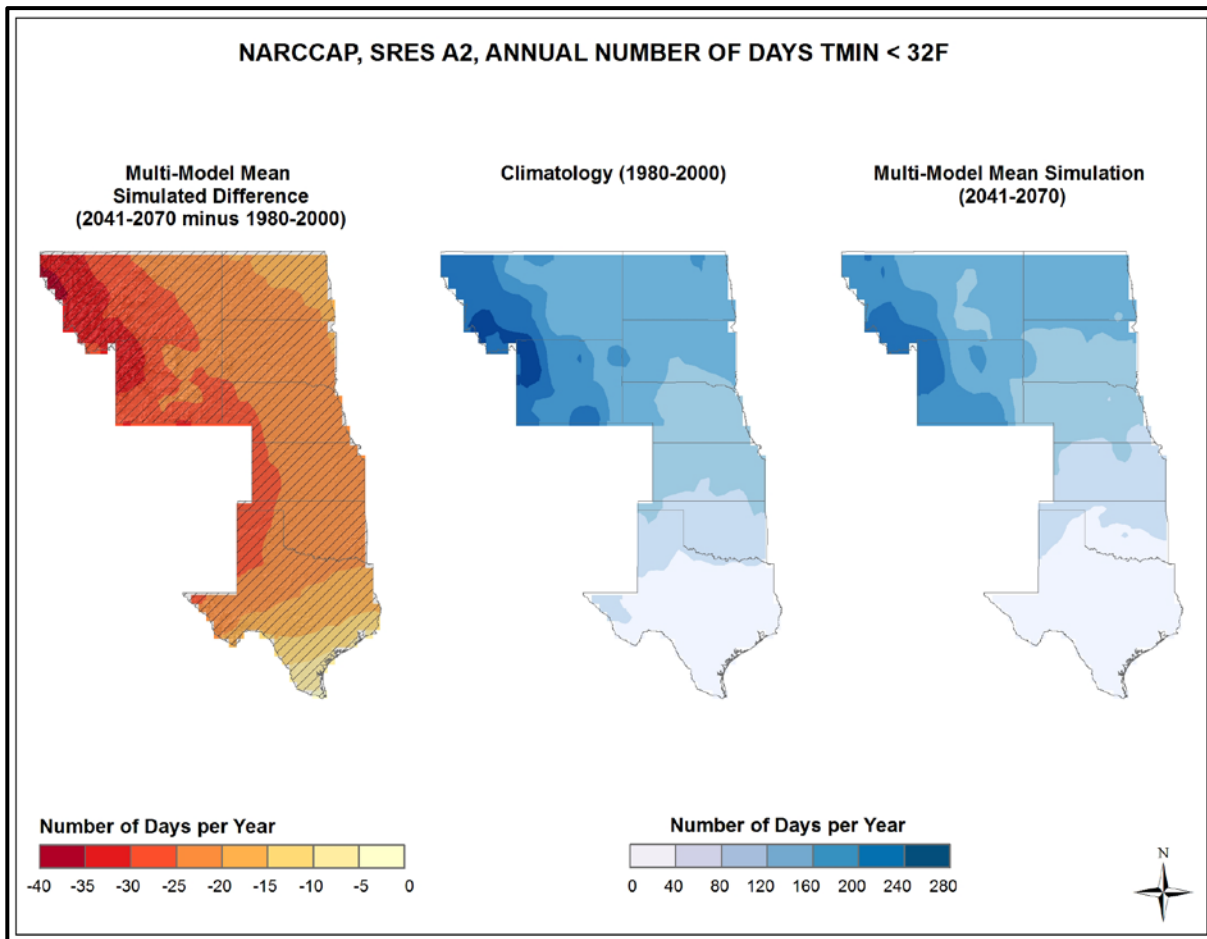


Figure 19. Simulated difference in the mean annual number of days with a minimum temperature less than 32°F ($T_{min} < 32^{\circ}\text{F}$) for the Great Plains region, for the 2041-2070 time period with respect to the reference period of 1980-2000 (left). Color with hatching (category 3) indicates that more than 50% of the models show a statistically significant change in the number of days, and more than 67% agree on the sign of the change (see text). Mean annual number of days with $T_{min} < 32^{\circ}\text{F}$ for the 1980-2000 reference period (center). Simulated mean annual number of days with $T_{min} < 32^{\circ}\text{F}$ for the 2041-2070 future time period (right). These are multi-model means from 8 NARCCAP regional climate simulations for the high (A2) emissions scenario. Changes are downward everywhere. Decreases are largest in the northwest of the region and smallest in the far south.

Consecutive warm days can have large impacts on a geographic area and its population and are analyzed here as one metric of heat waves. Figure 20 shows the NARCCAP multi-model mean change in the average annual maximum number of consecutive days with maximum temperatures exceeding 95°F between 2055 and the model reference period of 1980-2000, for the high (A2) emissions scenario. In Oklahoma and Texas, the average annual longest string of days with such high temperatures is simulated to increase by 16 days or more. In the central and southern portions of the region, the changes are smaller but still show increases of 4-16 days. Across the northern tier of the region, the increase in the number of consecutive days exceeding 95°F is the smallest, at 0-4 days. Recent climatology indicates that such measures of extreme hot periods have a large amount of interannual variability. Changes in the number of consecutive days over 95°F are not statistically significant for western Montana and Wyoming where the historical values are very low. All other grid points satisfy category 3, however, with the models indicating that changes across the Great Plains are statistically significant. The models also agree on the sign of change, i.e. the models are in agreement that the number of consecutive days above 95°F will increase throughout the region under this scenario.

3.5. Other Temperature Variables

The spatial distribution of the NARCCAP multi-model mean change in the average length of the freeze-free season between 2055 and the model reference period of 1980-2000, for the high (A2) emissions scenario, is shown in Fig. 21. The freeze-free season is defined as the period of time between the last spring frost (a daily minimum temperature of less than 32°F) and the first fall frost. The climatological trend of increasing freeze-free season length over the last century is simulated to continue, with at least 15 more days in the annual freeze-free season across the region. The largest increases are found across the high terrain of Wyoming and Montana, where values of greater than 30 days are simulated. The remainder of the region shows increases on the order of 3-4 weeks. All grid points satisfy category 3, with the models indicating that the changes in the length of the freeze-free season across the Great Plains are statistically significant. The models also agree on the sign of change, i.e. the models are in agreement that the freeze-free season length will increase throughout the region under this scenario.

Cooling and heating degree days are accumulative metrics related to energy use, more specifically regarding the cooling and heating of buildings, with a base temperature of 65°F, assumed to be the threshold below which heating is required and above which cooling is required. Heating degree days provide a measure of the extent (in degrees), and duration (in days), that the daily mean temperature is below the base temperature. Cooling degree days measure the extent and duration that the daily mean temperature is above the base temperature.

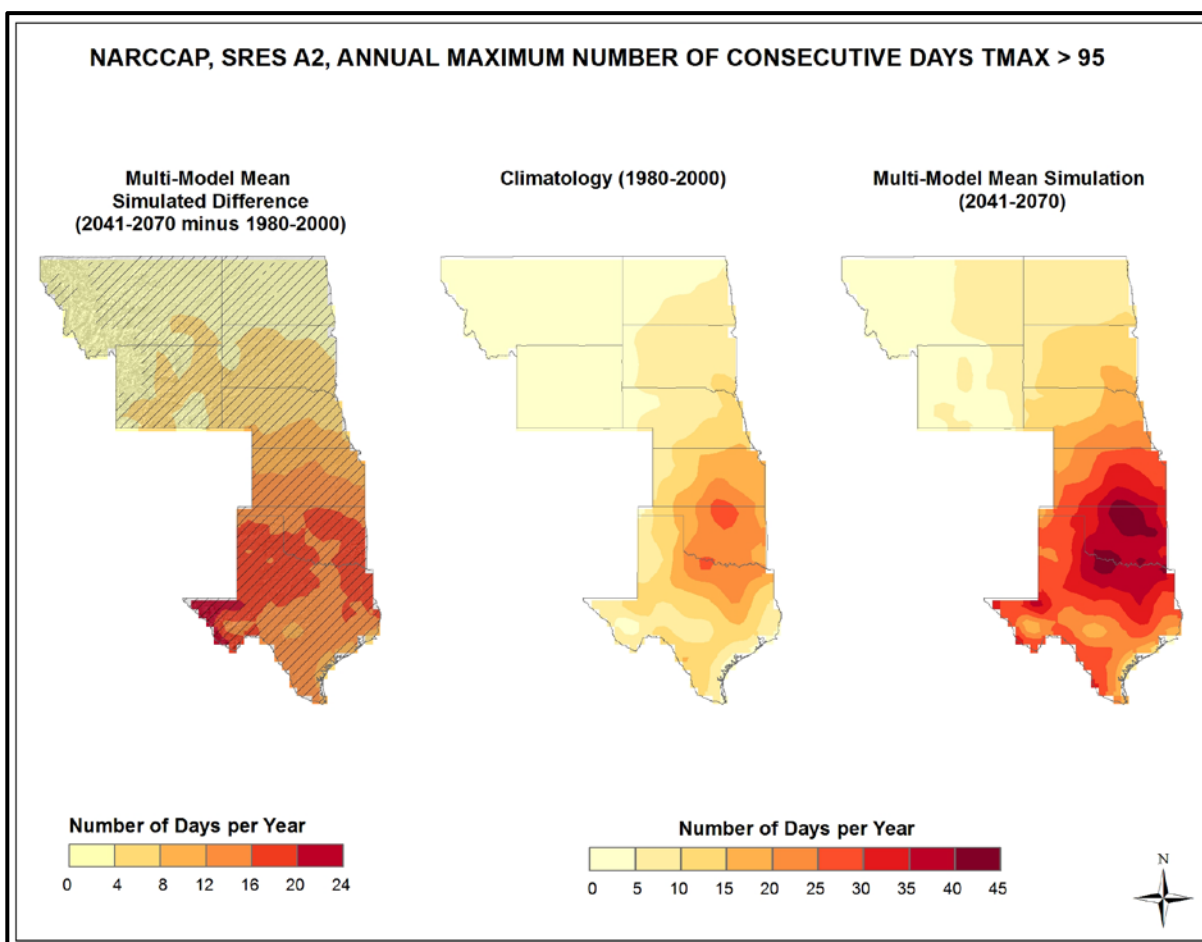


Figure 20. Simulated difference in the mean annual maximum number of consecutive days with a maximum temperature greater than 95°F ($T_{max} > 95^{\circ}F$) for the Great Plains region, for the 2041-2070 time period with respect to the reference period of 1980-2000 (left). Color only (category 1) indicates that less than 50% of the models show a statistically significant change in the number of consecutive days. Color with hatching (category 3) indicates that more than 50% of the models show a statistically significant change the number of consecutive days, and more than 67% agree on the sign of the change (see text). Mean annual number of consecutive days with $T_{max} > 95^{\circ}F$ for the 1980-2000 reference period (center). Simulated mean annual maximum number of consecutive days with $T_{max} > 95^{\circ}F$ for the 2041-2070 future time period (right). These are multi-model means from 8 NARCCAP regional climate simulations for the high (A2) emissions scenario. Note that left and right color scales are different. The changes are upward everywhere. Increases are largest in Texas and Oklahoma and decrease northward, in a pattern similar to the present-day climatology.

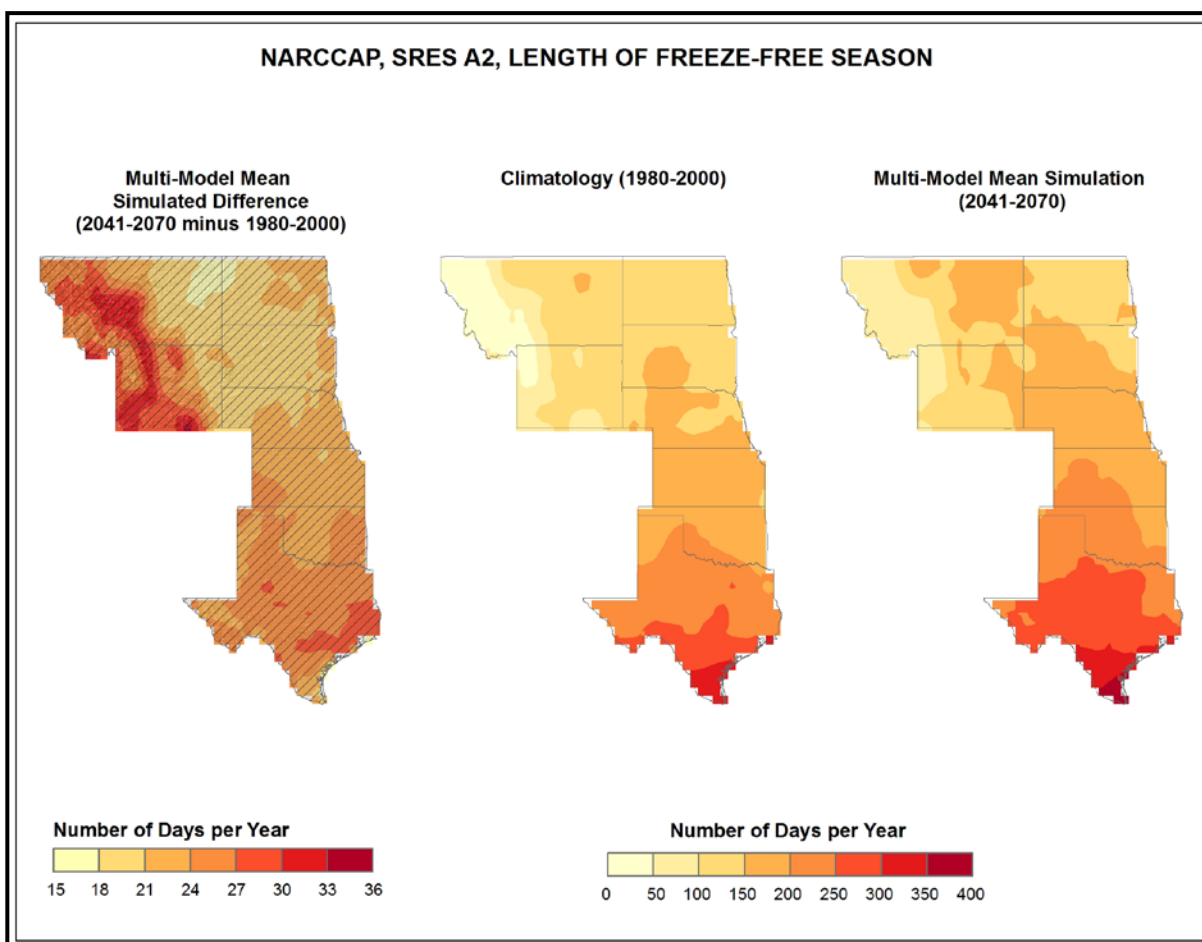


Figure 21. Simulated difference in the mean annual length of the freeze-free season for the Great Plains region, for the 2041-2070 time period with respect to the reference period of 1980-2000 (left). Color with hatching (category 3) indicates that more than 50% of the models show a statistically significant change in the length of the freeze-free season, and more than 67% agree on the sign of the change (see text). Mean annual length of the freeze-free season for the 1980-2000 reference period (center). Simulated mean annual length of the freeze-free season for the 2041-2070 future time period (right). These are multi-model means from 8 NARCCAP regional climate simulations for the high (A2) emissions scenario. Note that left and right color scales are different. The freeze-free season is simulated to become longer throughout the region, with increases mostly in the 20-30 day range.

Figure 22 shows the NARCCAP multi-model mean change in the average annual number of cooling degree days between 2055 and the model reference period of 1980-2000, for the high (A2) emissions scenario. In general, the changes are quite closely related to mean temperature with the warmest (coolest) areas showing the largest (smallest) changes. The hottest areas, such as Texas and Oklahoma, are simulated to have the largest increases of up to 1,000 cooling degree days (CDDs). Further north across Nebraska and the Dakotas, increases of 200-600 CDDs are simulated. Areas across the Rockies are shown to have the smallest increases, of less than 200 CDDs. The models indicate that the changes in cooling degree days across the Great Plains are statistically significant. The models also agree on the sign of change, with all grid points satisfying category 3, i.e. the models are in agreement that the number of CDDs will increase throughout the region under this scenario.

The NARCCAP multi-model mean change in the average annual number of heating degree days between 2055 and the model reference period of 1980-2000, for the high (A2) emissions scenario, is shown in Fig. 23. The largest changes are predicted to occur in higher elevation areas, where there are simulated decreases of up to 1,650 heating degree days (HDDs). The smallest decreases of 250-450 HDDs are simulated in southern Texas. The models once again indicate that the changes across the Great Plains are statistically significant. All grid points satisfy category 3, with the models also agreeing on the sign of change, i.e. the models are in agreement that the number of HDDs will decrease throughout the region under this scenario.

3.6. Tabular Summary of Selected Temperature Variables

The mean changes for select temperature-based variables derived from 8 NARCCAP simulations for 2055 with respect to the model reference period of 1971-2000, for the high (A2) emissions scenario, are summarized in Table 5. These were determined by first calculating the derived variable at each grid point. The spatially-averaged value of the variable was then calculated for the reference and future periods. Finally, the difference or ratio between the two periods was calculated from the spatially-averaged values. In addition, these same variables were calculated from the 8 CMIP3 daily statistically-downscaled (Daily_CMIP3) simulations for comparison.

For the NARCCAP simulations, the multi-model mean freeze-free period over the Great Plains region is simulated to increase by 24 days, comparable to the 24 days calculated for the CMIP3 daily statistically-downscaled data. The number of days with daily maximum temperatures greater than 90°F, 95°F, and 100°F are simulated to increase by 20, 18, and 15 days, respectively, for the NARCCAP models. Corresponding increases for the Daily_CMIP3 data are 29, 25, and 16 days, with values decreasing by a greater amount as the thresholds become more extreme.

The number of days with minimum temperatures of less than 32°F, 10°F, and 0°F are simulated to decrease by 23, 12, and 7 days, respectively, for the NARCCAP models. Corresponding values for the Daily_CMIP3 simulations are comparable decreases of 24, 10, and 6 days.

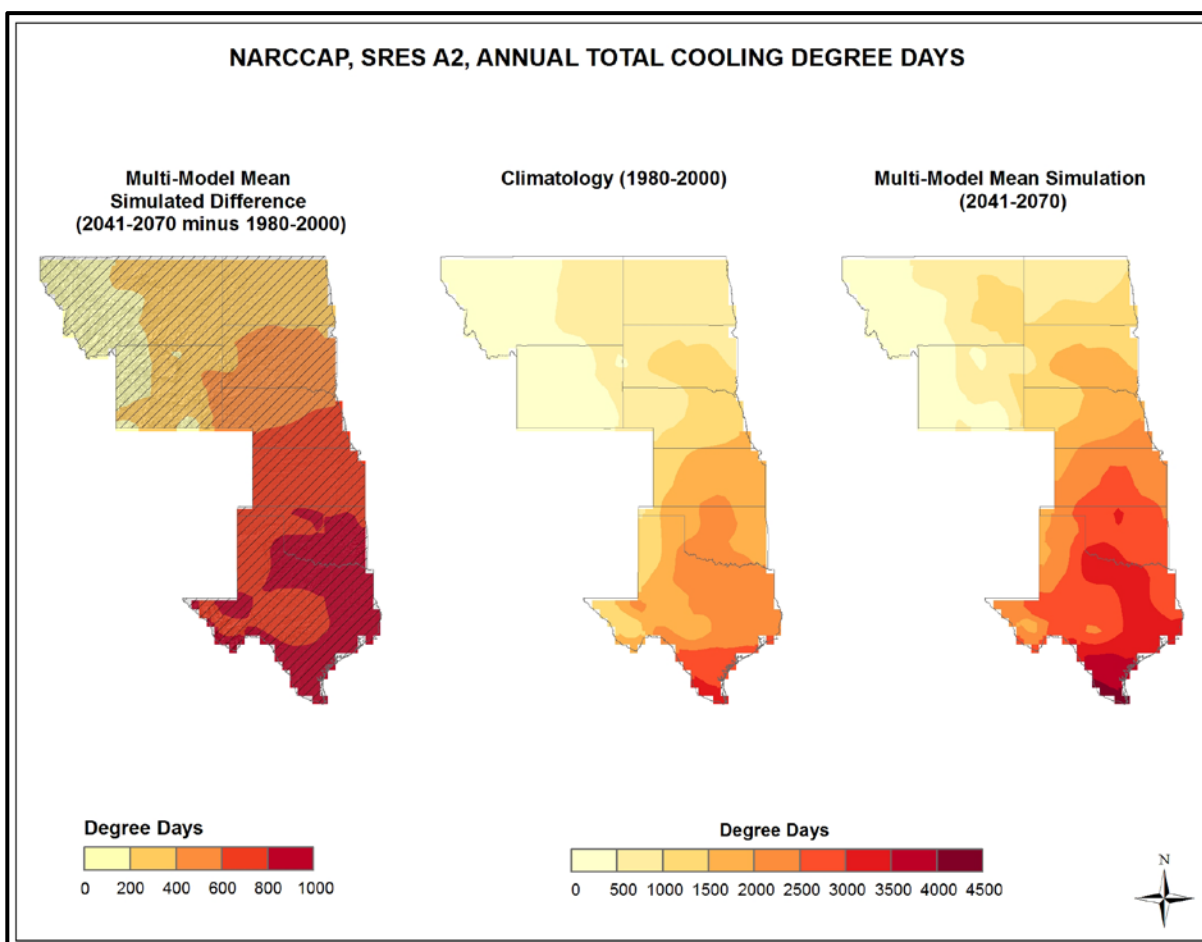


Figure 22. Simulated difference in the mean annual number of cooling degree days for the Great Plains region, for the 2041-2070 time period with respect to the reference period of 1980-2000 (left). Color with hatching (category 3) indicates that more than 50% of the models show a statistically significant change in the number of cooling degree days, and more than 67% agree on the sign of the change (see text). Mean annual number of cooling degree days for the 1980-2000 reference period (center). Simulated mean annual number of cooling degree days for the 2041-2070 future time period (right). These are multi-model means from 8 NARCCAP regional climate simulations for the high (A2) emissions scenario. Note that left and right color scales are different. There are increases everywhere, with the increases becoming larger from north to south.

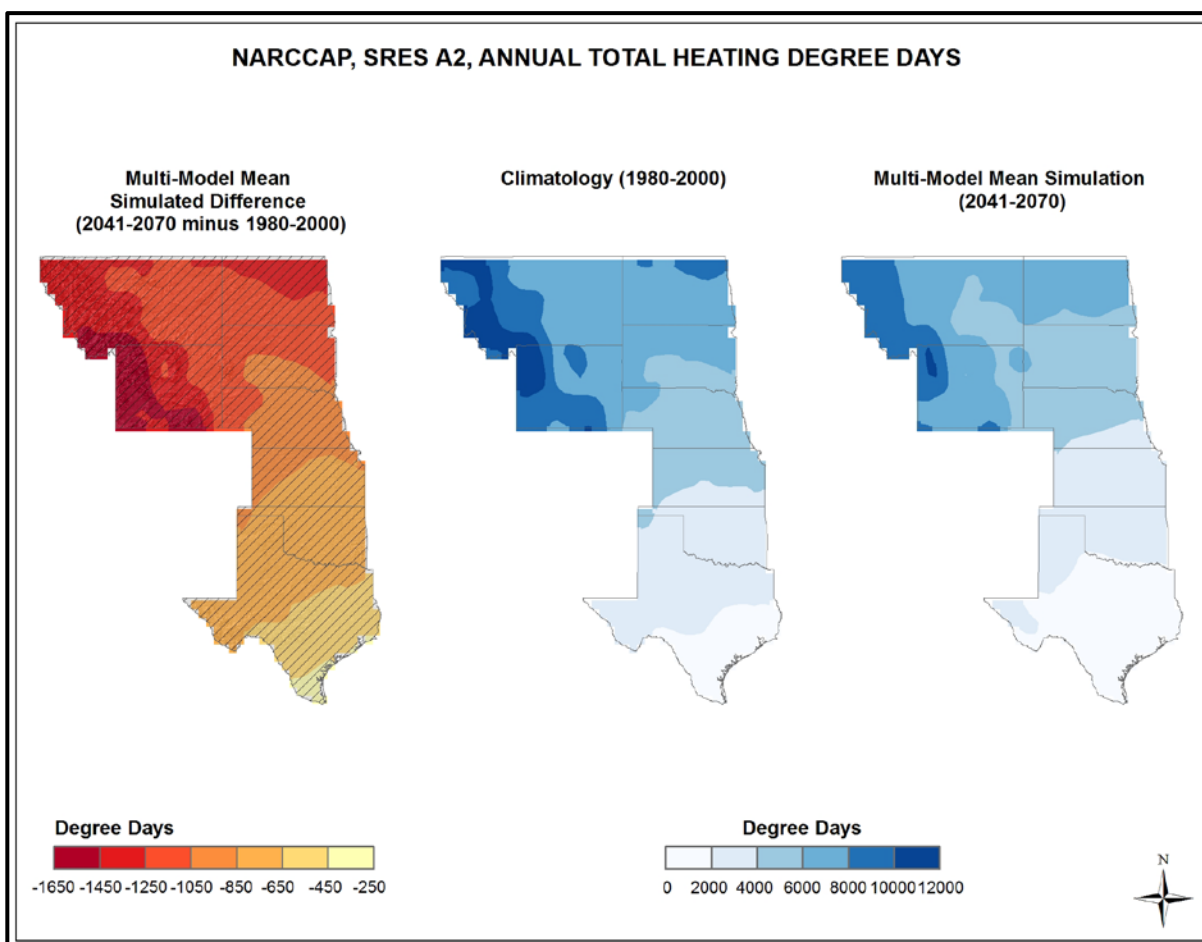


Figure 23. Simulated difference in the mean annual number of heating degree days for the Great Plains region, for the 2041-2070 time period with respect to the reference period of 1980-2000 (left). Color with hatching (category 3) indicates that more than 50% of the models show a statistically significant change in the number of heating degree days, and more than 67% agree on the sign of the change (see text). Mean annual number of heating degree days for the 1980-2000 reference period (center). Simulated mean annual number of heating degree days for the 2041-2070 future time period (right). These are multi-model means from 8 NARCCAP regional climate simulations for the high (A2) emissions scenario. There are decreases everywhere, with the largest decreases in high elevation areas.

Table 5. Multi-model means and standard deviations of the simulated annual mean change in select temperature variables from 8 NARCCAP simulations for the Great Plains region. Multi-model means from the 8 Daily_CMIP3 simulations are also shown for comparison. Analyses are for the 2041-2070 time period with respect to the reference period of 1971-2000, for the high (A2) emissions scenario.

Temperature Variable	NARCCAP	NARCCAP	Daily_CMIP3
	Mean	Standard Deviation	Mean
Freeze-free period	+24 days	4 days	+24 days
#days $T_{max} > 90^{\circ}\text{F}$	+20 days	6 days	+29 days
#days $T_{max} > 95^{\circ}\text{F}$	+18 days	6 days	+25 days
#days $T_{max} > 100^{\circ}\text{F}$	+15 days	6 days	+16 days
#days $T_{min} < 32^{\circ}\text{F}$	-23 days	3 days	-24 days
#days $T_{min} < 10^{\circ}\text{F}$	-12 days	3 days	-10 days
#days $T_{min} < 0^{\circ}\text{F}$	-7 days	3 days	-6 days
Consecutive #days $> 95^{\circ}\text{F}$	+62%	29%	+122%
Consecutive #days $> 100^{\circ}\text{F}$	+77%	47%	+222%
Heating degree days	-16%	2%	-17%
Cooling degree days	+48%	14%	+53%
Growing degree days (base 50°F)	+27%	5%	+29%

The multi-model mean annual maximum numbers of consecutive days exceeding 95°F and 100°F (our heat wave metric) are simulated to increase by 62% and 77% respectively for the NARCCAP data, a substantial increase in the length of such hot periods. These increases are even greater for the Daily_CMIP3 simulations, with values of 122% for the 95°F threshold, and 222% for the 100°F threshold.

Table 5 indicates that, for the high (A2) emissions scenario, the number of heating degree days are simulated by the NARCCAP simulations to decrease by 16% (17% for Daily_CMIP3), while the number of cooling degree days are simulated to increase by 48% (53% for Daily_CMIP3). The number of growing degree days (base 50°F) are also comparable for both data sets, increasing by 27% and 29% for NARCCAP and Daily_CMIP3, respectively.

3.7. Mean Precipitation

Figure 24 shows the spatial distribution of multi-model mean simulated differences in average annual precipitation for the three future time periods (2035, 2055, 2085) with respect to 1971-1999, for both emissions scenarios, for the 14 (B1) or 15 (A2) CMIP3 models. There is a pronounced north-south gradient in simulated precipitation changes. The southern regions show the largest decreases while northern areas show increases. This gradient increases in magnitude as time progresses for the high (A2) emissions scenario. The gradient in the low (B1) emissions scenario is largely unchanged between the time periods. The largest north-south differences are for the A2 scenario in 2085, varying from an increase in precipitation of 6-9% in the far north to a decrease of 9-12% in central Texas. Nominal differences occur for the A2 scenario in 2035, with increases of 3-6% in North and South Dakota and Montana, and decreases of 3-6% in west Texas. The agreement between models was once again assessed using the three categories described in Fig. 13. It can be seen that for the 2035 time period the changes in precipitation are not significant for most models (category 1) over the majority of grid points. This means that most models are in agreement that any

changes will be smaller than the normal year-to-year variations that occur. For the high emissions scenario in 2085, most models indicate changes that are larger than these normal variations (category 3) across the majority of the region. In this case, the models are mostly in agreement that precipitation will increase in the northern Great Plains and decrease in the southern Great Plains. In the center of the region, however, the models are in disagreement about the sign of the changes (category 2). For the low emissions scenario, model agreement can also be seen for the increases in the north, but not for the decreases in the south.

Table 6 shows the distribution of changes in annual mean precipitation for each future time period with respect to 1971-1999, for both emissions scenarios among the 14 (B1) or 15 (A2) CMIP3 models. The distribution of 9 NARCCAP simulations (for 2055, A2 scenario only) is also shown for comparison, with respect to 1971-2000. For all three time periods and both scenarios, the CMIP3 models simulate both increases and decreases in precipitation. All the median values are small (3% or less). The CMIP3 inter-model range of changes in precipitation (i.e. the difference between the highest and lowest model values) varies from 11% (for B1, 2035) to 29% (for A2, 2085). The range of the NARCCAP values is 13% (for A2, 2055). The interquartile range (the difference between the 75th and 25th percentiles) of precipitation changes across all the GCMs is less than 15%.

Table 6. Distribution of the simulated annual mean change in precipitation (%) from the 14 (B1) or 15 (A2) CMIP3 models for the Great Plains region. The lowest, 25th percentile, median, 75th percentile and highest values are given for the high (A2) and low (B1) emissions scenarios, and for each future time period (2021-2050, 2041-2070, and 2070-2099) with respect to the reference period of 1971-1999. Also shown are values from the distribution of 9 NARCCAP models for 2041-2070, A2 only, with respect to 1971-2000.

Scenario	Period	Lowest	25th Percentile	Median	75th Percentile	Highest
A2	2021-2050	-7	-2	0	3	7
	2041-2070	-12	-5	-2	4	8
	2070-2099	-18	-8	-3	6	11
	<i>NARCCAP (2041-2070)</i>	-5	0	3	4	8
B1	2021-2050	-7	-2	0	1	4
	2041-2070	-7	-3	1	4	6
	2070-2099	-10	-3	3	4	8

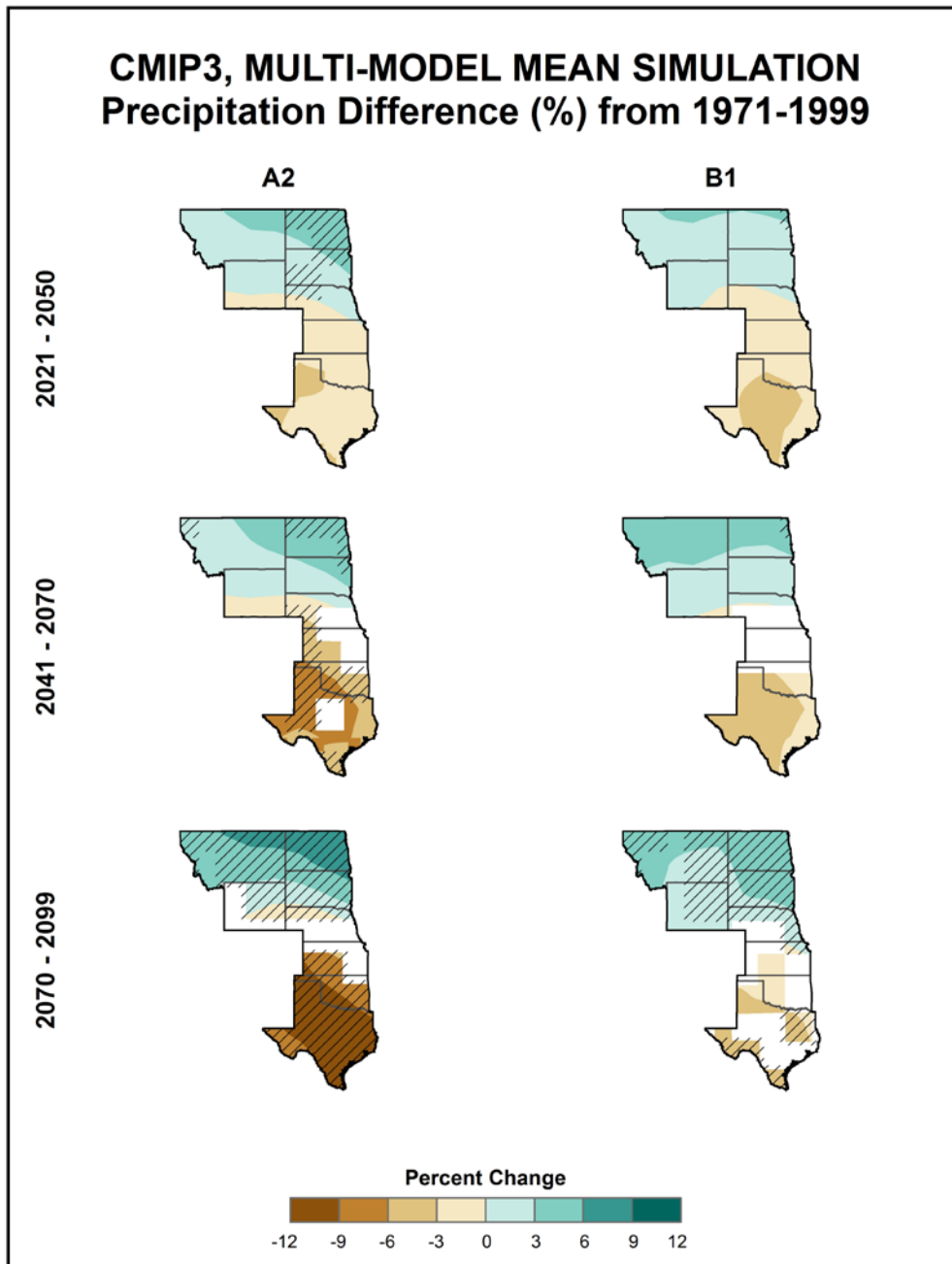


Figure 24. Simulated difference in annual mean precipitation (%) for the Great Plains region, for each future time period (2021-2050, 2041-2070, and 2070-2099) with respect to the reference period of 1971-1999. These are multi-model means for the high (A2) and low (B1) emissions scenarios from the 14 (B1) or 15 (A2) CMIP3 global climate simulations. Color only (category 1) indicates that less than 50% of the models show a statistically significant change in precipitation. Color with hatching (category 3) indicates that more than 50% of the models show a statistically significant change in precipitation, and more than 67% agree on the sign of the change. Whited out areas (category 2) indicate that more than 50% of the models show a statistically significant change in precipitation, but less than 67% agree of the sign of the change (see text). Generally, the models simulate increases in the northern Great Plains and decreases in the southern part of the region.

Figure 25 shows the multi-model mean annual and seasonal 30-year average precipitation change between 2041-2070 and 1971-2000 for the high (A2) emissions scenario, for 11 NARCCAP regional climate model simulations. The simulated annual changes in precipitation are mostly upward, with the largest increases occurring in North Dakota. Areas further south, however, such as west Texas, indicate decreases of more than 6%. Simulated winter changes are mostly positive, ranging from near zero in central Texas to over 15% across Wyoming, Montana and the Dakotas. Simulated changes in spring and fall are also mostly positive. The largest spatial variability occurs in the summertime, ranging as high as +15% (North Dakota) and as low as -20% (northwest Texas). The agreement between models was again assessed using the three categories described in Fig. 13. It can be seen that annually, and for all seasons, the simulated changes in precipitation are not statistically significant for most models over the majority of grid points (category 1). The models are also in disagreement about the sign of change (category 2) for two small areas in south-central Texas for the summer season. The models are in agreement (category 3), however, in some parts of the region, most notably in the Dakotas for the annual simulation, and across the Texas panhandle for summer.

Table 7 shows the distribution of changes in seasonal mean precipitation among the 14 (B1) or 15 (A2) CMIP3 models, between 2070-2099 and 1971-1999 for both emissions scenarios. On a seasonal basis, the range of model-predicted changes is quite large, when expressed as percentages. For example, in the high (A2) emissions scenario, the simulated changes in summer precipitation vary from a decrease of 37% to an increase of 12%. A majority of the models indicate increases in winter, spring, and fall precipitation. For summer, however, more models simulate decreases. In the low (B1) emissions scenario, the range of simulated precipitation changes is generally smaller, but the distribution of values is comparable to that of the A2 scenario. The central feature of the results in Table 7 is the large uncertainty in seasonal precipitation changes.

Table 7. Distribution of the simulated change in seasonal mean precipitation (%) from the 14 (B1) or 15 (A2) CMIP3 models for the Great Plains region. The lowest, 25th percentile, median, 75th percentile and highest values are given for the high (A2) and low (B1) emissions scenarios, and for the 2070-2099 time period with respect to the reference period of 1971-1999.

Scenario	Period	Season	Lowest	25th Percentile	Median	75th Percentile	Highest
A2	2070-2099	DJF	-19	0	6	10	15
		MAM	-14	-2	2	9	20
		JJA	-37	-27	-10	5	12
		SON	-29	-10	3	6	18
B1	2070-2099	DJF	-14	-2	2	6	10
		MAM	-11	0	4	8	11
		JJA	-18	-9	-2	5	13
		SON	-10	-7	3	4	11

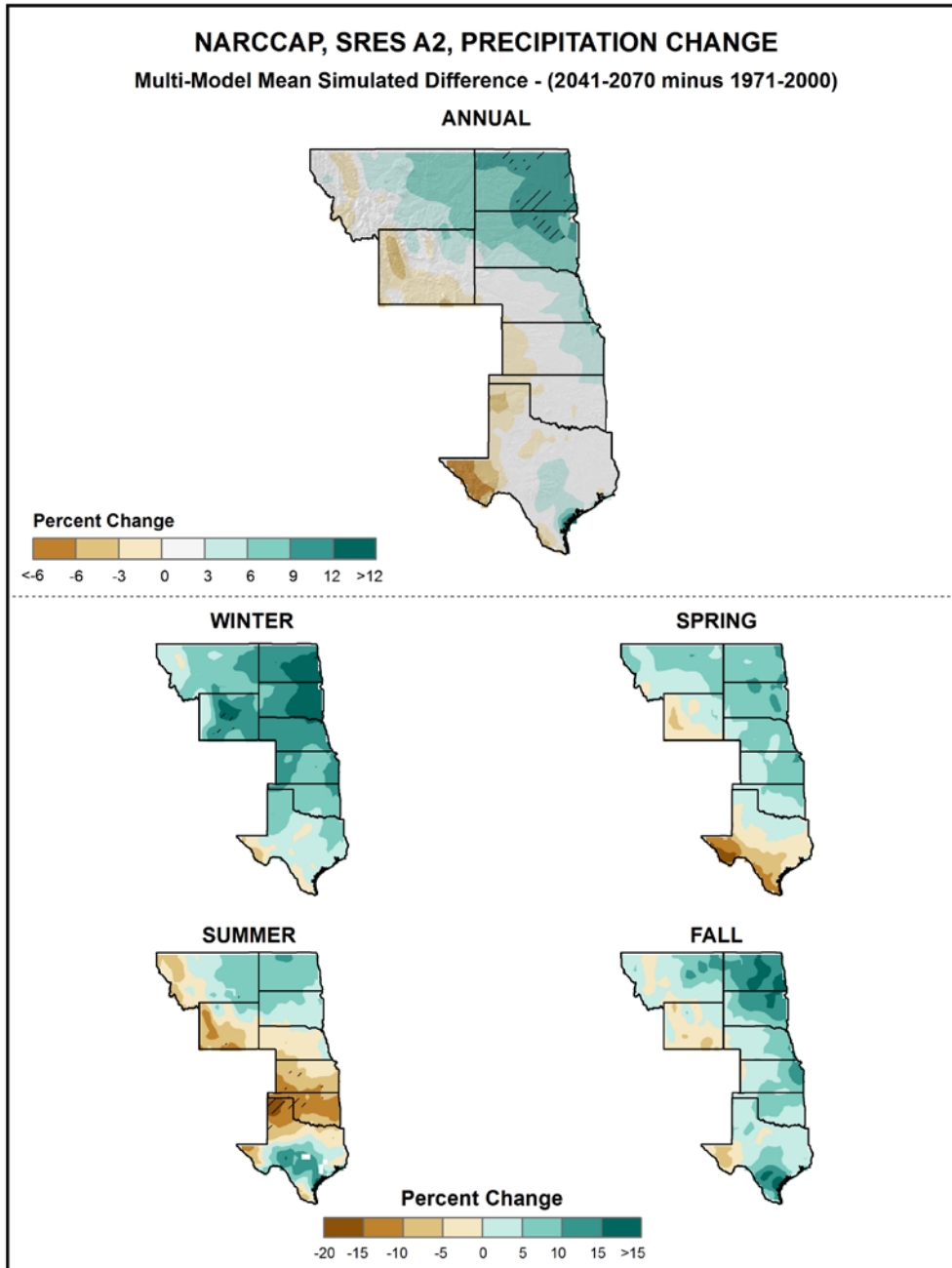


Figure 25. Simulated difference in annual and seasonal mean precipitation (%) for the Great Plains region, for 2041-2070 with respect to the reference period of 1971-2000. These are multi-model means from 11 NARCCAP regional climate simulations for the high (A2) emissions scenario. Color only (category 1) indicates that less than 50% of the models show a statistically significant change in precipitation. Color with hatching (category 3) indicates that more than 50% of the models show a statistically significant change in the number of days, and more than 67% agree on the sign of the change. Whited out areas (category 2) indicate that more than 50% of the models show a statistically significant change in precipitation, but less than 67% agree of the sign of the change (see text). Note that top and bottom color scales are unique, and different from that of Fig. 24. The annual change is upward in the northeast of the region and downward in the southwest, with large areas of little to no across the central Great Plains. Changes are mostly upward in the winter, spring, and fall, and downward in summer.

Figure 26 shows the change in annual mean precipitation for each future time period with respect to 1971-1999, for both emissions scenarios, averaged over the entire Great Plains region for the 14 (B1) or 15 (A2) CMIP3 models. In addition, averages for 9 NARCCAP simulations (relative to 1971-2000) and the 4 GCMs used in the NARCCAP experiment are shown for 2055 (A2 scenario only). Both the multi-model mean and individual model values are shown. A decrease in CMIP3 multi-model mean precipitation is simulated for each time period under the A2 scenario, however the B1 scenario indicates increases from 2055 onwards. The multi-model mean of the NARCCAP simulations is slightly greater than the CMIP3 multi-model mean, and comparable to that of the 4 GCMs used in the NARCCAP experiment (which do not include the 3 driest CMIP3 models). The range of individual model changes in Fig. 26 is large compared to the differences in the multi-model means, as also illustrated in Table 6. In fact, for both emissions scenarios, the individual model range is much larger than the differences in the CMIP3 multi-model means between time periods.

Figure 27 shows the change in seasonal mean precipitation for each future time period with respect to 1971-1999, for the high (A2) emissions scenario, averaged over the entire Great Plains region for the 15 CMIP3 models, as well as the NARCCAP models for 2055, relative to 1971-2000. Again, both the multi-model mean and individual model values are shown. There are differences seasonally, with the CMIP3 models generally simulating increases for the winter and spring seasons, and decreases the summer and fall seasons. The decreases are largest in the summer, ranging from -4% in 2035 to -9% in 2085. The NARCCAP models, which are displayed for 2055 only, have higher multi-model mean values than the CMIP3 models for all four seasons. This may in part be due to the choice of the 4 GCMs in the NARCCAP experiment (which do not include the driest CMIP3 models). As was the case for the annual precipitation changes in Fig. 26, the model ranges in Fig. 27 are large compared to the multi-model mean differences. This illustrates the large uncertainty in the precipitation estimates using these simulations.

3.8. Extreme Precipitation

Figure 28 shows the spatial distribution of the multi-model mean change in the average annual number of days with precipitation exceeding 1 inch, for 8 NARCCAP regional climate model simulations. Again this is the difference between the period of 2041-2070 and the 1980-2000 reference period for the high (A2) emissions scenario. In addition to this difference map, maps of the model simulations of the actual values for historical conditions (NARCCAP models driven by the NCEP Reanalysis II) and for the future are also displayed for comparison. Increases are simulated for nearly the entire region, generally of up to 30%, although greater in some northern areas. Slight decreases of up to 11% are simulated for small areas in the far western portions of the region. It can be seen that changes in days exceeding 1 inch are not statistically significant for most models (category 1) over the majority of grid points. This means that most models are in agreement that any changes will be smaller than the normal year-to-year variations that occur under this scenario. In some northern and central areas, however, most models indicate increases in days with precipitation of more than 1 inch that are larger than these normal variations (category 3).

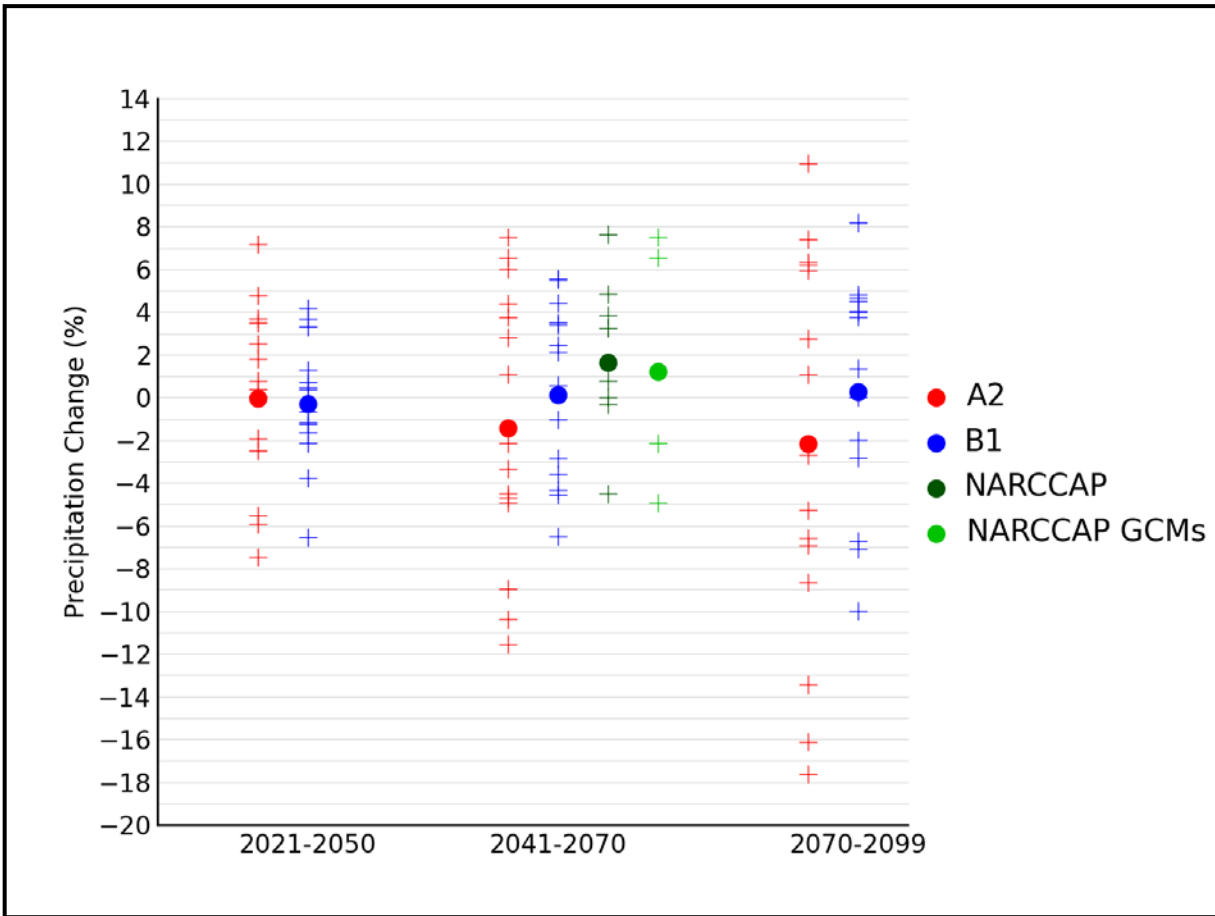


Figure 26. Simulated annual mean precipitation change (%) for the Great Plains region, for each future time period (2021-2050, 2041-2070, and 2070-2099) with respect to the reference period of 1971-1999. Values are given for the high (A2) and low (B1) emissions scenarios for the 14 (B1) or 15 (A2) CMIP3 models. Also shown for 2041-2070 (high emissions scenario only) are values (relative to 1971-2000) for 9 NARCCAP models, as well as for the 4 GCMs used to drive the NARCCAP simulations. The small plus signs indicate each individual model and the circles depict the multi-model means. The ranges of model-simulated changes are very large compared to the mean changes and to differences between the A2 and B1 scenarios.

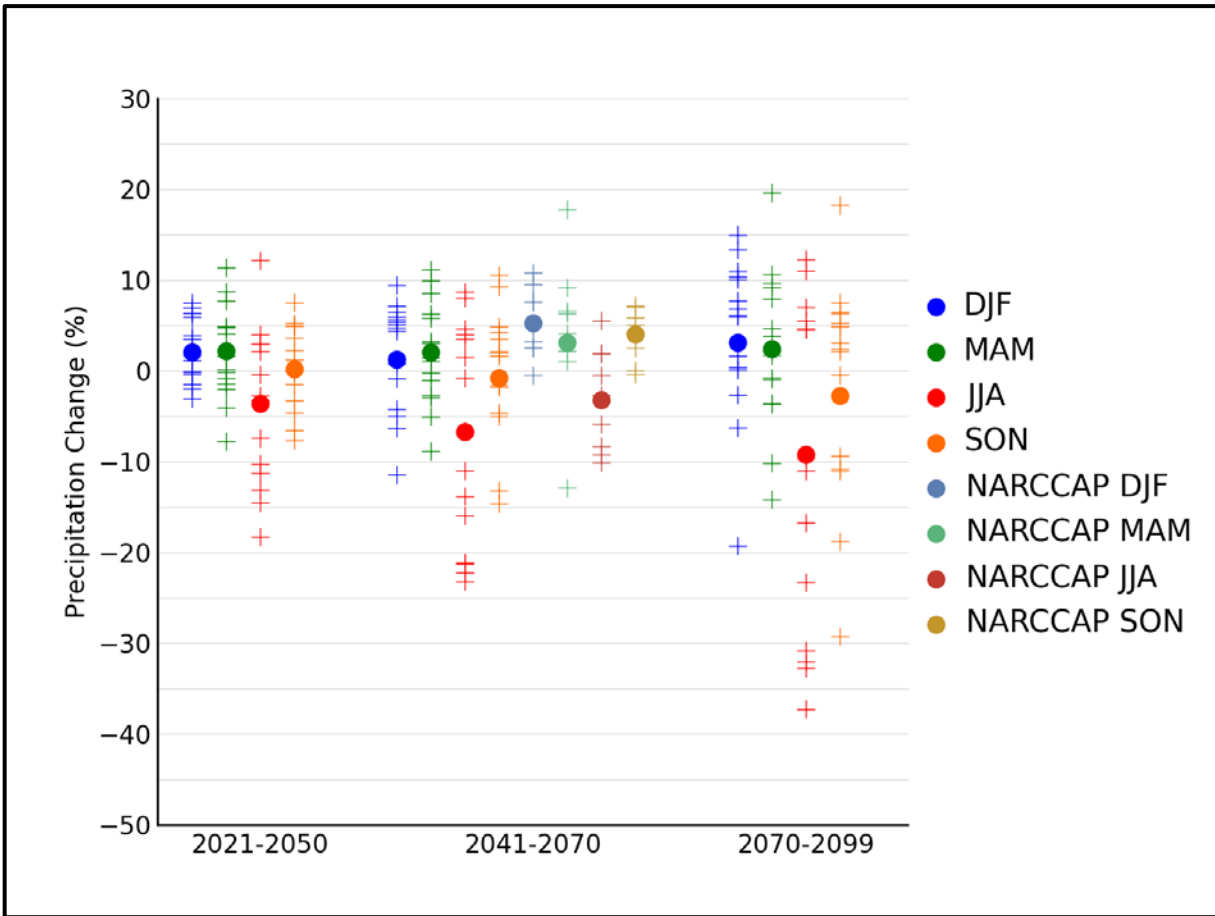


Figure 27. Simulated seasonal mean precipitation change (%) for the Great Plains region, for each future time period (2021-2050, 2041-2070, and 2070-2099) with respect to the reference period of 1971-1999. Values are given for all 15 CMIP3 models for the high (A2) emissions scenario. Also shown are values (relative to 1971-2000) for 9 NARCCAP model for 2041-2070. The small plus signs indicate each individual model and the circles depict the multi-model means. Seasons are indicated as follows: winter (DJF, December-January-February), spring (MAM, March-April-May), summer (JJA, June-July-August), and fall (SON, September-October-November). The ranges of model-simulated changes are large compared to the mean changes and to differences between the seasons.

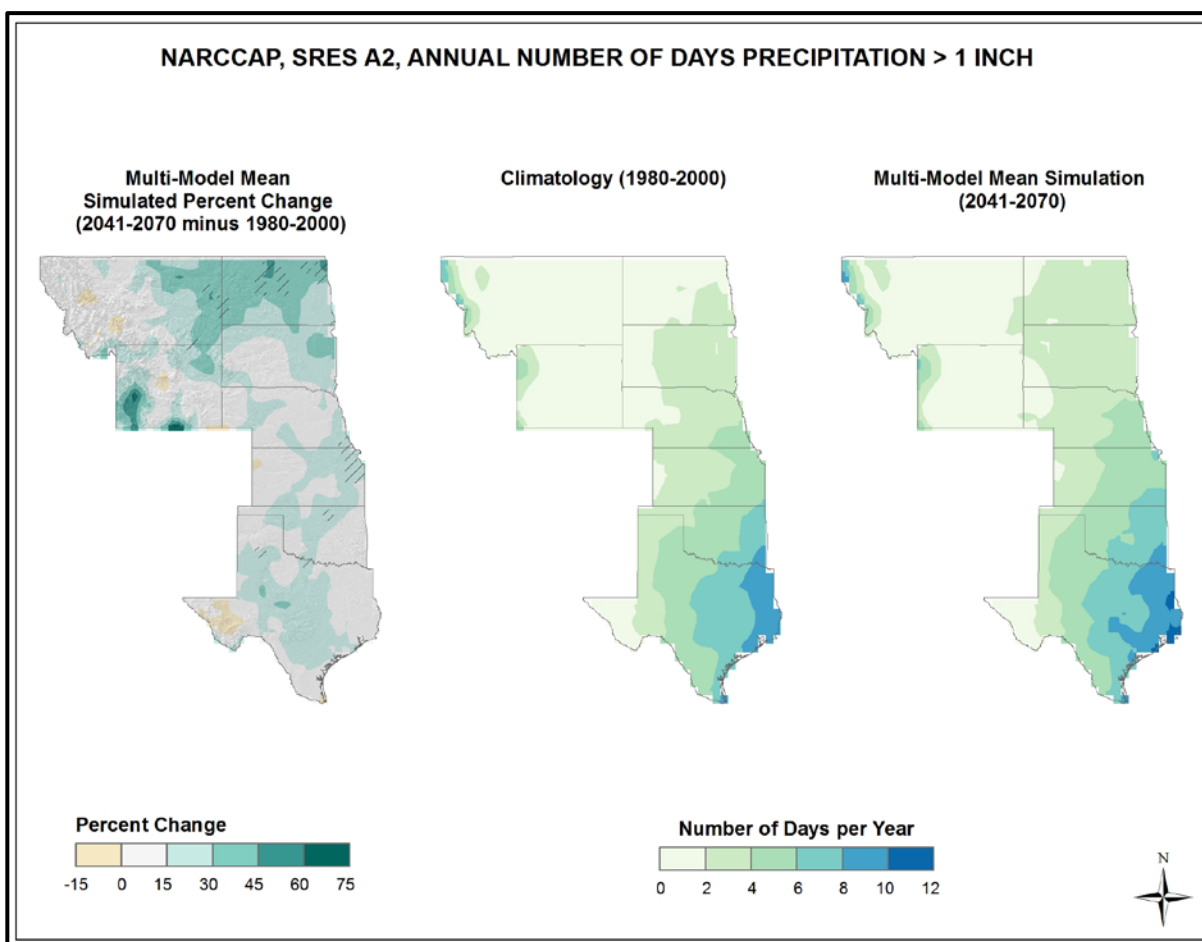


Figure 28. Simulated percentage difference in the mean annual number of days with precipitation of greater than one inch for the Great Plains region, for the 2041-2070 time period with respect to the reference period of 1980-2000 (left). Color only (category 1) indicates that less than 50% of the models show a statistically significant change in the number of days. Color with hatching (category 3) indicates that more than 50% of the models show a statistically significant change in the number of days, and more than 67% agree on the sign of the change (see text). Mean annual number of days with precipitation of greater than one inch for the 1980-2000 reference period (center). Simulated mean annual number of days with precipitation of greater than one inch for the 2041-2070 future time period (right). These are multi-model means from 8 NARCCAP regional climate simulations for the high (A2) emissions scenario. The models simulate mostly increases with the largest changes in the north.

Consecutive days with little or no precipitation reduce soil moisture levels and put stress on plants. Figure 29 shows the NARCCAP multi-model mean change in the average annual maximum number of consecutive days with precipitation less than 0.1 inches (3 mm) between 2055 and the model reference period of 1980-2000, for the high (A2) emissions scenario. The largest increases are simulated in the south, with increases of up to 13 days with little or no precipitation. By contrast, decreases of up to 8 days per year are simulated for parts of the north, including the Dakotas, Wyoming and Montana, i.e., the models indicate that these areas could experience shorter dry periods. Changes in the number of consecutive days with precipitation of less than 0.1 inches are not statistically significant for most models (category 1) over the majority of grid points. This means that most models are in agreement that any changes will be smaller than the normal year-to-year variations that occur under this scenario. However, for grid points where substantial increases are simulated, such as western Wyoming and central Texas, most models indicate statistically significant changes (category 3). In a few small areas throughout the region the models are in disagreement about the sign of the changes (category 2).

3.9. Tabular Summary of Selected Precipitation Variables

The mean changes for select precipitation-based variables derived from 8 NARCCAP simulations for 2055 with respect to the model reference period of 1971-2000, for the high (A2) emissions scenario, are summarized in Table 8. The same variables from the 8 CMIP3 statistically-downscaled (Daily_CMIP3) simulations are also shown for comparison. These spatially-averaged values were calculated as described for Table 5.

Table 8. Multi-model means and standard deviations of the simulated annual mean change in select precipitation variables from 8 NARCCAP simulations for the Great Plains region. Multi-model means from the 8 Daily_CMIP3 simulations are also shown for comparison. Analyses are for the 2041-2070 time period with respect to the reference period of 1971-2000, for the high (A2) emissions scenario.

Precipitation Variable	NARCCAP		Daily_CMIP3
	Mean	Standard Deviation	Mean
#days > 1 inch	+17%	6%	+15%
#days > 2 inches	+34%	22%	+38%
#days > 3 inches	+47%	39%	+65%
#days > 4 inches	+56%	58%	+98%
Consecutive #days < 0.1 inches	+3 days	+1 day	+1 day

For the NARCCAP data, the multi-model mean number of days with precipitation exceeding 1, 2, 3, and 4 inches are simulated to increase (+17% for 1 inch, +34% for 2 inches, +47% for 3 inches, and +56% for 4 inches) for the A2 scenario. The multi-model means from the Daily_CMIP3 simulations are higher than their NARCCAP counterparts, especially for the highest thresholds. Similar to the temperature variables in Table 5, greater increases are seen for the more extreme thresholds in Table 8, due to a lower number of occurrences in the 1971-2000 reference period. The average annual maximum number of consecutive days with precipitation less than 0.1 inches is simulated to increase by 3 days. The corresponding Daily_CMIP3 value is an increase of 1 day.

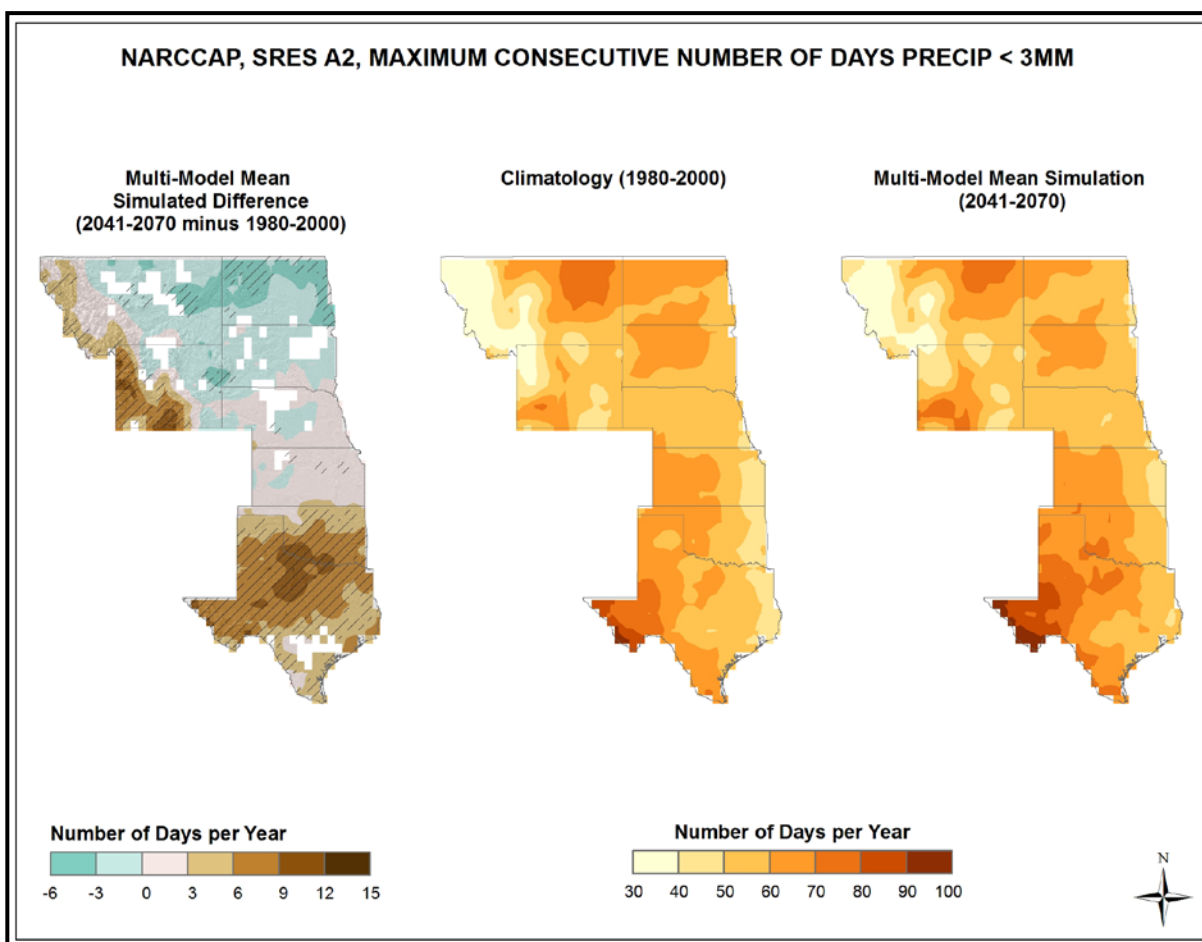


Figure 29. Simulated difference in the mean annual maximum number of consecutive days with precipitation of less than 0.1 inches/3 mm for the Great Plains region, for the 2041-2070 time period with respect to the reference period of 1980-2000 (left). Color only (category 1) indicates that less than 50% of the models show a statistically significant change in the number of consecutive days. Color with hatching (category 3) indicates that more than 50% of the models show a statistically significant change in the number of consecutive days, and more than 67% agree on the sign of the change. Whited out areas (category 2) indicate that more than 50% of the models show a statistically significant change in the number of consecutive days, but less than 67% agree of the sign of the change (see text). Mean annual maximum number of consecutive days with precipitation of less than 0.1 inches/3 mm for the 1980-2000 reference period (center). Simulated mean annual maximum number of consecutive days with precipitation of less than 0.1 inches/3 mm for the 2041-2070 future time period (right). These are multi-model means from 8 NARCCAP regional climate simulations for the high (A2) emissions scenario. The models simulate increases over most of the region, with slight decreases in the north.

3.10. Comparison Between Model Simulations and Observations

In this section, some selected comparisons between CMIP3 model simulations and observations are presented. These are limited to annual and seasonal temperature and precipitation. The model simulations of the 20th century that are shown herein are based on estimated historical forcing of the climate system, including such factors as greenhouse gases, volcanic eruptions, solar variations, and aerosols. Also shown are the simulations of the 21st century for the high (A2) emissions scenario.

In these comparisons, both model and observational data are expressed as deviations from the 1901-1960 average. As explained in Section 2.4 (Climatic Trends), acceleration of the anthropogenic forcing occurs shortly after 1960. Thus, for the purposes of comparing net warming between periods of different anthropogenic forcing, 1960 is a rational choice for the ending date of a reference period. It is not practical to choose a beginning date earlier than about 1900 because many model simulations begin in 1900 or 1901 and the uncertainties in the observational time series increase substantially prior to 1900. Therefore, the choice of 1901-1960 as the reference period is well suited for this purpose (comparing the net warming between periods of different anthropogenic forcing). However, there are some uncertainties in the suitability of the 1901-1960 reference period for this purpose. Firstly, there is greater uncertainty in the natural climate forcings (e.g., solar variations) during this time period than in the latter half of the 20th century. If there are sizeable errors in the estimated natural forcings used in climate models, then the simulations will be affected; this type of error does not represent a model deficiency. Secondly, the 1930s “Dust Bowl” era is included in this period. The excessive temperatures experienced then, particularly during the summers, are believed to be caused partially by poor land management through its effects on the surface energy budget. Climate models do not incorporate land management changes and there is no expectation that models should simulate the effects of such. Thirdly, there are certain climate oscillations that occur over several decades. These oscillations have important effects on regional temperatures. A 60-year period is too short to sample entire cycles of some of these, and thus only represents a partial sampling of the true baseline climate.

Figure 30 shows observed (using the same data set as shown in Fig. 8) and simulated decadal mean annual temperature changes for the U.S. Great Plains from 1900 to 2100, expressed as deviations from the 1901-1960 average. The observed rate of warming from 1910s into the 1930s is not simulated by any of the models. Conversely, the observed cooling from the 1930s into the 1970s is greater than any model simulation; however, since 1980, the observed rate of warming is similar to that of the models.

For the summer season (Fig. 31), the strikingly anomalous warmth of the 1930s is not simulated by any model. Observed temperatures are lower than any model simulation in the 1910s for the summer season and during the 1950s for the spring season. For summer and fall, the overall 20th century change in observed temperatures is small and less than the model simulations. This lack of 20th century warming in the central United States is well-known and has been dubbed the “warming hole”. Research on the causes of this feature is active and ongoing. The observed overall rate of warming in the winter and spring is within the range of the model simulations.

The 21st century portions of the time series indicate that the simulated future warming is much larger than the observed and simulated temperature changes for the 20th century.

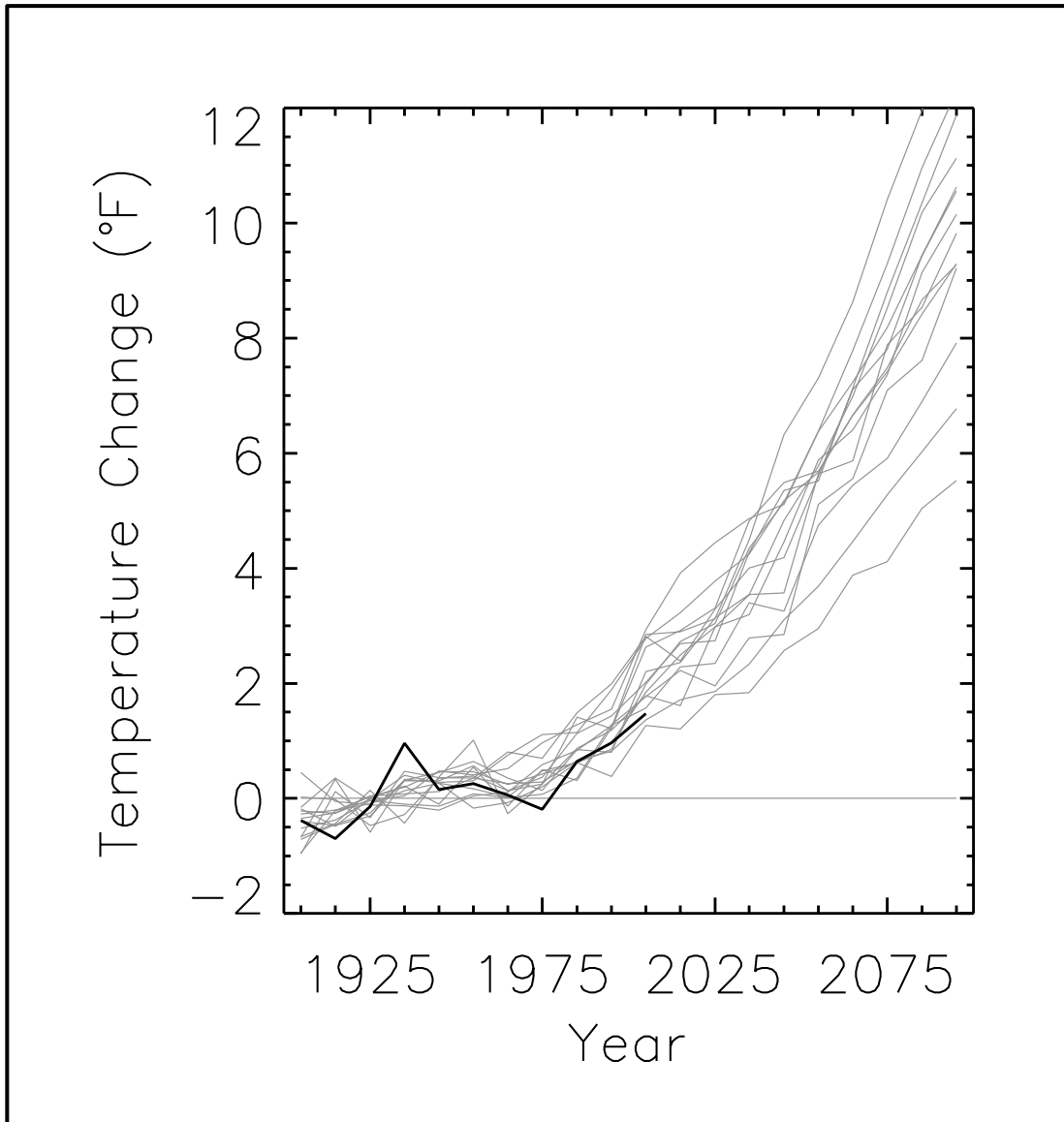


Figure 30. Observed decadal mean annual temperature change (deviations from the 1901-1960 average, °F) for the U.S. Great Plains (black line). Based on a new gridded version of COOP data from the National Climatic Data Center, the CDDv2 data set (R. Vose, personal communication, July 27, 2012). Gray lines indicate the 20th and 21st century simulations from 15 CMIP3 models, for the high (A2) scenario. The early 20th century rate of warming is not simulated by the models, but the late-century rate of warming is similar to the rate of warming in the models.

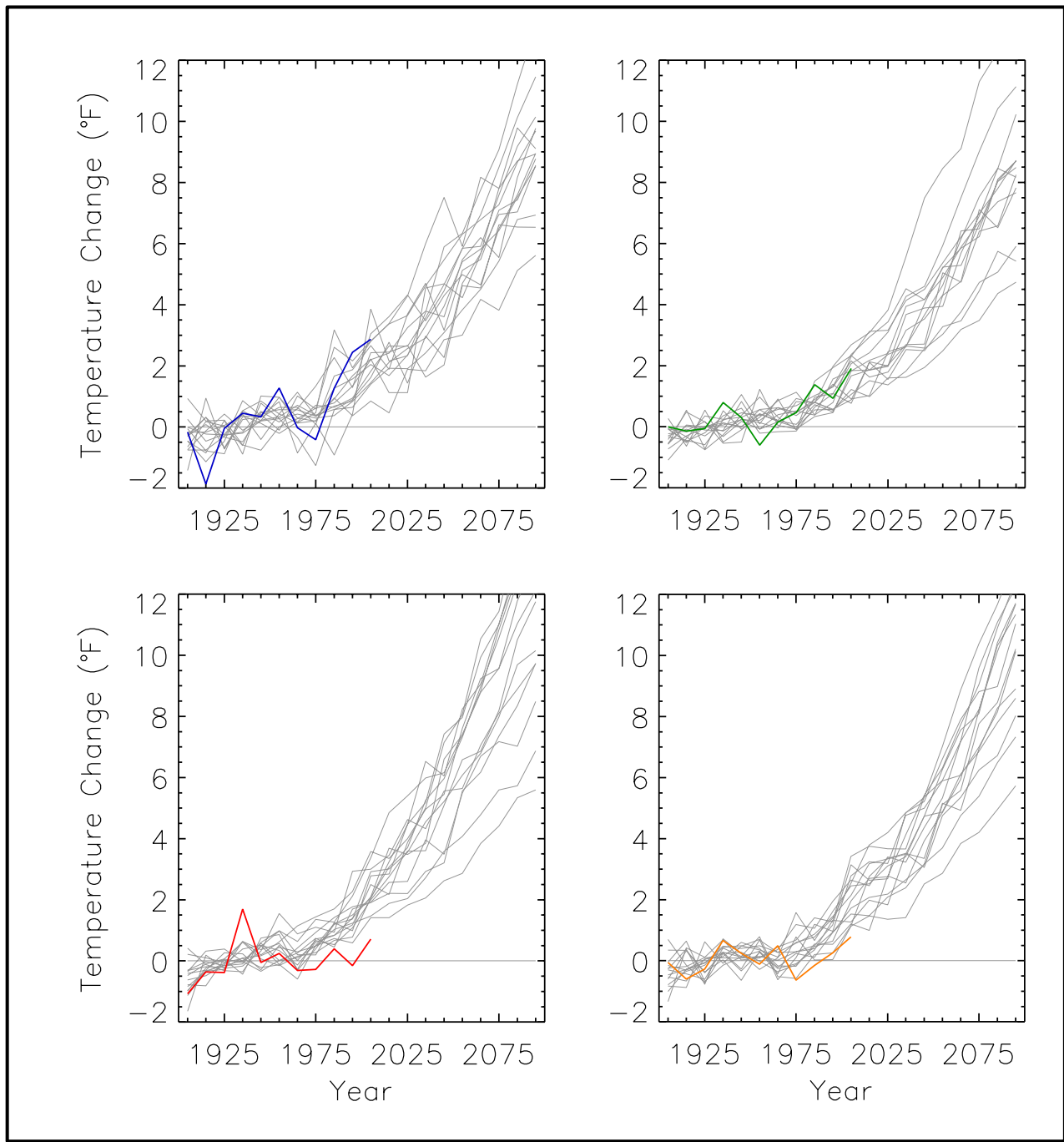


Figure 31. Observed decadal mean temperature change (deviations from the 1901-1960 average, °F) for the U.S. Great Plains for winter (top left, blue line), spring (top right, green line), summer (bottom left red line), and fall (bottom right, orange line). Based on a new gridded version of COOP data from the National Climatic Data Center, the CDDv2 data set (R. Vose, personal communication, July 27, 2012). Gray lines indicate 20th and 21st century simulations from 15 CMIP3 models, for the high (A2) scenario. The observed amount of overall 20th century warming is less than model simulations in summer and fall.

Observed and model-simulated decadal mean precipitation changes (using the same data set as shown in Fig. 9) can be seen in Fig. 32 for annual and Fig. 33 for seasonal values. In general, the model variability is considerably less than observed. For the annual time series, the observed anomalies are more negative than any model simulation in the 1930s and 1950s and more positive in the 1940s and 1990s. For the seasons, there are also decadal periods where the observed values are not within the envelope of the model simulations. The overall observed trends are within the envelope of the model simulations. The 21st century portions of the time series show increased variability among the model simulations. It can be seen that the majority of the models simulate an overall increase in precipitation for the winter.

The CMIP3 archive contains a total of 74 simulations of the 20th century, 40 simulations of the 21st century for the high (A2) emissions scenario, and 32 simulations of the 21st century for the low (B1) emissions scenario from a total of 23 different models (many models performed multiple simulations for these periods). An exploratory analysis of the entire archive was performed, limited to temperature and to the year as a whole. As before, the data were processed using 1901-1960 as the reference period to calculate anomalies.

Figure 34 compares observations of annual temperature with the entire suite of model simulations. For each model, the annual anomalies were first calculated using the 1901-1960 period as the reference. Then the mean 1901-1960 value from the observations was added to each annual anomaly, essentially removing the model mean bias. In this presentation, the multi-model mean and the 5th and 95th percentile bounds of the model simulations are shown. The mean and percentile values were calculated separately for each year. Then, the curves were smoothed with a 10-year moving boxcar average. The observational time series is not smoothed. During the first half of the 20th century, the observed annual values vary around the model mean because that is the common reference period. These values only fall outside the 5th/95th percentile bounds for the model simulations during the 1930s. For the rest of the observational time period, the values are generally within the 5th/95th percentile bounds, with a few values below the 5th percentile bound but none above the 95th percentile bound. The rate of observed warming from the mid-1970s onwards is similar to that of the multi-model mean, a similar result to that found in Fig. 30 for a subset of the CMIP3 models.

On decadal time scales, climate variations arising from natural factors can be comparable to or larger than changes arising from anthropogenic forcing. An analysis of change on such time scales was performed by examining the decadal changes simulated by the CMIP3 models with respect to the most recent historical decade of 2001-2010. Figure 35 shows the simulated change in decadal mean values of annual temperature for each future decadal time period with respect to the most recent historical decade of 2001-2010, averaged over the entire Great Plains region for the 14 (B1) or 15 (A2) CMIP3 models. For the 2011-2020 decade, the temperature increases are not statistically significant relative to the 2001-2010 decade for most of the models. As the time period increases, more of the individual models simulate statistically significant temperature changes, with all being significant at the 95% confidence level by 2035 for the high emissions scenario (2065 for the low emissions scenario). By the mid-to-late 21st century, all of the model decadal mean values lie outside the 10-90th percentile range of the historical annual temperature anomalies. As also shown in Fig. 30, the model simulations show increased variability over time, with the inter-model range of temperature changes for 2091-2100 being more than double that for 2051-2060 (for the high emissions scenario).

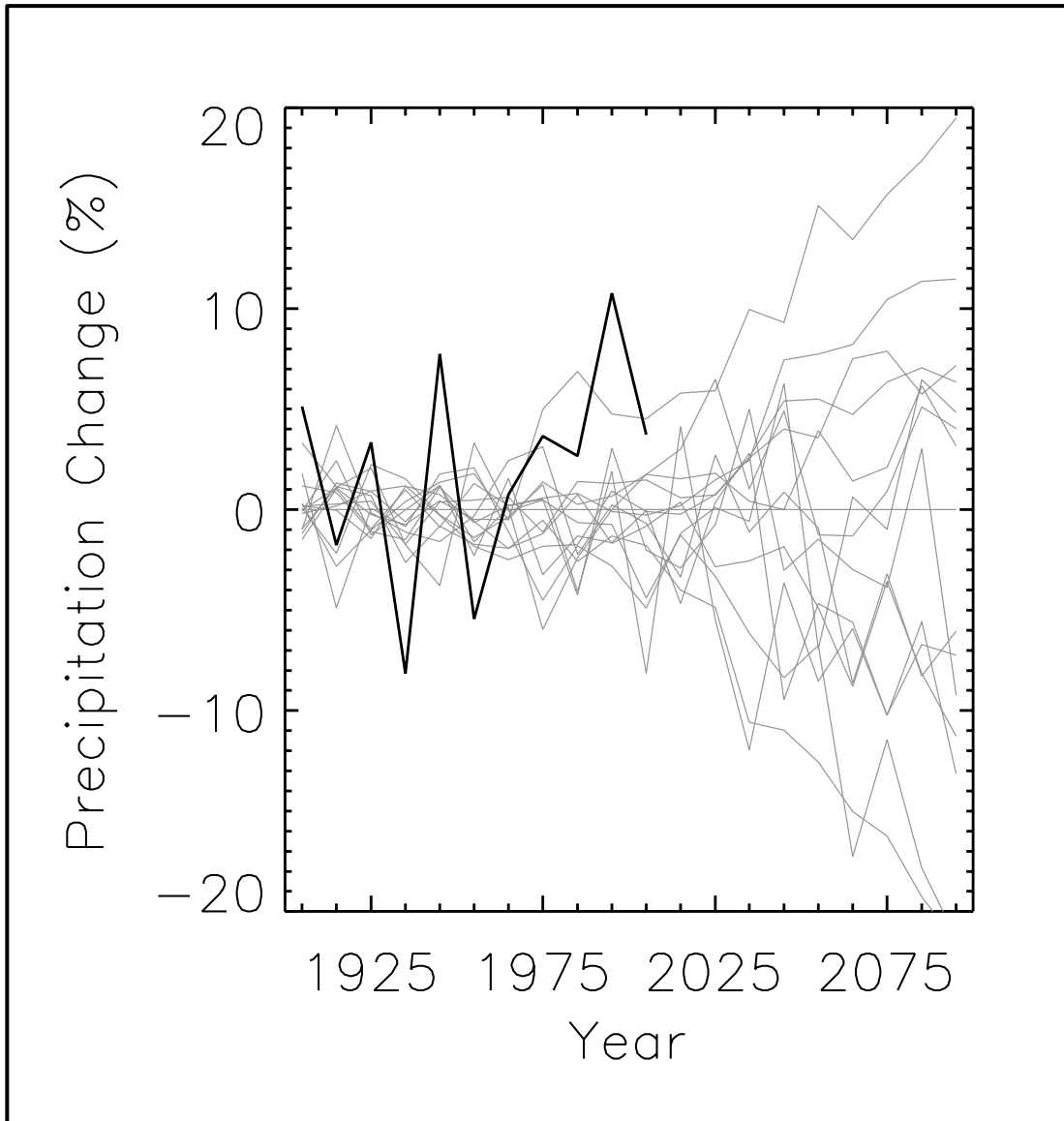


Figure 32. Observed decadal mean annual precipitation change (deviations from the 1901-1960 average, %) for the U.S. Great Plains (black line). Based on a new gridded version of COOP data from the National Climatic Data Center, the CDDv2 data set (R. Vose, personal communication, July 27, 2012). Gray lines indicate the 20th and 21st century simulations from 15 CMIP3 models, for the high (A2) scenario. Observed precipitation variations are mostly within the model simulations.

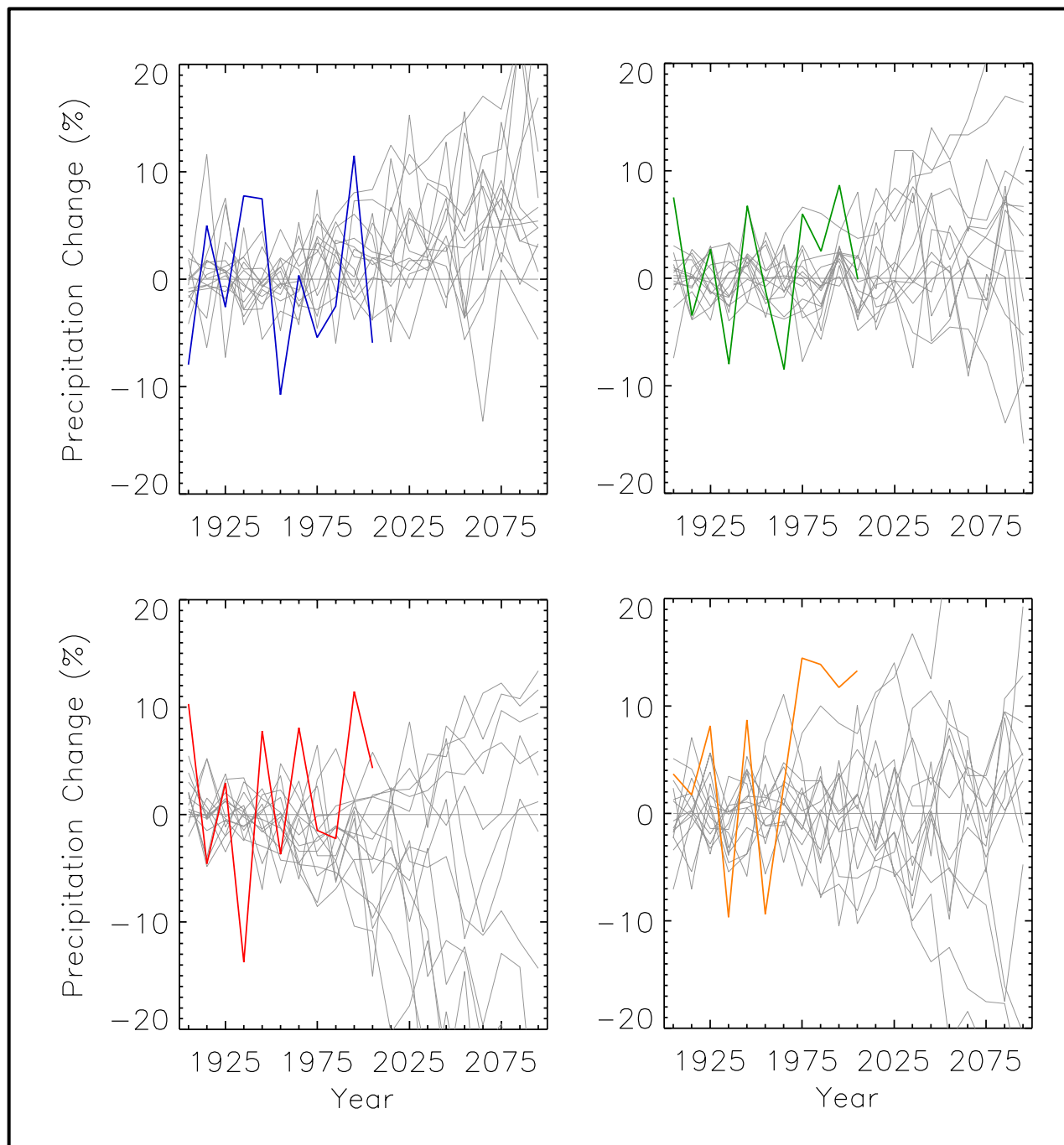


Figure 33. Observed decadal mean precipitation change (deviations from the 1901-1960 average, %) for the U.S. Great Plains for winter (top left, blue line), spring (top right, green line), summer (bottom left red line), and fall (bottom right, orange line). Based on a new gridded version of COOP data from the National Climatic Data Center, the CDDv2 data set (R. Vose, personal communication, July 27, 2012). Gray lines indicate 20th and 21st century simulations from 15 CMIP3 models, for the high (A2) scenario. Observed seasonal precipitation variations are within model simulations for all seasons.

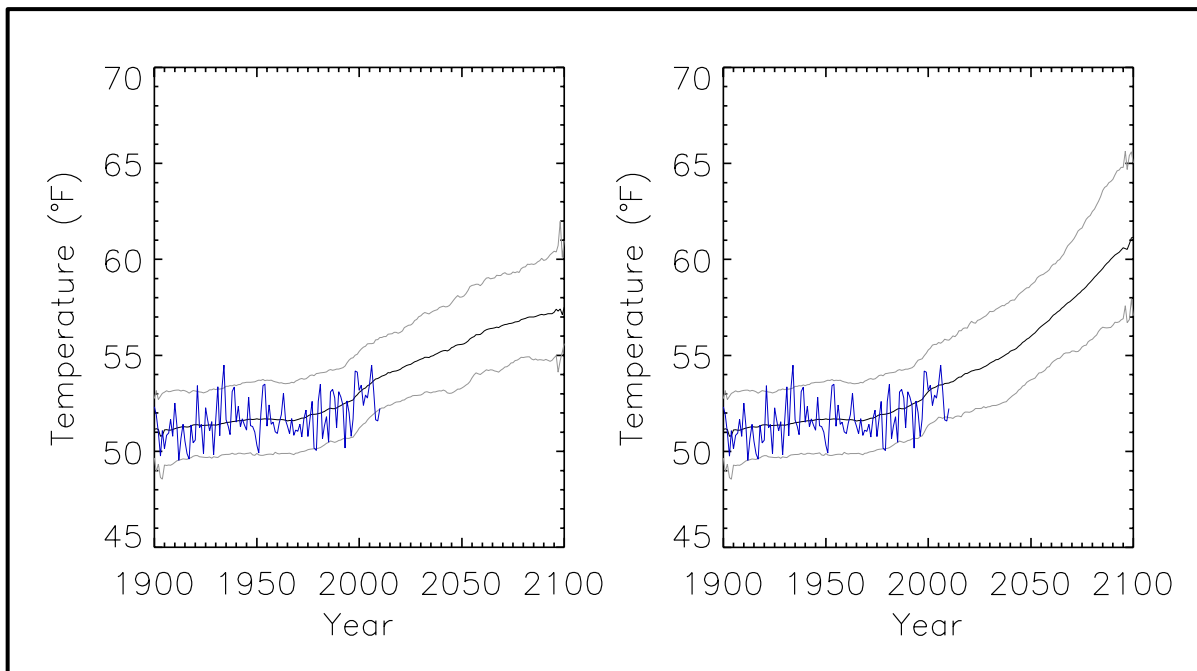


Figure 34. Time series of mean annual temperature for the Great Plains region from observations (blue) and from all available CMIP3 global climate model simulations (black and grey). Black represents the mean and grey indicates the 5 and 95% limits of the model simulations. Model mean and percentile limits were calculated for each year separately and then smoothed. Results are shown for the low (B1) emissions scenario (left) and the high (A2) emissions scenario (right). A total of 74 simulations of the 20th century were used. For the 21st century, there were 40 simulations for the high emissions scenario and 32 for the low emissions scenario. For each model simulation, the annual temperature values were first transformed into anomalies by subtracting the simulation's 1901-1960 average from each annual value. Then, the mean bias between model and observations was removed by adding the observed 1901-1960 average to each annual anomaly value from the simulation. For each year, all available model simulations were used to calculate the multi-model mean and the 5th and 95th percentile bounds for that year. Then, the mean and 5th and 95th percentile values were smoothed with a 10-year moving boxcar average.

The corresponding simulated change in decadal mean values of annual precipitation can be seen in Fig. 36. Unlike for temperature, many of the model values of precipitation change are not statistically significant in all decades out to 2091-2099. For the high (A2) emissions scenario (Fig. 36, top) positive changes in multi-model mean precipitation are simulated up to the 2041-2050 period, with mostly negative changes indicated after this time. Also, the variability in the model simulations becomes greater over time, with a larger number of models lying outside the 10-90th percentile range for each increasing time period. However, for the low (B1) emissions scenario (Fig. 36, bottom) increases in multi-model mean precipitation are simulated for all time periods, with little change in variability over time

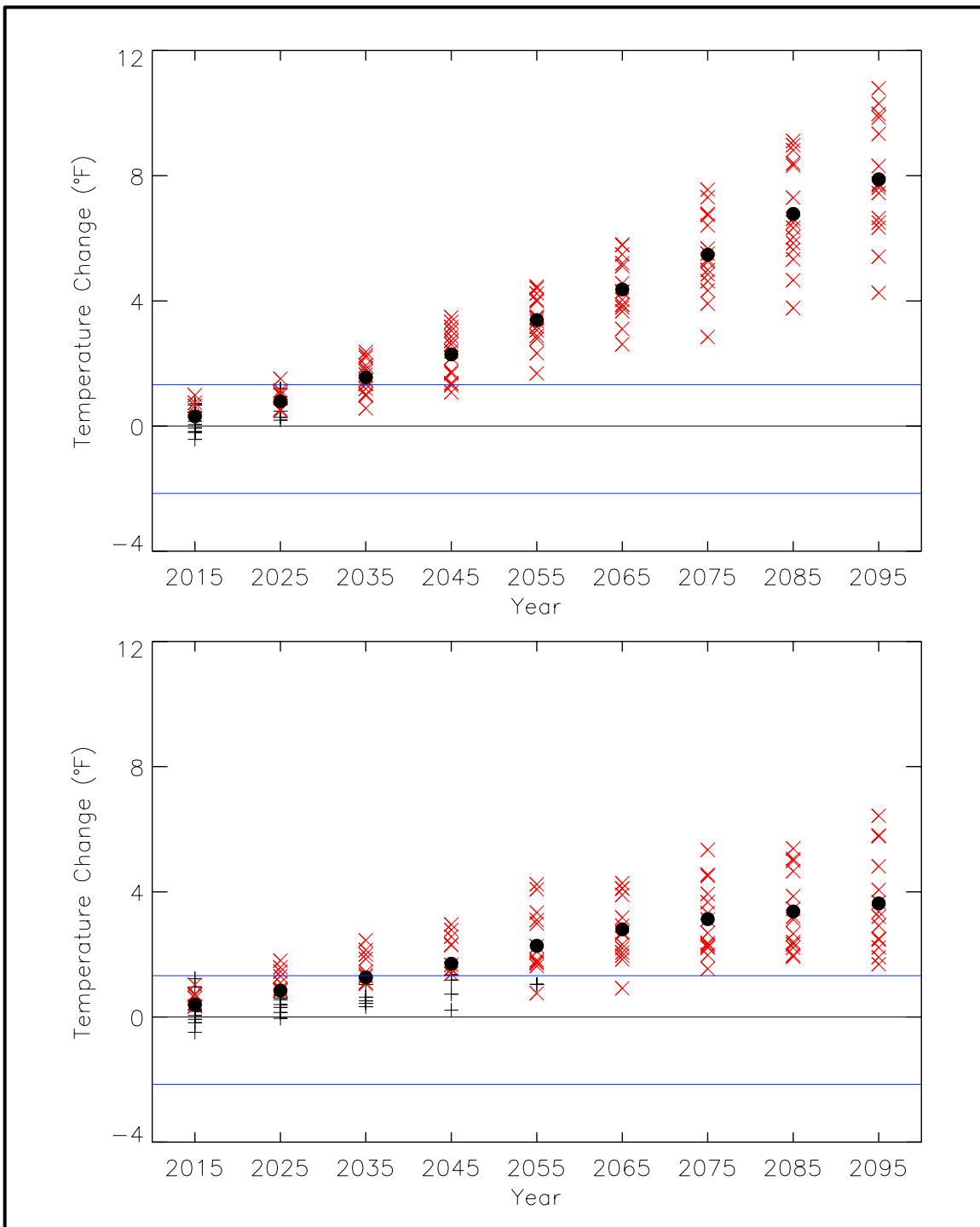


Figure 35. Simulated decadal mean change in annual temperature ($^{\circ}\text{F}$) for the U.S. Great Plains for each future decadal time period (represented by their approximate midpoints, e.g., 2015 = 2011-2020), with respect to the reference period of 2001-2010. Values are given for the high (A2, top) and low (B1, bottom) emissions scenarios for the 14 (B1) or 15 (A2) CMIP3 models. Large circles depict the multi-model means. Each individual model is represented by a black plus sign (+), or a red x if the value is statistically significant at the 95% confidence level. Blue lines indicate the 10th and 90th percentiles of 30 annual anomaly values from 1981-2010. The model simulated warming by 2015 is not statistically significant but by mid-21st century, all models simulate statistically significant warming.

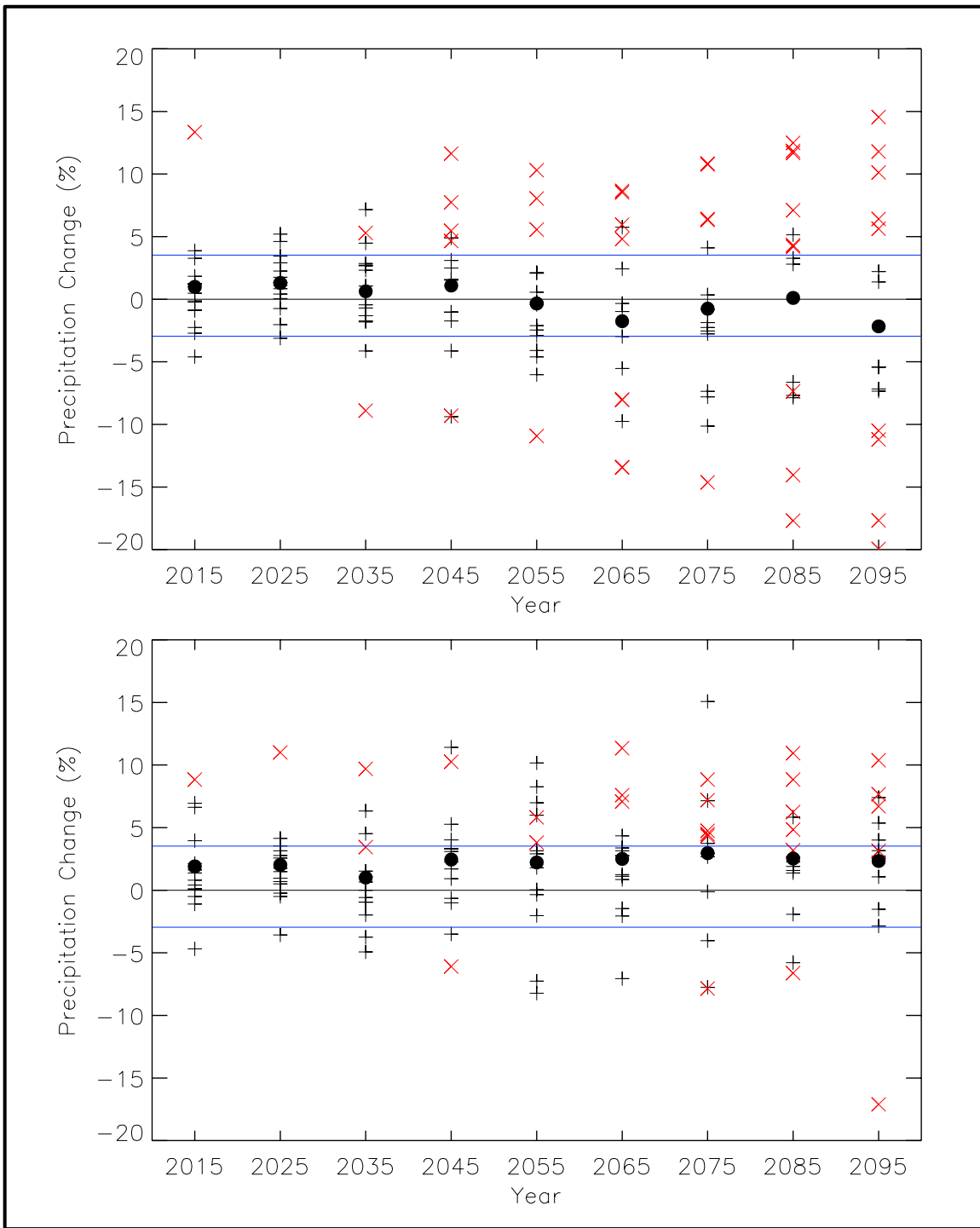


Figure 36. Simulated decadal mean change in annual precipitation (%) for the U.S. Great Plains for each future decadal time period (represented by their approximate midpoints, e.g., 2015 = 2011-2020), with respect to the reference period of 2001-2010. Values are given for the high (A2, top) and low (B1, bottom) emissions scenarios for the 14 (B1) or 15 (A2) CMIP3 models. Large circles depict the multi-model means. Each individual model is represented by a black plus sign (+), or a red x if the value is statistically significant at the 95% confidence level. Blue lines indicate the 10th and 90th percentiles of the 30 annual anomaly values from 1981-2010. Many models simulate precipitation changes that are not statistically significant out to the end of the 21st century.

4. SUMMARY

The primary purpose of this document is to provide physical climate information for potential use by the authors of the 2013 National Climate Assessment report. The document contains two major sections. One section summarizes historical conditions in the U.S. Great Plains and primarily focuses on trends in temperature and precipitation metrics that are important in the region. The core observational data set used is that of the National Weather Service's Cooperative Observer Network (COOP).

The second section summarizes climate model simulations for two scenarios of the future path of greenhouse gas emissions: the IPCC SRES high (A2) and low (B1) emissions scenarios. These simulations incorporate analyses from multiple sources, the core source being Coupled Model Intercomparison Project 3 (CMIP3) simulations. Additional sources consist of statistically- and dynamically-downscaled data sets, including simulations from the North American Regional Climate Change Assessment Program (NARCCAP). Analyses of the simulated future climate are provided for the periods of 2021-2050, 2041-2070, and 2070-2099, with changes calculated with respect to an historical climate reference period (1971-1999, 1971-2000, or 1980-2000). The resulting climate conditions are to be viewed as scenarios, not forecasts, and there are no explicit or implicit assumptions about the probability of occurrence of either scenario. The basis for these climate scenarios (emissions scenarios and sources of climate information) were considered and approved by the National Climate Assessment Development and Advisory Committee.

Some key characteristics of the historical climate include:

- Climatic phenomena that have major impacts on the Great Plains include droughts, floods, winter storms, convective storms, heat waves, cold waves, hurricanes, and sea-level rise.
- Temperatures have generally been above the 1901-1960 average for the last 20 years, both annually and seasonally. Eight of the past ten summers (2002-2011) have been above the 1901-1960 average. Northern states in the region have experienced the most change in their long-term average temperatures (e.g., North Dakota had the fastest increase in annual average temperature over the last 130 years, nationwide).
- Temperature trends are statistically significant (at the 95% level) for all seasons in the northern Great Plains and all seasons except summer and fall in the southern Great Plains.
- Annual precipitation for the Great Plains was greater than normal during the 1990s, less than normal during the early 2000s, and greater than normal during the last few years except for 2011. Trends in precipitation are not statistically significant for any season.
- Extreme cold and hot periods exhibit a large amount of interannual variability. The frequency of extreme cold periods has generally been low since 1990, averaging 65% below the long-term mean. The recent tendency toward fewer extreme cold events is more prominent in the north than in the south. Historical occurrence of extreme hot events is dominated by the severe heat of the 1930s.
- Occurrence of extreme (heavy) precipitation events also exhibits substantial interannual and decadal-scale variability. Since 1990, there have been several of years with a very high frequency of extreme precipitation events, with the greatest overall value of 1-day events occurring in 2007.

- There has been a generally increasing trend in freeze-free season length since the early 20th century. The average freeze-free season length during 1991-2010 was about 6 days longer than during 1961-1990.

The climate characteristics simulated by climate models for high (A2) and low (B1) emissions scenarios have the following key features:

- Both the CMIP3 and NARCCAP simulations indicate that spatial variations in annual temperature increases are relatively small, with the greatest warming simulated for the northeastern portion of the region under the high (A2) emissions scenario. The CMIP3 models indicate that temperature increases across the Great Plains are statically significant for all three future time periods and both emissions scenarios.
- CMIP3 models simulate average temperature increases of 2.8°F by 2035, 4.4°F by 2055, and nearly 8°F by 2085 for the high (A2) emissions scenario. Simulated increases under the low (B1) emissions scenario are very similar to those of the A2 scenario by 2035, but are considerably smaller by 2085. Seasonal temperature increases are simulated to be largest in summer and smallest in spring.
- The range of model-simulated temperature changes is substantial, indicating substantial uncertainty in the magnitude of warming associated with each scenario. However, in each model simulation, the warming is unequivocal and large compared to historical variations. This is also true for all of the derived temperature variables described below.
- NARCCAP model simulations indicate increases in the number of days with a maximum temperature of more than 95°F. The largest increase (more than 30 days) is simulated to occur in the southwest corner of Texas. The smallest increases (less than 10 days) are seen in the far northern portion of the region in high elevation areas.
- Simulated increases in the number of consecutive days above 95°F are 12 days or more in Oklahoma and Texas. In the central and northern portions of the region, the changes are smaller, generally in the range of increases of 4-12 days. Across the far northern tier of the region, the increase in the number of consecutive days exceeding 95°F is less than 4 days (for the A2 scenario at mid-century).
- Simulated decreases in the number of days with a minimum temperature below 10°F are largest (25 days or more) for the northern half of the region, near the Canadian border and in high elevation areas, whereas little or no change is simulated in the southern areas. Decreases in the number of days with a minimum temperature below 32°F are largest (more than 28 days) in the northwestern part of the region (for the A2 scenario at mid-century).
- The freeze-free season is simulated to become longer throughout the region, with increases mostly in the 20-30 day range (for the A2 scenario at mid-century).
- Cooling degree days (CDDs) are simulated to increase throughout the region, with the greatest increases (up to 1000) occurring in the southeastern Great Plains. Smaller increases of 200-600 CDDs are simulated for areas farther north. Areas across the Rocky Mountains are simulated to have the smallest increases of less than 200 CDDs (for the A2 scenario at mid-century).

- Heating degree days (HDDs) are simulated to decrease throughout the region, with the largest decreases (up to 1650 HDDs) occurring in high elevation areas of the northwest. The smallest decreases (250-450 HDDs) are simulated in southern Texas (for the A2 scenario at mid-century).
- Southern regions show the largest simulated decreases in average annual precipitation, while northern areas show increases. NARCCAP models show increases across most of the region in all seasons except summer. For the most part, these changes are either not statistically significant or the models do not agree on the sign of the change. An exception is the modeled changes in the far northern and far southern portions of the region for 2070-2099 under the high (A2) emissions scenario where the models simulate statistically significant increases and decreases, respectively. For most time periods and locations, the range of model-simulated precipitation changes is considerably larger than the multi-model mean change. Thus, there is great uncertainty associated with future precipitation changes in these scenarios.
- Nearly the entire region is simulated to see increases (up to 27%) in the annual number of days with precipitation exceeding 1 inch (for the A2 scenario at mid-century), with small areas in the far western portions of the region simulated to see slight decreases (up to 23%). However, these changes are mostly not statistically significant.
- Consecutive days with little or no precipitation (less than 0.1 inches) are simulated to increase in the south by 3-13 days per year and decrease in parts of the north by up to 8 days per year (for the A2 scenario at mid-century). The decreases in Texas and Oklahoma are mostly statistically significant.
- Most models do not indicate a statistically significant change in temperature (with respect to 2001-2010) for the near future; however, as the time advances through the 21st century, a greater number of models simulate statistically significant temperature changes, with all being significant at the 95% confidence level by 2035 (for the high emissions scenario).
- Many of the modeled values of decadal precipitation change are not statistically significant, with respect to 2001-2010, out to 2091-2099.

A comparison of model simulations of the 20th century with observations indicates the following:

- The observed changes in temperature are generally within the envelope of modeled changes on an annual basis. Graphs of the annual and summer season indicate that the observed rate of increase in temperature from the 1920s to the Dust Bowl era of the 1930s and the subsequent rate of decrease from the 1930s to the 1940s are greater than any model. Simulations of temperature in the 21st century indicate that future warming is much larger than the observed and simulated values for the 20th century.
- The variability in observed annual precipitation change tends to be higher than that of the models, though overall observed trends are within the envelope of model simulations.

5. REFERENCES

- Aberdeen News, cited 2011: Excessive heat kills at least 1,700 cattle across the state. [Available online at <http://www.aberdeennews.com/farmforum/news/aan-excessive-heat-kills-at-least-1700-cattle-across-the-state-20110721,0,5204476.story>.]
- AchutaRao, K., and K.R. Sperber, 2002: Simulation of the El Niño Southern Oscillation: Results from the Coupled Model Intercomparison Project. *Clim. Dyn.*, **19**, 191–209.
- Arakawa, A., 2004: The cumulus parameterization problem: Past, present, and future. *J. Climate*, **17**, 2493-2525.
- Bader D. C., C. Covey, W. J. Gutowski Jr., I. M. Held, K. E. Kunkel, R. L. Miller, R. T. Tokmakian, and M. H. Zhang, 2008: *Climate models: An Assessment of Strengths and Limitations*. U.S. Climate Change Science Program Synthesis and Assessment Product 3.1. Department of Energy, Office of Biological and Environmental Research, 124 pp.
- Bengtsson, L., K. I. Hodges, M. Esch, N. Keenlyside, L. Kornbluh, J.-J. Luo, and T. Yamagata, 2007: How may tropical cyclones change in a warmer climate? *Tellus A*, **59**, 539-561.
- Black, R. E., 1971: A Synoptic Climatology of Blizzards on the North-central Plains of the United States. NOAA Tech. Memo., NWS CR-39, 38 pp.
- Brooks, H., C. Doswell, and M. Kay, 2003: Climatological estimates of local daily tornado probability for the United States. *Weather Forecast.*, **18**, 626-640.
- Cerruti, B. J., and S. G. Decker, 2011: The Local Winter Storm Scale: A measure of the intrinsic ability of winter storms to disrupt society. *Bull. Am. Meteorol. Soc.*, **92**, 721-737.
- Changnon, S., K. Kunkel, and B. Reinke, 1996: Impacts and responses to the 1995 heat wave: A call to action. *Bull. Amer. Meteor. Soc.*, **77**, 1497-1506.
- Changnon, S., and T. Karl, 2003: Temporal and spatial variations of freezing rain in the contiguous United States: 1948-2000. *J. Appl. Meteorol.*, **42**, 1302-1315.
- Changnon, S., D. Changnon, and T. Karl, 2006: Temporal and spatial characteristics of snowstorms in the contiguous United States. *J. Appl. Meteorol. Climatol.*, **45**, 1141-1155.
- Church, J. A., and N. J. White, 2006: A 20th century acceleration in global sea-level rise. *Geophys. Res. Lett.*, **33**, L01602.
- Donoghue, J. F., 2011: Sea level history of the northern Gulf of Mexico coast and sea level rise scenarios for the near future. *Climatic Change*, 1-17.
- Douglas, M., R. Maddox, K. Howard, and S. Reyes, 1993: The Mexican Monsoon. *J. Climate*, **6**, 1665-1677.
- Dufresne, J.-L., and S. Bony. 2008. An assessment of the primary sources of spread of global warming estimates from coupled ocean–atmosphere models. *J. Climate*, **21**, 5135-5144.
- Elsner, J. B., J. P. Kossin, and T. H. Jagger, 2008: The increasing intensity of the strongest tropical cyclones. *Nature*, **455**, 92-95.
- Emanuel, K., 2005: Increasing destructiveness of tropical cyclones over the past 30 years. *Nature*, **436**, 686-688.

- Enz, J. W., 2003: North Dakota Topographic, Climate, and Agricultural Overview. North Dakota State University. [Available online at <http://www.ndsu.edu/ndsco/publication/ndsco/ndclimate.pdf>.]
- Fall, S., A. Watts, J. Nielsen-Gammon, E. Jones, D. Niyogi, J. R. Christy, and R. A. Pielke Sr, 2011: Analysis of the impacts of station exposure on the US Historical Climatology Network temperatures and temperature trends. *J. Geophys. Res.*, **116**, D14120.
- Goldenberg, S., C. Landsea, A. Mestas-Nunez, and W. Gray, 2001: The recent increase in Atlantic hurricane activity: Causes and implications. *Science*, **293**, 474-479.
- Gu, L., and Coauthors, 2008: The 2007 Eastern U.S. Spring freeze: Increased cold damage in a warming world? *BioScience*, **58**, 253-262.
- Hayhoe, K., and Coauthors, 2004: Emission pathways, climate change, and impacts on California. *P. Natl. Acad. Sci. USA*, **101**, 12422-12427.
- Hayhoe, K., and Coauthors, 2008: Regional climate change projections for the Northeast USA. *Mitig. Adapt. Strateg. Glob. Change*, **13**, 425-436.
- Hayhoe, K. A., 2010: A standardized framework for evaluating the skill of regional climate downscaling techniques. Ph.D. thesis, University of Illinois, 153 pp. [Available online at <https://www.ideals.illinois.edu/handle/2142/16044>.]
- Herrero, M. P., and R. Johnson, 1980: High temperature stress and pollen viability of maize. *Crop Science*, **20**, 796-800.
- Hoerling, M., J. Eischeid, D. Easterling, T. Peterson, and R. Webb, 2010: Understanding and Explaining Hydro-climate Variations at Devils Lake. A NOAA Climate Assessment. 22 pp. [Available online at http://www.esrl.noaa.gov/psd/csi/images/NOAA_Climate_Assessment_DevilsLake.pdf.]
- Holland, G. J., and P. J. Webster, 2007: Heightened tropical cyclone activity in the North Atlantic: natural variability or climate trend? *Philos. Trans. Roy. Soc. A*, **365**, 2695-2716.
- Hoyos, C. D., P. A. Agudelo, P. J. Webster, and J. A. Curry, 2006: Deconvolution of the factors contributing to the increase in global hurricane intensity. *Science*, **312**, 94-97.
- Hubbard, K., and X. Lin, 2006: Reexamination of instrument change effects in the US Historical Climatology Network. *Geophys. Res. Lett.*, **33**, L15710.
- IPCC, 2000: *Special Report on Emissions Scenarios: A Special Report of Working Group III of the Intergovernmental Panel on Climate Change*, N. Nakicenovic, and R. Swart, Eds., Cambridge University Press, 570 pp.
- , 2007a: *Climate Change 2007: The Physical Science Basis. Contribution of Working Group I to the Fourth Assessment Report of the Intergovernmental Panel on Climate Change*, Solomon, S., D. Qin, M. Manning, Z. Chen, M. Marquis, K.B. Averyt, M. Tignor, and H.L. Miller, Eds., Cambridge University Press, 996 pp.
- , 2007b: *Climate Change 2007: Synthesis Report. Contribution of Working Groups I, II and III to the Fourth Assessment Report of the Intergovernmental Panel on Climate Change*, Pachauri, R. K, and Reisinger, A., Eds., IPCC, 104 pp.
- , cited 2012: IPCC Data Distribution Centre. [Available online at http://www.ipcc-data.org/ddc_co2.html.]

- Jones, P. D., P. Y. Groisman, M. Coughlan, N. Plummer, W. C. Wang, and T. R. Karl, 1990: Assessment of urbanization effects in time series of surface air temperature over land. *Nature*, **347**, 169-172.
- Kalkstein, L. S., and R. E. Davis, 1989: Weather and human mortality: an evaluation of demographic and interregional responses in the United States. *Ann. Assoc. Am. Geogr.*, **79**, 44-64.
- Karl, T. R., and R. G. Quayle, 1981: The 1980 summer heat wave and drought in historical perspective. *Mon. Wea. Rev.*, **109**, 2055-2073.
- Karl, T. R., C. N. Williams Jr, P. J. Young, and W. M. Wendland, 1986: A model to estimate the time of observation bias associated with monthly mean maximum, minimum and mean temperatures for the United States. *J. Appl. Meteorol.*, **25**, 145-160.
- Karl, T. R., H. F. Diaz, and G. Kukla, 1988: Urbanization: Its detection and effect in the United States climate record. *J. Climate*, **1**, 1099-1123.
- Karl, T. R., J. M. Melillo, and T. C. Peterson, Eds, 2009: *Global Climate Change Impacts in the United States*. Cambridge University Press, 188 pp.
- Knight, D. B., and R. E. Davis, 2009: Contribution of tropical cyclones to extreme rainfall events in the southeastern United States. *J. Geophys. Res.*, **114**, D23102.
- Knutson, T. R., and Coauthors, 2010: Tropical cyclones and climate change. *Nature Geosci.*, **3**, 157-163.
- Knutti, R., 2010: The end of model democracy? *Climatic Change*, **102**, 395-404.
- Kocin, P. J., A. D. Weiss, and J. J. Wagner, 1988: The great arctic outbreak and east coast blizzard of February 1899. *Weather Forecast.*, **3**, 305-318.
- Kolker, A. S., M. A. Allison, and S. Hameed, 2011: An evaluation of subsidence rates and sea-level variability in the northern Gulf of Mexico. *Geophys. Res. Lett.*, **38**, L21404.
- Kruk, M. C., E. J. Gibney, D. H. Levinson, and M. Squires, 2010: A Climatology of inland winds from tropical cyclones for the eastern United States. *J. Appl. Meteorol. Climatol.*, **49**, 1538-1547.
- Kunkel, K. E., D. R. Easterling, K. Redmond, and K. Hubbard, 2003: Temporal variations of extreme precipitation events in the United States: 1895-2000. *Geophys. Res. Lett.*, **30**.
- Kunkel, K. E., M. Palecki, L. Ensor, K. G. Hubbard, D. Robinson, K. Redmond, and D. Easterling, 2009: Trends in twentieth-century US snowfall using a quality-controlled dataset. *J. Atmos. Oceanic Technol.*, **26**, 33-44.
- Kunkel, K. E., D. R. Easterling, D. A. R. Kristovich, B. Gleason, L. Stoecker, and R. Smith, 2010: Recent increases in US heavy precipitation associated with tropical cyclones. *Geophys. Res. Lett.*, **37**, L24706.
- Kunkel, K. E., and Coauthors, 2012: Monitoring and understanding changes in extreme storm statistics: state of knowledge. *Bull. Amer. Meteor. Soc.*, in press.
- Landsea, C., B. Harper, K. Hoarau, and J. Knaff, 2006: Can we detect trends in extreme tropical cyclones? *Science*, **313**, 452-454.
- Landsea, C., 2007: Counting Atlantic tropical cyclones back in time. *Eos Trans. AGU*, **88**, 197-203.

- LSU, cited 2012: Climate Trends. [Available online at [http://charts.srcc.lsu.edu/trends/.](http://charts.srcc.lsu.edu/trends/)]
- Mader, T. L., 2003: Environmental stress in confined beef cattle. *J. Anim. Sci.*, **81**, E110-E119.
- Mäkinen, T. M., 2007: Human cold exposure, adaptation, and performance in high latitude environments. *Am. J. Hum. Biol.*, **19**, 155-164.
- Mann, M. E., and K. A. Emanuel, 2006: Atlantic hurricane trends linked to climate change. *Eos Trans. AGU*, **87**, 233, 244.
- Maurer, E. P., A. W. Wood, J. C. Adam, D. P. Lettenmaier, and B. Nijssen, 2002: A long-term hydrologically based dataset of land surface fluxes and states for the conterminous United States. *J. Climate*, **15**, 3237–3251.
- McGeehin, M. A., and M. Mirabelli, 2001: The potential impacts of climate variability and change on temperature-related morbidity and mortality in the United States. *Environ. Health Persp.*, **109**, 185.
- Meehl, G. A., W. M. Washington, T. M. L. Wigley, J. M. Arblaster, and A. Dai, 2003: Solar and greenhouse gas forcing and climate response in the twentieth century. *J. Climate*, **16**, 426-444.
- Meehl, G. A., and Coauthors, 2007: Global climate projections. *Climate Change 2007: The Physical Basis. Contribution of Working Group I to the Fourth Assessment Report of the Intergovernmental Panel on Climate Change*, Solomon, S., D. Qin, M. Manning, Z. Chen, M. Marquis, K.B. Averyt, M. Tignor, and H.L. Miller, Eds., Cambridge University Press, 747-845.
- Menne, M. J., C. N. Williams, and R. S. Vose, 2009: The US Historical Climatology Network monthly temperature data, version 2. *Bull. Am. Meteorol. Soc.*, **90**, 993-1007.
- Menne, M. J., C. N. Williams, and M. A. Palecki, 2010: On the reliability of the U.S. surface temperature record. *J. Geophys. Res.*, **115**, D11108.
- Monahan, A.H., and A. Dai, 2004: The spatial and temporal structure of ENSO nonlinearity. *J. Climate*, **17**, 3026–3036.
- NARCCAP, cited 2012: North American Regional Climate Change Assessment Program. [Available online at [http://www.narccap.ucar.edu/.](http://www.narccap.ucar.edu/)]
- NDSU, cited 2012: The Fargo Flood Homepage. [Available online at <http://www.ndsu.edu/fargoflood/>]
- Needham, H., and B. D. Keim, 2011: Storm surge: physical processes and an impact scale. *Recent Hurricane Research-Climate, Dynamics, and Societal Impacts*, Lupo E., Ed. InTech, 385-407.
- Nielsen-Gammon, J., cited 2011: Climate of Texas. [Available online at [http://atmo.tamu.edu/osc/library/osc_pubs/climate_of_texas.pdf.](http://atmo.tamu.edu/osc/library/osc_pubs/climate_of_texas.pdf)]
- NOAA, 2008: The Easter freeze of April 2007: A climatological perspective and assessment of impacts and services, NOAA/NESDIS Technical Report 2008-01. [Available online at [http://www1.ncdc.noaa.gov/pub/data/techrpts/tr200801/Easter%20Freeze_revised%20April%2028.pdf.](http://www1.ncdc.noaa.gov/pub/data/techrpts/tr200801/Easter%20Freeze_revised%20April%2028.pdf)]
- , cited 2010: Sea Level Online, NOAA Tides and Currents webpage. [Available online at [http://tidesandcurrents.noaa.gov/sltrends/sltrends.shtml.](http://tidesandcurrents.noaa.gov/sltrends/sltrends.shtml)]
- , cited 2011a: Billion Dollar Weather/Climate Disasters. [Available online at [http://www.ncdc.noaa.gov/billions/.](http://www.ncdc.noaa.gov/billions/)]

- , cited 2011b: State of the Climate Drought August 2011. [Available online at <http://www.ncdc.noaa.gov/sotc/drought/2011/8.>]
- , cited 2011c: State of the Climate National Overview August 2011 [Available online at <http://www.ncdc.noaa.gov/sotc/national/2011/8.>]
- , cited 2012a: Cooperative Observer Program. [Available online at [http://www.nws.noaa.gov/om/coop/.](http://www.nws.noaa.gov/om/coop/)]
- , cited 2012b: NCEP/DOE AMIP-II Reanalysis. [Available online at [http://www.cpc.ncep.noaa.gov/products/wesley/reanalysis2/.](http://www.cpc.ncep.noaa.gov/products/wesley/reanalysis2/)]
- Norton, C. W., P.-S. Chu, and T. A. Schroeder, 2011: Projecting changes in future heavy rainfall events for Oahu, Hawaii: A statistical downscaling approach. *J. Geophys. Res.*, **116**, D17110.
- NWS, 1993: Cooperative Program Operations. National Weather Service Observing Handbook No. 6, 56 pp. [Available online at [http://www.srh.noaa.gov/srh/dad/coop/coophb6.pdf.](http://www.srh.noaa.gov/srh/dad/coop/coophb6.pdf)]
- O'Connor, J., and C. Fean, 1955: The Record-Breaking Cold Wave of Mid-November 1955 in the Northwest. *Mon. Wea. Rev.*, **83**, 279.
- Ojima, D., L. Garcia, E. Elgaali, K. Miller, T. G. F. Kittel, and J. Lockett, 1999: Potential climate change impacts on water resources in the Great Plains. *J. Am. Water Resour. As.*, **35**, 1443-1454.
- Overland, J. E., M. Wang, N. A. Bond, J. E. Walsh, V. M. Kattsov, and W. L. Chapman, 2011: Considerations in the selection of global climate models for regional climate projections: The Arctic as a case study. *J. Climate*, **24**, 1583-1597.
- Owens, B. F., and C. W. Landsea, 2003: Assessing the skill of operational Atlantic seasonal tropical cyclone forecasts. *Weather Forecast.*, **18**, 45-54.
- Pathak, T. B., K.G. Hubbard, and M.D. Shulski: Soil Temperature, 2012: A guide for planting agronomic and horticulture crops in Nebraska. NebGuide, G2122. [Available online at [http://www.ianrpubs.unl.edu/epublic/live/g2122/build/g2122.pdf.](http://www.ianrpubs.unl.edu/epublic/live/g2122/build/g2122.pdf)]
- PCMDI, cited 2012: CMIP3 Climate Model Documentation, References, and Links. [Available online at [http://www-pcmdi.llnl.gov/ipcc/model_documentation/ipcc_model_documentation.php.](http://www-pcmdi.llnl.gov/ipcc/model_documentation/ipcc_model_documentation.php)]
- Penland, S., and K. E. Ramsey, 1990: Relative sea-level rise in Louisiana and the Gulf of Mexico: 1908-1988. *J. Coastal Res.*, 323-342.
- Quayle, R. G., D. R. Easterling, T. R. Karl, and P. Y. Hughes, 1991: Effects of recent thermometer changes in the cooperative station network. *Bull. Am. Meteorol. Soc.*, **72**, 1718-1723.
- Quiroz, R. S., 1984: The climate of the 1983-84 winter—a season of strong blocking and severe cold in North America. *Mon. Wea. Rev.*, **112**, 1894-1912.
- Randall, D.A., and Coauthors, 2007: Climate models and their evaluation. *Climate Change 2007: The Physical Basis. Contribution of Working Group I to the Fourth Assessment Report of the Intergovernmental Panel on Climate Change*, Solomon, S., D. Qin, M. Manning, Z. Chen, M. Marquis, K.B. Averyt, M. Tignor, and H.L. Miller, Eds., Cambridge University Press, 590-662.
- Rosenberg, N. J., D. J. Epstein, D. Wang, L. Vail, R. Srinivasan, and J. G. Arnold, 1999: Possible impacts of global warming on the hydrology of the Ogallala aquifer region. *Climatic Change*, **42**, 677-692.

- Roth, D., 2010: Texas Hurricane History. [Available online at <http://www.hpc.ncep.noaa.gov/research/txhur.pdf>.]
- Schubert, S. D., M. J. Suarez, P. J. Pegion, R. D. Koster, and J. T. Bacmeister, 2004: On the cause of the 1930s Dust Bowl. *Science*, **303**, 1855-1859.
- Schwartz, R. M., and T. W. Schmidlin, 2002: Climatology of blizzards in the conterminous United States, 1959-2000. *J. Climate*, **15**, 1765-1772.
- St. Pierre, N. R., B. Cobanov, and G. Schmitkey, 2003: Economic losses from heat stress by U.S. livestock industries. *J. Dairy Sci.*, **86**, E52-E77.
- Tebaldi, C., J. M. Arblaster, and R. Knutti, 2011: Mapping model agreement on future climate projections. *Geophys. Res. Lett.*, **38**, L23701.
- U.S. Census Bureau, cited 2011: Metropolitan and Micropolitan Statistical Areas. [Available online at <http://www.census.gov/popest/data/metro/totals/2011/>.]
- USEPA, cited 2011: Area Designations for 2008 Ground-level Ozone Standards. [Available online at <http://www.epa.gov/ozonedesignations/2008standards/final/region6f.htm>.]
- USGS, cited 2011: Elevation of Devils Lake. [Available online at <http://nd.water.usgs.gov/devilslake/data/dlelevation.html>.]
- Vecchi, G. A., and B. J. Soden, 2007: Increased tropical Atlantic wind shear in model projections of global warming. *Geophys. Res. Lett.*, **34**, L08702.
- Vecchi, G. A., and T. R. Knutson, 2008: On estimates of historical North Atlantic tropical cyclone activity. *J. Climate*, **21**, 3580-3600.
- Vose, R. S., C. N. Williams, Jr., T. C. Peterson, T. R. Karl, and D. R. Easterling, 2003: An evaluation of the time of observation bias adjustment in the U.S. Historical Climatology Network. *Geophys. Res. Lett.*, **30**, 2046.
- Walsh, J. E., A. S. Phillips, D. H. Portis, and W. L. Chapman, 2001: Extreme cold outbreaks in the United States and Europe, 1948-99. *J. Climate*, **14**, 2642-2658.
- Webster, P. J., G. J. Holland, J. A. Curry, and H. R. Chang, 2005: Changes in tropical cyclone number, duration, and intensity in a warming environment. *Science*, **309**, 1844-1846.
- Wilby, R. L., and T. Wigley, 1997: Downscaling general circulation model output: a review of methods and limitations. *Prog. Phys. Geog.*, **21**, 530.
- Williams, C. N., M. J. Menne, and P. W. Thorne, 2011: Benchmarking the performance of pairwise homogenization of surface temperatures in the United States. *J. Geophys. Res.*, **52**, 154-163.
- Young, B., 1981: Cold stress as it affects animal production. *J. Anim. Sci.*, **52**, 154.

6. ACKNOWLEDGEMENTS

6.1. Regional Climate Trends and Important Climate Factors

Document and graphics support was provided by Brooke Stewart of the Cooperative Institute for Climate and Satellites (CICS), and by Fred Burnett and Clark Lind of TBG Inc. Analysis support was provided by Russell Vose of NOAA's National Climatic Data Center (NCDC).

6.2. Future Regional Climate Scenarios

We acknowledge the modeling groups, the Program for Climate Model Diagnosis and Intercomparison (PCMDI) and the WCRP's Working Group on Coupled Modelling (WGCM) for their roles in making available the WCRP CMIP3 multi-model dataset. Support of this dataset is provided by the Office of Science, U.S. Department of Energy. Analysis of the CMIP3 GCM simulations was provided by Michael Wehner of the Lawrence Berkeley National Laboratory, and by Jay Hnilo of CICS. Analysis of the NARCCAP simulations was provided by Linda Mearns and Seth McGinnis of the National Center for Atmospheric Research, and by Art DeGaetano and William Noon of the Northeast Regional Climate Center. Additional programming and graphical support was provided by Byron Gleason of NCDC, and by Andrew Buddenberg of CICS.

A partial listing of reports appears below:

- NESDIS 102 NOAA Operational Sounding Products From Advanced-TOVS Polar Orbiting Environmental Satellites. Anthony L. Reale, August 2001.
- NESDIS 103 GOES-11 Imager and Sounder Radiance and Product Validations for the GOES-11 Science Test. Jaime M. Daniels and Timothy J. Schmit, August 2001.
- NESDIS 104 Summary of the NOAA/NESDIS Workshop on Development of a Coordinated Coral Reef Research and Monitoring Program. Jill E. Meyer and H. Lee Dantzer, August 2001.
- NESDIS 105 Validation of SSM/I and AMSU Derived Tropical Rainfall Potential (TRaP) During the 2001 Atlantic Hurricane Season. Ralph Ferraro, Paul Pellegrino, Sheldon Kusselson, Michael Turk, and Stan Kidder, August 2002.
- NESDIS 106 Calibration of the Advanced Microwave Sounding Unit-A Radiometers for NOAA-N and NOAA-N=. Tsan Mo, September 2002.
- NESDIS 107 NOAA Operational Sounding Products for Advanced-TOVS: 2002. Anthony L. Reale, Michael W. Chalfant, Americo S. Allegrino, Franklin H. Tilley, Michael P. Ferguson, and Michael E. Pettey, December 2002.
- NESDIS 108 Analytic Formulas for the Aliasing of Sea Level Sampled by a Single Exact-Repeat Altimetric Satellite or a Coordinated Constellation of Satellites. Chang-Kou Tai, November 2002.
- NESDIS 109 Description of the System to Nowcast Salinity, Temperature and Sea nettle (*Chrysaora quinquecirrha*) Presence in Chesapeake Bay Using the Curvilinear Hydrodynamics in 3-Dimensions (CH3D) Model. Zhen Li, Thomas F. Gross, and Christopher W. Brown, December 2002.
- NESDIS 110 An Algorithm for Correction of Navigation Errors in AMSU-A Data. Seiichiro Kigawa and Michael P. Weinreb, December 2002.
- NESDIS 111 An Algorithm for Correction of Lunar Contamination in AMSU-A Data. Seiichiro Kigawa and Tsan Mo, December 2002.
- NESDIS 112 Sampling Errors of the Global Mean Sea Level Derived from Topex/Poseidon Altimetry. Chang-Kou Tai and Carl Wagner, December 2002.
- NESDIS 113 Proceedings of the International GODAR Review Meeting: Abstracts. Sponsors: Intergovernmental Oceanographic Commission, U.S. National Oceanic and Atmospheric Administration, and the European Community, May 2003.
- NESDIS 114 Satellite Rainfall Estimation Over South America: Evaluation of Two Major Events. Daniel A. Vila, Roderick A. Scofield, Robert J. Kuligowski, and J. Clay Davenport, May 2003.
- NESDIS 115 Imager and Sounder Radiance and Product Validations for the GOES-12 Science Test. Donald W. Hillger, Timothy J. Schmit, and Jamie M. Daniels, September 2003.
- NESDIS 116 Microwave Humidity Sounder Calibration Algorithm. Tsan Mo and Kenneth Jarva, October 2004.
- NESDIS 117 Building Profile Plankton Databases for Climate and EcoSystem Research. Sydney Levitus, Satoshi Sato, Catherine Maillard, Nick Mikhailov, Pat Cadwell, Harry Dooley, June 2005.
- NESDIS 118 Simultaneous Nadir Overpasses for NOAA-6 to NOAA-17 Satellites from 1980 and 2003 for the Intersatellite Calibration of Radiometers. Changyong Cao, Pubu Ciren, August 2005.
- NESDIS 119 Calibration and Validation of NOAA 18 Instruments. Fuzhong Weng and Tsan Mo, December 2005.
- NESDIS 120 The NOAA/NESDIS/ORA Windsat Calibration/Validation Collocation Database. Laurence Connor, February 2006.
- NESDIS 121 Calibration of the Advanced Microwave Sounding Unit-A Radiometer for METOP-A. Tsan Mo, August 2006.

- NESDIS 122** JCSDA Community Radiative Transfer Model (CRTM). Yong Han, Paul van Delst, Quanhua Liu, Fuzhong Weng, Banghua Yan, Russ Treadon, and John Derber, December 2005.
- NESDIS 123** Comparing Two Sets of Noisy Measurements. Lawrence E. Flynn, April 2007.
- NESDIS 124** Calibration of the Advanced Microwave Sounding Unit-A for NOAA-N'. Tsan Mo, September 2007.
- NESDIS 125** The GOES-13 Science Test: Imager and Sounder Radiance and Product Validations. Donald W. Hillger, Timothy J. Schmit, September 2007.
- NESDIS 126** A QA/QC Manual of the Cooperative Summary of the Day Processing System. William E. Angel, January 2008.
- NESDIS 127** The Easter Freeze of April 2007: A Climatological Perspective and Assessment of Impacts and Services. Ray Wolf, Jay Lawrimore, April 2008.
- NESDIS 128** Influence of the ozone and water vapor on the GOES Aerosol and Smoke Product (GASP) retrieval. Hai Zhang, Raymond Hoff, Kevin McCann, Pubu Ciren, Shobha Kondragunta, and Ana Prados, May 2008.
- NESDIS 129** Calibration and Validation of NOAA-19 Instruments. Tsan Mo and Fuzhong Weng, editors, July 2009.
- NESDIS 130** Calibration of the Advanced Microwave Sounding Unit-A Radiometer for METOP-B. Tsan Mo, August 2010.
- NESDIS 131** The GOES-14 Science Test: Imager and Sounder Radiance and Product Validations. Donald W. Hillger and Timothy J. Schmit, August 2010.
- NESDIS 132** Assessing Errors in Altimetric and Other Bathymetry Grids. Karen M. Marks and Walter H.F. Smith, January 2011.
- NESDIS 133** The NOAA/NESDIS Near Real Time CrIS Channel Selection for Data Assimilation and Retrieval Purposes. Antonia Gambacorta, Chris Barnet, Walter Wolf, Thomas King, Eric Maddy, Murty Divakarla, Mitch Goldberg, April 2011.
- NESDIS 134** Report from the Workshop on Continuity of Earth Radiation Budget (CERB) Observations: Post-CERES Requirements. John J. Bates and Xuepeng Zhao, May 2011.
- NESDIS 135** Averaging along-track altimeter data between crossover points onto the midpoint gird: Analytic formulas to describe the resolution and aliasing of the filtered results. Chang-Kou Tai, August 2011.
- NESDIS 136** Separating the Standing and Net Traveling Spectral Components in the Zonal-Wavenumber and Frequency Spectra to Better Describe Propagating Features in Satellite Altimetry. Chang-Kou Tai, August 2011.
- NESDIS 137** Water Vapor Eye Temperature vs. Tropical Cyclone Intensity. Roger B. Weldon, August 2011.
- NESDIS 138** Changes in Tropical Cyclone Behavior Related to Changes in the Upper Air Environment. Roger B. Weldon, August 2011.
- NESDIS 139** Computing Applications for Satellite Temperature Datasets: A Performance Evaluation of Graphics Processing Units. Timothy F.R. Burgess and Scott F. Heron, December 2011.
- NESDIS 140** Microburst Nowcasting Applications of GOES. Kenneth L. Pryor, September 2011.
- NESDIS 141** The GOES-15 Science Test: Imager and Sounder Radiance and Product Validations. Donald W. Hillger and Timothy J. Schmit, November 2011.

NOAA SCIENTIFIC AND TECHNICAL PUBLICATIONS

The National Oceanic and Atmospheric Administration was established as part of the Department of Commerce on October 3, 1970. The mission responsibilities of NOAA are to assess the socioeconomic impact of natural and technological changes in the environment and to monitor and predict the state of the solid Earth, the oceans and their living resources, the atmosphere, and the space environment of the Earth.

The major components of NOAA regularly produce various types of scientific and technical information in the following types of publications

PROFESSIONAL PAPERS – Important definitive research results, major techniques, and special investigations.

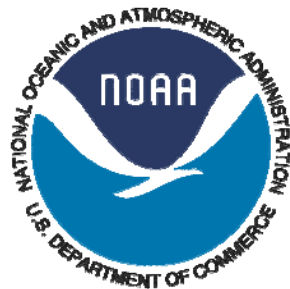
CONTRACT AND GRANT REPORTS – Reports prepared by contractors or grantees under NOAA sponsorship.

ATLAS – Presentation of analyzed data generally in the form of maps showing distribution of rainfall, chemical and physical conditions of oceans and atmosphere, distribution of fishes and marine mammals, ionospheric conditions, etc.

TECHNICAL SERVICE PUBLICATIONS – Reports containing data, observations, instructions, etc. A partial listing includes data serials; prediction and outlook periodicals; technical manuals, training papers, planning reports, and information serials; and miscellaneous technical publications.

TECHNICAL REPORTS – Journal quality with extensive details, mathematical developments, or data listings.

TECHNICAL MEMORANDUMS – Reports of preliminary, partial, or negative research or technology results, interim instructions, and the like.



U.S. DEPARTMENT OF COMMERCE
National Oceanic and Atmospheric Administration
National Environmental Satellite, Data, and Information Service
Washington, D.C. 20233